Modelling forces on buoyant macro plastics and their cross-sectional distribution in rivers

T. M. van Welsenes

TUDelft

Deltares

Modelling forces on buoyant macro plastics and their cross-sectional distribution in rivers

by

T.M. van Welsenes

August 21, 2019

To obtain the degree of Master of Science in Civil Engineering at Delft University of Technology

To be defended publicly on 25 September, 2019 at 14:30 PM

An electronic version of this thesis is available at http://repository.tudelft.nl

TUDelft   **Deltares**

PREFACE

It is November 2018 Bali, Indonesia. After a long dry period heavy rain starts to develop, changing the local landscape. Dry riverbanks fill with water and the streets are washed clean by the rain. On this day, our team of TU Delft students, on a plastic pollution study in Indonesia, heads out into the storm. Although most people return to a hideout, our team is dedicated to measure the plastic pollution output of the local rivers during the storm. It is expected that the first storm of the rainy season will wash a significant amount of plastic trash into the rivers and eventually the ocean. For our research this is vital data.

At arrival at one of the measurement locations, we see that the river is 3 times as deep. Quickly, the trawl (measurement tool for plastic transport) is lowered into the river. But due to the large amounts of trash the trawl is filled within seconds and the load becomes too large for the trawl to hold. Quickly, measuring the plastic transport in the river was no longer our concern but saving our trawl was now a priority. After extracting the trawl we see that within a minute the trawl is filled with 20 kilograms of trash, a large part being plastic material.

Plastic material is found in abundance and the pollution problem seems to be out of control. My experiences in Bali taught me that the problem is real and yes, we can do something about it. As a result I started to dive deeper into the plastic pollution problem; together with my project team Pantai Project was founded, a research program that motivates and helps students to contribute to the plastic pollution problem globally, and I started to focus my master thesis on riverine plastic pollution. The need for understanding and modelling of macro plastic transport sparked my interest. With joy I arrived at Deltares where I found a mutual in riverine plastic pollution with Frans Buschman.

I would like to express my gratitude to my supervisor at Deltares, Frans Buschman. Our mutual interest in the research topic, many meetings and interesting discussions have led to insights which proved to be invaluable to this thesis. Thanks to Wim Uijttewaal who provided very valuable insights with his expertise and sharing the enthusiasm for research on riverine plastic pollution. Thanks to Erik Mosselman and Jeremy Bricker who helped me to approach the study from different perspectives and provided valuable feedback.

Thomas van Welsenes

Rotterdam, September 2019

NOMENCLATURE

Abbreviations

BBO   Basset-Boussinesq-Oseen equation
LWD   Large Woody Debris

Symbols

A_w	m^2	Air contact area
ρ_w	kg/m^3	Air density
D	m	Channel depth
L	m	Channel length
B	m	Channel width
δ	m	Characteristic length scale eddy
Q	m^3/s	Discharge
C_D	-	Drag coefficient
μ_c	Pa/s	Dynamic viscosity
τ_e	s	Eddy timescale
ν_t		Eddy viscosity
K		Eddy diffusivity
a_f	m/s^2	Fluid acceleration
A_f	m^2	Fluid contact area
ρ_f	kg/m^3	Fluid density
m_f	kg	Fluid mass
U_f	m/s	Fluid velocity
g	m/s^2	Gravity constant
ν_e	m^2/s	Kinematic viscosity
λ_0	m	Kolmogorov microscale
U_m	m/s	Mean fluid velocity
a_p	m/s^2	Particle acceleration
ρ_p	kg/m^3	Particle density
d_p	m	Particle diameter
D_p	m^2/s	Particle diffusivity
m_p	kg	Particle mass
τ_p	s	Particle response time
U_p	m/s	Particle velocity
p	N/m^2	Pressure
r	m	Radius
τ	N/m^2	Shear stress
U_f^*	m/s	Shear velocity
Stk	-	Stokes number
t	s	Time
ϵ_t	m^2/s	Transverse mixing coefficient
D_{disp}	m	Transverse particle dispersion
∇	-	Vector differential operator
U_w	m/s	Wind velocity
x	m	Coordinate along x-axis
y	m	Coordinate along y-axis
z	m	Coordinate along z-axis

ABSTRACT

Concerns regarding plastic pollution arise as large quantities of plastic enter the ocean and affect wildlife and possibly human health. Rivers form a dominant pathway for macro plastic particles into the ocean. Plastic pollution in rivers can result in blockage, where it affects water quality and ecology. This increases risks of flooding and provides health concerns. To prevent further dispersion of plastics into the ocean and reduce health and flood risks, reduction of plastic concentrations in rivers is desired. Buoyant macro plastics are a dominant polluter and understanding their cross-sectional distribution in rivers could promote areas for efficient extraction or monitoring. As field measurements are expensive and time consuming it is desired to accelerate research with modelling techniques. To improve modelling of buoyant macro plastics and translate cross-sectional distributions it is necessary to model relative motion of buoyant macro plastic particles to the flow and one another.

Previous research has shown that the understanding of macro plastic forces and transport is limited. The range of macro plastic properties complicates modelling approaches to macro plastic transport. To simplify, a classification of macro plastics is introduced according to cornerstones in behaviour. A basic force model is constructed (derived from riverine wood transport studies) to provide an understanding of the effect of size, density, wind and discharge on transport of different macro plastic types. This new understanding is applied to a variety of flow features induced by a range of river elements (river bend, channel widening, river confluence and groyne) to develop a hypotheses on the cross-sectional distribution of the different macro plastic objects in these environments. These hypotheses are tested in a numerical transport model. A theoretical background study on particle response times and Stokes numbers is performed to identify a relation between the particle response time and relative particle dispersion (compared to the flow). This provides a possibility for translating the transport of the different macro plastic objects into the numerical model. To define numerical modelling input of different buoyant macro plastic objects, particle response times are calculated and translated to horizontal particle dispersion coefficients in D-WAQ PART (software package of choice). Each of the previously formulated river elements is modelled as well in the numerical model.

The modelling results show that river bends cause an increase in particle concentrations along the river bend. Channel widening increases the concentration along the boundaries. A river confluence increases the concentration along the tributary side of the channel. A groyne increases the macro plastic concentration along the groyne-free side of the channel. These results show that particle response times and their relation to Stokes number and particle dispersion propose an interesting tool for the modelling of relative particle motion towards the flow and the different macro plastic objects.

This study identifies the significance, diversity and complexity of macro plastic particles in riverine environments. It highlights the need for classification and simplification to facilitate modelling and still be able to obtain relevant results. Describing macro plastics according to cornerstones in behaviour provides an efficient tool to simplify modelling. Coupling of different macro plastic classes to a range of riverine environments and understanding the differences in their cross-sectional distribution provides practical use.

CONTENTS

LIST OF FIGURES

LIST OF TABLES

1

INTRODUCTION

1.1. CONTEXT

Plastic materials are part of our everyday lives and for good reasons. They are cheap, strong, light, versatile (Thompson, Moore, Vom Saal, & Swan, 2009) and highly resistant against environmental influences (Sascha Klein, 2018). It is estimated that the annual plastic production is exceeding 300 million tonnes, while increasing exponentially (Thompson et al., 2009). This claim, supported by others such as *The Facts 2017* (2017) and Gourmelon (2015), imposes significant responsibility on the management of plastic material. Large-scale global plastic production is a result of its many societal benefits as the use of plastic water bottles provide transport of clean drinking water globally and food packaging reduce food wastage and improve the expiration date of perishable foods (Andrady & Neal, 2009).

Population levels, economic growth and urbanization accelerate in developing countries and so does the municipal solid-waste generation. As proper waste handling is lagging behind, large quantities of mismanaged waste are produced in developing countries (Guerrero, Maas, & Hogland, 2013). Consequently, large quantities of plastic materials end up in the environment and endure due to their persistence.Jambeck et al. (2015) calculated that around 4 to 12 million tonnes of plastics enter the ocean annually via land-based sources. Although the estimate is rough, it does provide an indication of the size of the problem.

Besides the negative aesthetics of plastic littering, the flow of plastic waste into the marine environment is known for harming wildlife. Birds, turtles and fish die in great quantities because of ingestion and entanglement, see Figure 1.1. Plastics function as persistent vehicles for hitchhiking microorganisms, travelling great distances and potentially accelerating the dispersal of aggressive invasive species in the marine environment (Gregory, 2009). As plastic materials harm marine life and enter the food chain, concerns for human health arise as well (Rochman et al., 2015).

(a) Entanglement of marine wild life (Chias, 2018)   (b) Ingestion of plastics by birds (Atkin, 2018)

Figure 1.1: The effects of marine plastic pollution on wildlife

Rivers are an important source of marine plastic pollution as they form a major pathway for plastics. It remains unclear how much plastic material is disposed yearly into the marine environment via rivers. L. C. Lebreton et

al. (2017) estimated that 1.15 to 2.41 million tonnes of plastics enter the ocean annually via rivers. Schmidt, Krauth, and Wagner (2017) calculated that 0.41 to 4 million tonnes of plastic enter the ocean each year. Both model predictions are based on the presumption that mismanaged plastic waste and riverine plastic output are positively correlated. However, both studies mention their models impose large uncertainties due to limited available data. To improve, more riverine studies should be performed.

Plastic pollution in rivers can result in blockage, where it affects the water quality and ecology, and increases the risk of flooding with potential damaging of surrounding residents as a result, see Figure 1.2. Over the years, large cities have been subjected to increased flood risks. Often, river blockage is mentioned as one of the causes for this increased risk (Marshall, 2005)(Peters et al., 2015). Health concerns have been addressed back in 1984 by Littler and Thomas (1984), suggesting a link between river blockage in combination with bad sanitation and an increase of typhus and cholera. In addition, standing water provides a breeding ground for mosquitoes and increase the risk of mosquito transmitted diseases (Peters et al., 2015). To prevent further dispersion of plastics into the ocean and reduce health and flood risks, reduction of plastic concentrations in rivers is desired.

Figure 1.2: Blockage due to plastic littering in a river in Indonesia (Shukman, 2018)

1.2. PROBLEM DEFINITION

The riverine plastic pollution problem has received little attention until recently (Thompson et al., 2009) and substantial research is lacking (Kooi et al., 2018). Blettler, Abrial, Khan, Sivri, and Espinola (2018) stated that plastic pollution studies are predominantly focused on oceanic plastics. Fewer studies have been applied on riverine plastics. A majority of these studies was conducted in western countries and focuses on micro plastics (< 0.5 cm) (Gasperi, Dris, Bonin, Rocher, & Tassin, 2014), despite the major concerns in developing countries and environmental impact of macro plastics (> 2, 5 cm) (Blettler et al., 2018). A lack of empirical data and the poor application of standardized sampling methods limit the understanding of the dynamic behaviour of plastics. Field measurements require expensive equipment and a multitude of people (van Emmerik et al., 2018). Research on the transport of plastic material along the riverbed is lacking but has been highlighted as an important area of riverine macro plastic transport (Morritt, Stefanoudis, Pearce, Crimmen, & Clark, 2014). The transport of plastic waste is complicated by the wide range of properties (size, shape and density) and changing conditions (wind, discharge and changing geometry and structures) (Kooi et al., 2018).

Buoyant macro plastics are a dominant polluter (Blettler et al., 2018) and understanding their cross-sectional distribution could provide areas of interest for monitoring and plastic extraction (Blettler et al., 2018). As measurements are expensive and time consuming (van Emmerik et al., 2018) it is desired to accelerate research with modelling techniques (Blettler et al., 2018). However, numerical modelling studies on riverine macro plastic transport are limitedly available as macro plastics have a range of properties and behaviour that is not well understood. Most modelling approaches focus on microplastics (Blettler et al., 2018) or model macro plastics homogeneously (Clara Chrzanowski, 2016)(Lammerts, 2016). Improved modelling of macro plastic transport can help understand and predict the cross-sectional distribution of buoyant macro plastics and identify areas of interest for monitoring or plastic extraction. This concludes to the following problem definition:

"As field measurements are expensive and time consuming it is desired to accelerate research with modelling approaches to identify areas of interest for monitoring or plastic extraction. Due to the range of macro plastic properties the understanding of macro plastic transport is limited. This hampers modelling approaches for riverine macro plastic transport."

1.3. RESEARCH SCOPE

This research focuses on the cross-sectional distribution of buoyant macro plastics in rivers and how this relates to macro plastic forces and river elements. The cross-sectional distribution is considered to be relevant for identifying areas of interest for monitoring and plastic extraction and to analyze behaviour. Buoyant macro plastics (densities lower than water) are a dominant marine polluter and increase the risk of flooding and river contamination. Therefore, the scope of this study is focused on buoyant macro plastics. Micro plastics and non-buoyant macro plastic transport are mentioned briefly.

Macroplastic behaviour is analyzed according to plastic characteristics (size and density) and river geometry and structures (riverbend, confluence, channel widening and groynes). To do so, rivers are analyzed in segments where small scale processes are treated limitedly and complete river basins are not considered. The effects of particle shape are neglected given the wide variety of shapes and its limited understanding. Plastics are modelled as spherical objects, neglecting rotation and orientation. Buoyant macro plastics are less sensitive to vertical mixing as opposed to non-buoyant material. For simplification purposes vertical mixing effects are neglected.

The numerical modelling uses Delft3D FLOW and D-WAQ PART. Delft3D is a powerful hydrodynamic model that can simulate 3D flow conditions. D-WAQ PART is a particle tracking module that is used in combination with the hydrodynamic output of Delft3D FLOW. Deltares is the owner of Delft3D FLOW and D-WAQ PART. This study is performed in collaboration with Deltares.

1.4. RESEARCH OBJECTIVE AND QUESTIONS

The following research objective is specified:

"Improve the modelling and understanding of buoyant macro plastic forces and their effect on the cross-sectional distribution of buoyant macro plastics in rivers"

To meet the research objective a number of research questions have been formulated and is listed below:

1. What are expected forces that drive buoyant macro plastic transport in rivers?
2. How can existing numerical modelling functionalities be used for the modelling of the cross-sectional buoyant macro plastic particle distribution in rivers?
3. What effects contribute to the cross-sectional distribution of buoyant macro plastics in rivers?

    (a) What is the effect of macro plastic characteristics (size and density)?

    (b) What are the effects of river geometry and structures?

    (c) What is the effect of external forcing (wind and discharge)?

4. How can the range of buoyant macro plastic behaviour in rivers be classified?
5. What areas along a river are of interest for macro plastic monitoring and the application of riverine plastic extraction?

1.5. COOPERATION WITH DELTARES

Deltares provides working space, laptop, access to its programs, necessary tools and personal guidance. The project was initiated based on a mutual interest in research of plastic pollution in the marine environment, following a meeting in December 2018. This master thesis is conducted independently of Deltares. Since current projects of Deltares align with the research topic cooperation is of mutual benefit. Deltares employees are experienced with plastic research and hydrodynamical and particle models, such as Delft3D, and therefore

provide an excellent work environment for this master thesis. Deltares provides a mentor *F. Buschman* during the time of research who is part of the thesis committee.

1.6. APPROACH

This study is divided into the following steps:

1. An exploratory study on existing research, methods for validation or verification and a theoretical background on turbulence in rivers and particle dispersion

2. Construction of a framework of buoyant macro plastic particle motion in rivers according to macro plastic characteristics and river elements

3. Analysis of the numerical models Delft3D FLOW and D-WAQ PART and translation of buoyant macro plastic characteristics into numerical parameters to model transport along a variety of river elements

4. Evaluation of research; providing a discussion, conclusion and recommendations

Figure 1.3 provides an overview of the four steps and their corresponding chapters.

EXPLORATORY STUDY
Goal: Provide theoretic background and methodology

- Chapter 2: Literature Study
- Chapter 3: Exploratory Study on Methods
- Chapter 4: Theoretical Background

FRAMEWORK ON BUOYANT MACRO PLASTIC PARTICLE MOTION
Goal: Develop a framework of buoyant macro plastic particle motion

- Chapter 5: Analytical Model
- Chapter 6: Flow Study

NUMERICAL MODELLING
Goal: Translate macro plastic transport into numerical modelling functionalities

- Chapter 7: Analysis on Numerical Parameters
- Chapter 8: Case Studies

EVALUATION
Goal: Present final discussion, recommendations and conclusions

- Chapter 9: Discussion and Recommendations
- Chapter 10: Conclusion

Figure 1.3: Overview of master thesis outline

I. EXPLORATORY STUDY

The goal of this step is to provide an overview of previous studies, explore available methods for developing validation or verification and provide theoretical background on river turbulence and particle dispersion.

The exploratory study consists of a literature study (chapter 2), an exploratory study on methods (chapter 3) and a theoretical background study (chapter 4). The literature study focuses on macro plastic characteristics (size and density), riverine transport, range of river elements, dynamics of particle motion and numerical macro plastic modelling studies.

In chapter 3, a variety of methods is analyzed for the development of a methodology. The range of methods is analyzed on their ability to provide validation or verification to the numerical model in step III. Methods that are excluded from the methodology are discussed as well. This, to describe their potential and required development for future riverine macro plastic research and prevent repeated work.

Chapter 4 provides background information on river turbulence and the relation between particle response times and particle dispersion. Particle response times provide a tool for describing relative particle motion. A theoretical background study is proposed to study the possibilities and limitations of translating riverine buoyant macro plastic transport (according to particle response times) from literature.

II. Framework of Buoyant Macro Plastic Particle Motion

The goal of this step is to classify and analyze riverine buoyant macro plastic transport for the development of a framework of buoyant macro plastic particle motion. These results are tested in step III.

To achieve the research objective first an improved description of buoyant riverine macro plastic transport is developed by constructing a framework of buoyant macro plastic particle motion, using an analytical model (chapter 5). Macro plastic transport is very complex and it is hard to translate behaviour into an analytical model. To simplify, a list of buoyant macro plastics types are developed and classified according to cornerstones in behaviour, e.g. dominance of buoyancy, massive particles and dominant added mass effect. Describing buoyant macro plastics according to cornerstones in behaviour is useful for formulating a framework in buoyant macro plastic particle motion and answering questions 1, 3(a), (c) and 4. Such a classification tool can help classify litter input in rivers and forecast its transport or identify monitoring locations in rivers that represent the litter input of a river.

The analytical model calculates the transport and response times for the macro plastic classes. The response times are used in step III to translate plastic particle transport into a numerical model. With the use of transport equations on wood and sediment a force model is constructed for buoyant macro plastics. A range of plastic objects, representative of each class, are used as input for the analytical model. This force model is used to analyze buoyant macro plastic transport drivers, the effects of macroplastic characteristics on buoyant macro plastic riverine transport and calculate particle response times. The analytical model delivers on question 1, 3(a) and (c).

Finally, a framework of buoyant macro plastic particle motion is constructed. This framework is used in the flow study (chapter 6) as a reference point for formulating hypotheses on buoyant macro plastic behaviour in a range of riverine environments. I.e. riverbends, channel widening, confluences and groynes. The hypotheses will be compared with the results of step III.

III. Numerical Modelling

The goal of this step is to translate the response time properties of each macro plastic class into numerical modelling functionalities (chapter 7). The performance of this translation is tested in chapter 8.

Numerical models are powerful tools for particle tracking. Successfully translation of macro plastic transport into a numerical model is useful for understanding and predicting plastic transport. This step answers research questions 2, 3(b), (c) and 5.

First, an analysis on numerical parameters is performed (chapter 7). The input parameters of Delft3D FLOW and D-WAQ PART are analyzed according to their relevance for simulating buoyant macro plastic transport (research question 2). A list of relevant parameters is proposed. A range of input values is attributed to each of the macro plastic classes, using the calculated response time (chapter 5) and its relation to dispersion. Finally, a case study is performed (chapter 8). A range of river elements, as proposed in chapter 6, is modeled in D-WAQ PART. The cross-sectional distribution of each buoyant macro plastics class, per river element, is analyzed compared with hypotheses from chapter 6 and results in chapter 5.

IV. Evaluation

The research is finalized in this phase. Chapter 9 provides the discussion and recommendations. Chapter 10 provides the final conclusion and delivers on the research objective and questions.

I. Exploratory Study

2

LITERATURE STUDY

2.1. CHARACTERISTICS OF MACRO PLASTICS

Research question 3(a) focuses on the relation between macro plastic characteristics and riverine macro plastic transport. A literature study was conducted on the characteristics traits of macro plastic material.

As described in Section 1.1, plastics consist of a wide variety of products, each with different shapes, sizes and densities/types (Kooi et al., 2018). Because of the large characteristic distribution, an attempt is made to define the range of properties according to these three key characteristics.

2.1.1. SHAPE

Plastics are used for a range of applications and vary greatly in shape. Limited information is available on the most dominant (macro) plastic shapes in rivers, hence it is complicated to construct a range of plastic shape properties and behaviour. Literature studies confirmed that the shape distribution of macro plastics is very large (Kooi et al., 2018). From personal experience, during macro plastic measurements in the rivers of Bali, it was found that most plastic litter consisted of plastic packaging and wrapping such as candy wrappers, plastic bags, bottle caps, water bottles and plastic cups (T. M. van Welsenes, van Utenhove, van Wijland, Memelink, & de Klerk, 2018).

2.1.2. SIZE

Plastic sizes range from > 10 cm fishing nets, bottles and plastic bags to < 100 nm nanosized plastic particles (Sascha Klein, 2018), and vary in behaviour. A variety of literature studies have identified different size classes for plastics. L. Lebreton et al. (2018) defined four different size classes for plastics; microplastics (0.05–0.5 cm), mesoplastics (0.5–5 cm), macro plastics (5–50 cm) and megaplastics (> 50 cm). Other studies defined nanoplastics from < 100 nm, < 1 μm to < 20 μm (Sascha Klein, 2018). Furthermore, González et al. (2016) defined macrolitter as > 2.5 cm, mesolitter as $0.5 - 2.5$ cm and microlitter as < 0.5 cm. For this research the latter size definitions are maintained.

2.1.3. DENSITY

The density range of plastics varies from 0.05 3 g/cm^3 for extruded Polystyrene (PS) and 1.4 g/cm^3 for Polyvinyl Chloride (PVC) (Kooi et al., 2018). However, considering only the most common produced plastics, the characteristic range is limited to 0.83 g/cm^3 to 1.37 g/cm^3. An overview of the most common produced plastics and their corresponding densities are displayed in Table 2.1.

Around 50% of the produced plastics have densities lower than water (< 1.0 g/cm^3) and consist of PP and PE. Examples are food packaging (PP), snack wrappers (PP), caps (PP) and reusable bags (PE) (*The Facts 2017*, 2017). PS has a density close to water ($\approx$ 1.0 g/cm^3)and consists of 6.7% of the total plastic production. "*Heavy Plastics*", such as PVC, PUR and PET have densities greater then water (>1.0 g/cm^3) and take up almost 25% of the total plastic production. However, PET is predominantly produced in the form of water bottles (*The Facts 2017*, 2017). An empty water bottle with a cap on will therefore have a much lower total density due to the entrapped air and show buoyant behaviour.

Resin	Symbol	Density (g/cm^3)	% of Market
Polypropylene	PP	0.83-0.85	19.3
Low-density Polyethylene	LDPE	0.91-0.93	17.3
High-density Polyethylene	HDPE	0.93 - 0.96	12.1
Polystyrene	PS	1.05	6.7
Polyvinyl Chloride	PVC	1.38	10
Polyurethane	PUR	1.20	7.5
Polyethylene terephthalate	PET	1.37	7.4

Table 2.1: Top produced plastic types in Europe (*The Facts 2017*, 2017) and their density (Andrady & Neal, 2009)

2.2. SOURCES AND SINKS OF PLASTIC IN RIVERS

To develop an understanding of (macro)plastic transport in rivers it is important to assess where it enters and leaves the system. The literature results are described in this section.

2.2.1. SOURCES

Most of the inflow or sources of plastics in rivers are land-based (Kooi et al., 2018) and are directly linked to human activity (Windsor et al., 2019). Wagner et al. (2014) proposed that roughly 70% to 80% of marine litter, of which most are plastics, originate from land-based sources and are emitted via rivers in the oceans. Potential sources for macro plastics in rivers are fisheries, beach litter, shipping activities, harbours and runoff from urban, touristic, agricultural and industrial areas. Microplastics are also emitted via waste water treatment plants. However, more research is required on these sources as little information is available on the amount and composition of (plastic) emission per source.

2.2.2. SINKS

Kooi et al. (2018) described a collection of source and sink processes. These are depicted in Figure 2.1 (a), a schematic impression of transport processes for synthetic polymers in rivers. The green circles indicate a source of plastics and red circles indicate (temporary) sinks. First an inflow of plastic material occurs, by any of the previous mentioned sources (see Section 2.2.1). During its lifetime through the river several processes result in (temporary) sinks of plastic. Beaching is the accumulation of plastics along the riverbank, entrapment is accumulation due to vegetation and/or structures and turbulent entrapment results from the formation of eddies. Eventually the plastic material will be emitted in to the sea (sink). Beaching and (turbulent) entrapment can function as sources as turbulence and flood events can re-introduce the plastics. Quantitative contributions for each of the sinks is not available and require more research.

(a) Schematic representation of source (green) and sinks (red) of plastics in rivers

(b) Schematic representation of settling, aggregation and bio-fouling
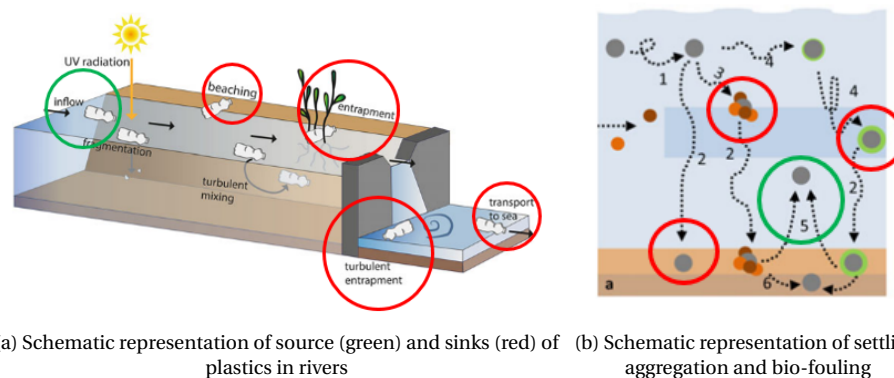
Figure 2.1: Sources and sinks along a river (Kooi et al., 2018)

Van Franeker (1985) and Rebolledo, Van Franeker, Jansen, and Brasseur (2013) discussed the occurrence of plastic ingestion in wild life. However, quantitative measurements are barely available. It is suggested to be negligible by Kooi et al. (2018), when considering macro plastic river transport.

2.3. River Geometries and Structures

A variety of geometric features and structures occur along a river. These features impact the hydrodynamic conditions and possibly the cross-sectional macro plastic distribution. This study provides an entry point for the Flow Study to analyze macro plastic behaviour along various river elements and is imperative for answering the third research question.

2.3.1. River Geometries

River bend

Rivers can have minimal curvature (straight) or high curvature. Curved channels induce helical flow patterns and become more pronounced for an increase in curvature (Huang, Jia, Hsun-Chuan, & Sam, 2009) (Ottevanger, Blanckaert, & Uijttewaal, 2012). Graf and Blanckaert (2002) described the typical cross sectional flow conditions that develop along a river bend, see Figure 2.2 for a schematization. Along the bend a centrifugal force operates towards the inner bank. This force is less towards the bottom, due to bottom friction, and higher at the top. As a result a circular movement in the flow develops which is referred to as a secondary flow (Einstein, 1926). Along the surface the flow is directed towards the outer bank and at the bottom flow is directed towards the inner bank. Near the outer-bank an outer-bank cell develops.
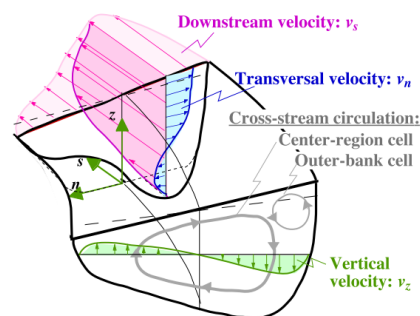
Figure 2.2: Schematic of flow in a river bend (Graf & Blanckaert, 2002)

Garcia et al. (2012) further schematized the flow patterns occurring through a meandering river. Figure 2.3 shows the schematization and five existing flow patterns. First, as the flow approaches the bend the flow starts to converge (1). Along the bend the velocity profile changes into a pool profile and at the same time a point bar (accumulation point of fine sediments due to low flow velocities) develops along the inner bend and a pool (local scour) develops along the outer bend (2). As the flow leaves the bend diverging of the flow occurs (3). Further downstream of the bend the velocity profile changes into a riffle profile (4). Finally, the flow approaches a new river bend. Here a bank embayment and helical flow pattern develop along the outer bend. A point bar accompanied by a gyre develop along the inner bend. Strongly curved channels induce a greater degree of helicity and lead to maximum pool scouring (large local erosion).

Channel Widening/Narrowing

Battjes and Labeur (2017) described unsteady flow in open channels. Local stagnant flows can develop due to angular profiles in the channel or at rounded changes where the curvature radius is too small. This is the case for channel widening and narrowing, where the changes in channel dimensions occur abruptly. A schematic of a channel widening is provided in Figure D.2 and a channel narrowing in Figure 2.5. The stagnant flow develops near/around the abrupt adjustment in channel width.

River Confluence

A river confluence consists of two rivers merging into a single channel, where the mainstream channel is the longest of the two and the tributary channel the shortest (Penna et al., 2018). In Figure 2.6 a river confluence and occurring flow patters are schematized. Penna et al. (2018) define six different flow patterns along the
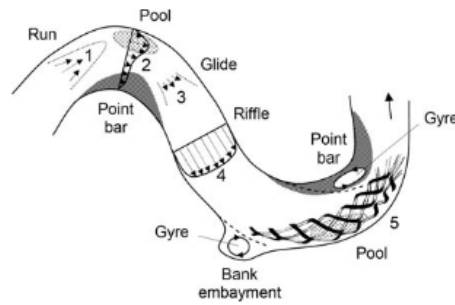
Figure 2.3: Schematic of a meandering river and occurring flow patterns (Garcia et al., 2012)
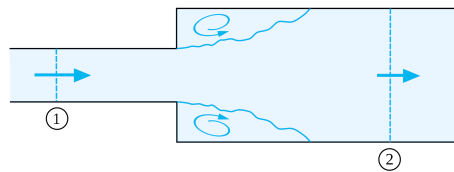
Figure 2.4: Schematic of a channel widening and occurring flow patterns (*Borda-Carnot Equation*, 2018)
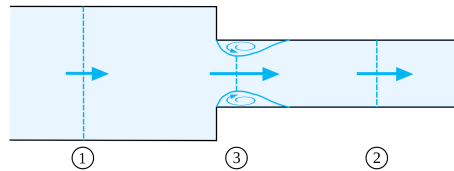
Figure 2.5: Schematic of a channel narrowing and occurring flow patterns (*Borda-Carnot Equation*, 2018)

river confluence. Stagnating flow develops in the upstream junction corner where flow velocities are strongly reduced. The formation of an eddie downstream of the junction is formed in the flow separation zone. The flow deflection zone, where both streams enter in the confluence. A maximum velocity zone downstream of the confluence. A Flow recovery area downstream of the confluence, where the flow no longer is affected by the disturbed hydrodynamics. Two dominant shear stress layers where the velocity gradients are the largest. The size and magnitude of each zone depends on factors, such as the geometry, junction angle, cross-sectional area and flow. Best and Reid (1984) suggested that the separation zone increases in correlation with the junction angle and discharge ratio between the main- and tributary channel. Shumate (1998) found that the separation zone varies in size along the water depth, where it is larger near the surface. Penna et al. (2018) suggest that an increase in junction angle results in a longer and wider stagnant zone in the upstream junction corner.
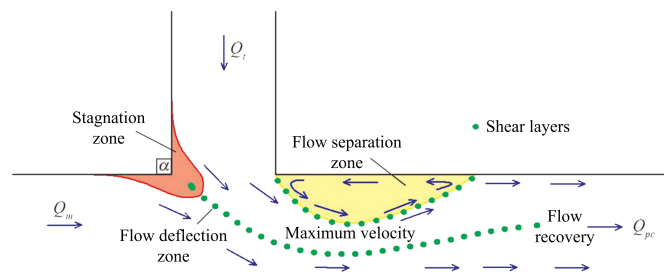
Figure 2.6: Schematic of a river confluence and occurring flow patterns (Penna et al., 2018)

2.3.2. River Structures

Groyne
Tingsanchali and Maheswaran (1990) provided a 2D depth averaged flow computation near a single groyne. A simple schematic of the effect of a groyne on the flow conditions in a river channel is shown in Figure 2.7. As the groyne obstructs the flow a recirculating zone occurs behind the groyne that circulates with the flow direction.
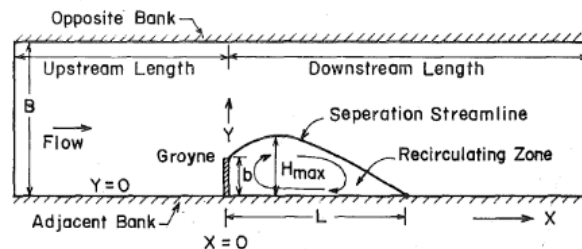
Figure 2.7: Schematic of a groyne in a river channel (Tingsanchali & Maheswaran, 1990)

Uijttewaal (2005) described the effects of a groyne layout on the flow in groyne fields. The primary function of groynes in the Netherlands is to maintain the mean velocity in the main channel sufficiently high. In addition stagnant zones develop in between the groynes. Figure 2.8 represents a graphic of flow conditions through a groyne field. The figure shows the development of large eddies in between the groynes.
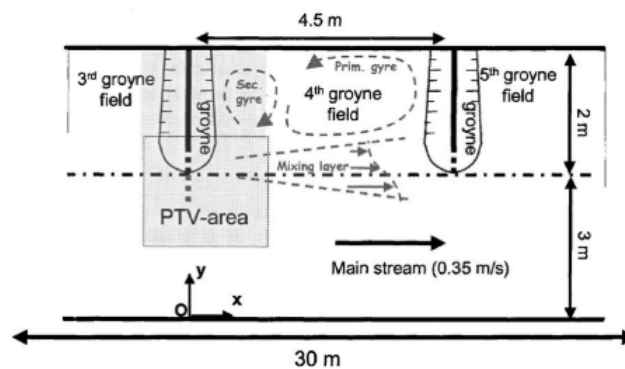
Figure 2.8: Schematic of flow conditions in a groyne field (Uijttewaal, 2005)

2.4. Macro plastic Transport in Rivers

To pursue the first and second research objective an understanding of the current knowledge on macro plastic transport in rivers, via a literature study, is necessary. Here, a distinction is made between external and intrinsic transport effects on macro plastic particles.

2.4.1. External Effects

Advective Transport
Ji (2008) noted the dominance of advective transport (transport by bulk motion) in rivers in the longitudinal direction. As a result macro plastic transport is driven by this advective transport. This downstream discharge is driven by gravitational forces as a result from the bed level gradient (Kooi et al., 2018). Flow velocities decrease near the riverbank and riverbed, see Figure 2.9 (a) and Figure 2.9 (b).

(a) Verticle velocity profile   (b) Horizontal velocity profile
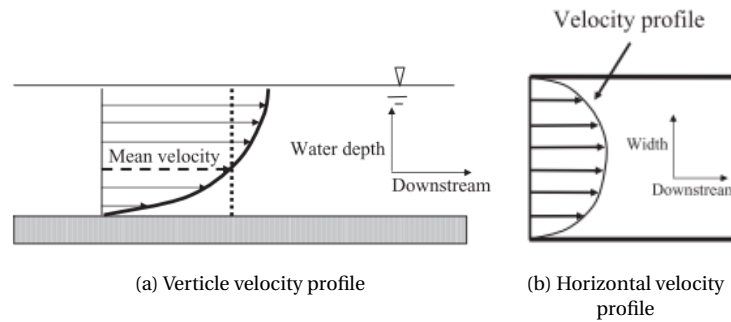
Figure 2.9: Velocity profiles of a river (Ji, 2008)

WIND

Kooi et al. (2018) described the importance of wind on floating macro plastic objects. Over time the wind tends to push these materials towards the riverbanks, resulting in beaching. Larger materials are subject to larger wind forces as their contact surface area increases. It is therefore expected that large materials are found near the riverbanks. Once the material is beached, they can re-enter the river during a flood event when the water level and discharge increase.

FRAGMENTATION

Fragmentation, or in other words degradation, heavily affects the fate of plastics as it changes the size and shape of the material. Fragmentation of plastics is dominated by four processes namely (Sascha Klein, 2018);

- Physical degradation (abrasive forces, heating/cooling, wetting/drying)
- Photodegradation (UV light interaction)
- Chemical degradation (oxidation, hydrolysis)
- Biodegradation by organisms

Often, synthetic polymers age because of environmental influences such as photo- and/or chemical degradation of additives which results in property changes and embrittlement. Weakening of plastic material makes them more subjective to frictional forces (physical degradation) causing further degradation creating microplastics or even nanoplastics. Degradation however is much slower than the residence time of most plastics in rivers (Kooi et al., 2018) and therefore this is expected to be of little relevance to plastic transport.

SETTLING

In Section 2.2 three settling processes were indicated, as described by Kooi et al. (2018). Two are a result of external conditions, namely aggregation and fouling. These are described below.

Aggregation is the attachment of particles to the transported (plastic) material and thus increasing its density. This can eventually result in sinking of plastic material and therefore manipulating its fate. Aggregation has a significant effect on smaller particles as the surface area to volume ratio is profoundly larger. As this study focuses on macro plastics aggregation is not considered.

Fouling is the attachment of bio-organics onto the transported substance. This increases the density overtime and can eventually lead to sinking as well. Again, smaller particles are more subjective to fouling and this process is therefore neglected in this study.

Depending on the density of macro plastics either the particles has a falling velocity (where the objects density is larger than the fluid density) or a rising velocity (where the object density is smaller than the fluid density). When neglecting turbulent flow conditions, high density particles tend to settle at the riverbed and low density particles tend to float at the surface level.

2.4.2. INTERNAL EFFECTS

Kooi et al. (2018) concluded that the great range of macro plastic properties will ultimately result in a wide variety of transport patterns for individual macro plastic particles. The density of a particle determines whether it is buoyant or non-buoyant. Floating debris is mainly transported by flow, while non-buoyant plastic debris is subject to advective, dispersive and settling processes. Larger items tend to catch more wind and accumulate on riverbanks or get caught by near shore vegetation.

2.5. MATERIAL TRANSPORT IN RIVERS

As there is limited literature on plastic transport, the study has been extended to include other materials in transport that have similarities with plastic transport. These consist of wood and sediment. For each of these materials the range of properties concerning shape, size and density are studied, for comparing purposes with plastics. Understanding these transport processes provides an entry point for developing a force model and assessing the first and second research question. For each material a summary is provided in this section. An extension of the literature study is provided in Appendix A.

2.5.1. WOOD

Wood transport is relatively well described and shows similarities in size and density with macro plastics.

WOOD CHARACTERISTICS

Braudrick et al. (1997) described that wood logs are cylindrical in shape and have length dimensions that can reach the river width. From this study a density range for wood types in Northwest-America was stated to vary between 392 kg/m^3 - 537 kg/m^3. Table 2.2 provides an overview of the different kinds of wood. A general overview of the characteristics concerning shape, size and density is provided in Table 2.3.

Classification	Density g/m^3
Douglas fir	0.54
Bigleaf maple	0.547
Western hemlock	0.51
Stika spruce	0.45
Old-growth redwood	0.45
Black cottonwood	0.39
Western red cedar	0.36

Table 2.2: Density of common wood species in Northwest-America with 12% moisture content (Braudrick et al., 1997) (Brown, 1974)

Density	Size	Shape
0.39 g/m^3 - 0.54 g/m^3	Order of metres	Cylindrical

Table 2.3: Property range of wood logs in rivers

TRANSPORT OF WOOD IN RIVERS

Braudrick et al. (1997) described the transport of large woody debris (LWD) in river channels. LWD can be transported by either debris flow or stream flow. Bigger streams are able to transport LWD further downstream where smaller pieces move further than larger pieces. This demonstrates the importance for piece length to channel width in wood log transport. The threshold for LWD transport is defined by the threshold of flotation. Depending on the density of wood the flotation threshold varies.

Braudrick and Grant (2000) described the movement of right-circular cylindrical logs in uniform flow, lying on a smooth immobile planar stream bed in rivers, using a force balance. When this balance is in equilibrium the log starts moving. Figure A.1 shows the force diagram of a cylindrical log lying parallel (Figure A.1 (a)) and normal to the flow (Figure A.1 (b)).

(a) Log lying parallel to flow   (b) Log lying normal to flow
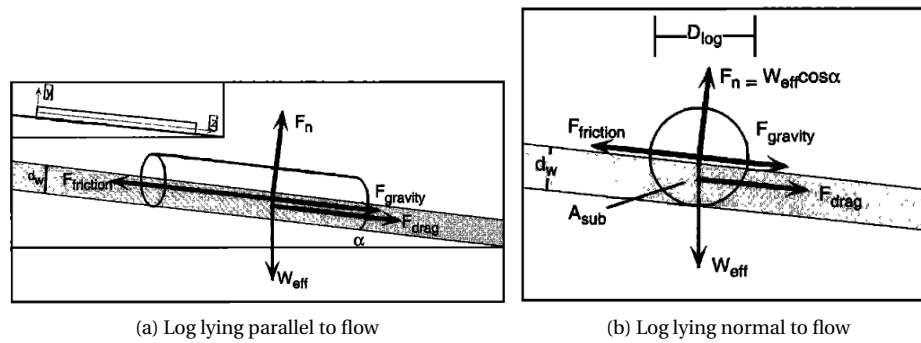
Figure 2.10: Log transport in a river (Braudrick & Grant, 2000)

2.5.2. SEDIMENT

SEDIMENT CHARACTERISTICS

Sediments often consist of fine particles but have been described relatively well. As some macro plastics are non-buoyant, similar to sediment, it provides a candidate for further review.

Wentworth (1922) described that sediment consists of a variety of materials, and therefore varies in size and density, and provided a range of solid particle size classifications for sediment transport. A range of sizes is described in Table 2.4. The density range of sediments is described in Table 2.5. Sediment particles are in general spherical or angular in shape. This information provides the property range of sediments as given by Table 2.6.

Classification	Size
Clay (fine to coarse)	0.24 - 4 μm
Silt (fine to coarse)	4 - 62 μm
Sand (fine to coarse)	62 - 2000 μm
Gravel (fine to coarse)	4 - 32 mm
Cobbles (small to coarse)	32 - 256 mm
Boulders (small to large)	256 - 4096 mm

Table 2.4: Size classifications of sediment particles (Wentworth, 1922)

Classification	Density
Clay/Silt	1600 - 2000
Sand	1500 - 1750
Gravel	1500
Stone	2250 - 3000

Table 2.5: Density classifications of sediment particles (Materialen, n.d.)

Density	Size	Shape
1600 kg/m^3 - 3000 kg/m^3	0.24 x 10^{-6} m - 4.096 m	Spherical or angular

Table 2.6: Property range of sediments in rivers

TRANSPORT OF SEDIMENT IN RIVERS

Bosboom and Stive (2015) pointed out that in still and clear water sediment particles accelerate up to a certain fall velocity and transport downwards until they settle at the riverbed. The fall velocity follows from a force

balance between the downward directed gravitational force (minus the buoyancy effect) and the upward directed drag force. Schulz, Wilde, and Albertson (1954) stated that the fall velocity of an isolated particle in water is influenced mainly by its size, shape and density. For particles with a density lower than water the buoyancy forces will dominate the gravity force and result in a rising velocity; as a consequence the drag force and gravity forces rotate 180°.

Armanini (2018) and Bosboom and Stive (2015) suggest that the flow regime surrounding a particle influences the experienced drag . Bigger particles are more likely to induce a higher Reynolds number, which results in a lower drag coefficient. In addition, the shape of a sediment particle effects the drag coefficient as well. Armanini (2018) described the effect of the shape factor on the drag coefficient. However, the shape factor does not describe the real conditions properly as natural particles are highly variable in their shape and size.

Particles that are settled on the riverbed only transport when the exerted shear stress by the water movement is large enough. When a certain threshold is reached, the critical shear stress, the particle initiates motion (Bosboom & Stive, 2015).

2.5.3. OIL

Oil is a buoyant material and is affected by wind transport, similar to macro plastics, and therefore provides a candidate for further study.

OIL CHARACTERISTICS

In Table A.1 the density is given for various types of crude oil (*Engineering Toolbox*, 2019). The range of properties is described in Table A.2. As shape and size are not applicable to a fluid such as oil only a density value is provided.

Classification	Density kg/m^3
Crude oil 48° API	790
Crude oil 40° API	825
Crude oil 35.6° API	847
Crude oil 32.6° API	862
Crude oil, California	915
Crude oil, Mexican	973
Crude oil, Texas	873

Table 2.7: Density of various types of crude oil (*Engineering Toolbox*, 2019)

Density kg/m^3	Size	Shape
790 - 973	-	-

Table 2.8: Property range of oil

TRANSPORT OF OIL IN RIVERS

Shen and Yapa (1988) used a computer model to model oil slick transformations in rivers. It is suggested that advective transport due to flow is dominant in rivers over wind, especially in the longitudinal direction. Horizontal diffusion of oil in rivers is mainly dependant on the shear velocity, depth of flow and wind condition. The mechanical spreading of oil in open water is dominated by gravitational, viscous and surface-tension forces.

As mathematical descriptions of oil are difficult to translate to macro plastic behaviour, oil is not used in the analytical model.

2.6. PARTICLE DYNAMICS OF MOTION

To understand the transport of macro plastic particles a basic understanding of particle dynamics is desired. In this topic important equations on particle dynamics of motion are studied and coupled to macro plastic transport.

2.6.1. MAXEY-RILEY EQUATION

From the literature study two particle dynamics equations are found, namely the Basset-Bousinesq-Oseen Equation (BBO) and the Maxey-Riley equation (Zhu, 1998) (Cartwright et al., 2010). Both equations describe the particle trajectories relative to flow. The Maxey-Riley equation is preferred over the BBO equation as the Maxey-Riley equation describes the trajectory of a finite-size particle. The Maxey-Riley equation, as formulated by Cartwright et al. (2010), describes the particle trajectory for small spherical particles with low Reynolds numbers, see Equation 2.1 and 2.2.

$$m_p a_p = \underbrace{m_f \frac{D}{Dt} U_f}_{\text{term 1}} - \underbrace{\frac{1}{2} m_f \left(a_p - \frac{D}{Dt} \left[U_f + \frac{1}{10} a_f^2 \nabla^2 U_f \right] \right)}_{\text{term 2}}$$

$$- \underbrace{6\pi a_f \rho_f \nu_e q(t)}_{\text{term 3}} + \underbrace{(m_p - m_f) g}_{\text{term 4}} - \underbrace{6\pi a_f^2 \rho_f \nu_e \int_0^t d\tau \frac{dq(\tau)/d\tau}{\sqrt{\pi \nu_e (t - \tau)}}}_{\text{term 5}} \tag{2.1}$$

$$q(t) \equiv U_p(t) - U_f(t) - \frac{1}{6} a^2 \nabla^2 U_f \tag{2.2}$$

When looking at Equation 2.1 multiple terms can be identified. The first term on the right side of the equation is the acceleration term and describes the force exerted on the particle by the flow. The second term describes the added-mass effect. The third term is Stokes drag as a result of the fluid viscosity. Stokes drag holds for small particles with low Reynolds numbers. This does not hold for macro plastic The fourth term describes Stokes drag due to the buoyant force. The final integral term is called the Basset-Bousinesq history term. The terms with the factor $a^2 \nabla^2$ are called the Faxén corrections and account for spatial variation of the flow field across the particle.

Macro plastic particles are not small and do not induce low Reynolds numbers. Therefore, Stokes drag can be neglected (term 3). For further simplification the Basset-Bousinesq history term is neglected as it is difficult to implement. The Faxén corrections are not relevant for macro plastic particles as the spatial variation of the flow field is small compared to the particle diameter. This leads to a simplified formulation of the Maxey-Riley equation where drag forces, added mass and buoyant forces are included, see Equation 2.3. This simplified formulation for the Maxey-Riley equation is used in chapter 5 to calculate buoyant macro plastic particle trajectories.

$$m_p a_p = \underbrace{m_f \frac{D}{Dt} U_f}_{\text{term 1}} - \underbrace{\frac{1}{2} m_f \left(a_p - \frac{D}{Dt} U_f \right)}_{\text{term 2}} + \underbrace{(m_p - m_f) g}_{\text{term 4}} \tag{2.3}$$

2.6.2. OTHER FORCES

LIFT FORCE

Yang, Hou, Wang, Lin, and Fu (2012) described the effect of the Saffman lift on moving particles in a microchannel. The lift force pushes a particle towards the centre of the channel if the particle speed is lower than fluid speed ($U_p < U_f$). The particle is pushed towards the wall if the particle moves faster than the fluid speed ($U_p > U_f$). Li and Ahmadi (1992) noted that the Saffman lift force is restricted to small particle Reynolds number and is therefore assumed to be only relevant for sub-micron particles. Therefore, for this study the Saffman lift force is neglected.

Another lift force is the Magnus force. When a ball rotates in the clockwise direction flow accelerates along the top while flow below the particle is slowed down. This results in a pressure difference. Hence, a lift force

develops. The resulting pressure force can be described according to Equation 2.4. As rotation is neglected in this study the Magnus force is not included.

$$F_{Magnus} = \Delta p A \tag{2.4}$$

PRESSURE FIELD

Bahrami (2009) describes the pressure gradient force on an arbitrary fluid with size $\Delta x, \Delta y$ and Δz. The pressure gradient force is a result of the local fluid pressure gradient around the particle. The net pressure in the x-direction is given by Equation 2.5. This is similar to the net forces acting in the y- and z- direction. Combing the pressure force in all directions results in Equation 2.6. In a river channel the pressure gradient is directed downstream and is responsible the for the developing flow velocity (von Planta et al., 2018).

$$dF_{x,press} = p\,dy\,dz - \left(p + \frac{\delta p}{\delta x}dx\right)dy\,dz = -\frac{\delta p}{\delta x}dx\,dy\,dz \tag{2.5}$$

$$F_{press} = -\nabla p \tag{2.6}$$

2.6.3. PARTICLE RESPONSE TIME

The particle response time describes the particle responsiveness towards the flow regime. Therefore, the particle response time is considered to be a relevant parameter for defining relative motion between a particle and the flow. It is desired to describe buoyant macro plastic particle transport according to particle response times to formulate how they behave relative towards the flow and different macro plastic objects. In chapter 5 calculations are made on response times for buoyant macro plastic particles.

For a submerged particle the particle response time is described according to equation 2.7 (Schwarzkopf, Sommerfeld, Crowe, & Tsuji, 2011). The particle response time is dependant on the density (ρ_p), particle diameter (d_p) and the fluid dynamic viscosity (μ_c). This study focuses on buoyant macro plastic particles which are emerged. As a result, the relation between particle response times and size/density changes. This is further discussed in chapter 4.

$$\tau_p = \frac{\rho_p (d_p)^2}{18\mu_c} \tag{2.7}$$

2.6.4. STOKES NUMBER

The Stokes number characterizes the relative particle transport to the flow in a turbulent environment and is calculated by dividing the particle response time with the characteristic time of the flow. A visualization of particle transport along an eddie and how this relates to different values for the Stokes number is visualized in Figure 2.11. Equation 2.8 describes the Stokes number, where τ_p is the particle response time and τ_e is the eddy timescale (Finlay, 2019). The eddy timescale represents the amount of time a particle travels within an eddy. This value changes according to the mean flow velocity (U_m) and the characteristics length of the eddy (δ), see Equation 2.9.

If $Stk >> 1$, the particle is dominated by its inertia and tends to follow its initial trajectory. For low stokes numbers $Stk << 1$, particles tend to follow the fluid trajectory closely. Behaviour of particles with stokes numbers close to one $Stk \sim 1$ is a lot more complicated as small changes in relative motion towards the flow can have a large effect on the particles transport (Piccinini, 2011) as particles can shoot out of the eddy. This is displayed in Figure 2.11. How this relates to riverine buoyant macro plastics transport is discussed in chapter 4.

$$Stk = \frac{\tau_p}{\tau_e} \tag{2.8}$$

$$\tau_e = \frac{\delta}{U_m} \tag{2.9}$$
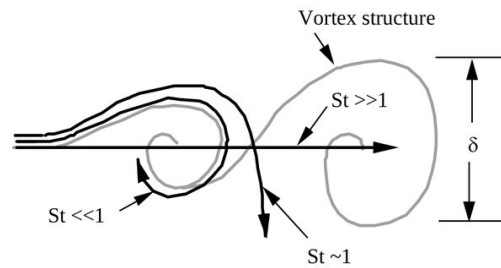
Figure 2.11: Particle trajectory compared with flow for various Stokes numbers Piccinini (2011)

2.7. NUMERICAL MODELLING OF MACRO PLASTIC TRANSPORT

Numerical models can provide an efficient tool to analyze complicated transport processes of macro plastics in rivers. Existing numerical functionalities are used in this research. Hence, a literature study on numerical modelling approaches of macro plastic transport follows. Note that these studies use passive tracer assumptions for the modelling of macro plastics. Relating to transport of wood and sediment the tracer assumption does not always hold, as is expected for buoyant macro plastics. This study imposes to improve on the passive tracer assumption and model relative particle motion towards the flow.

Blettler et al. (2018) described that studies on macro plastics are scarce and are often focused on oceanic environments, despite the importance of rivers as marine polluters. It is suggested that a limited amount of modelling studies towards macro plastic transport in rivers are available.

A few studies on the modelling of macro plastic transport in rivers have been performed. In 2016, a study performed by Clara Chrzanowski (2016) analyzed the effects of wind and emission locations on the formation of hotspots in the Port of Rotterdam with use of the particle model Delft3D PART by performing a passive tracer simulation. They concluded that the wind was a dominant factor in the formation of accumulation spots in the Port of Rotterdam. Figure 2.12 shows that for South-West wind conditions (ZW) the hotspots form predominantly in northern banks and branches of the river, whereas for North-East wind conditions (NO) the hotspots occurred mainly in the southern branches of the river.
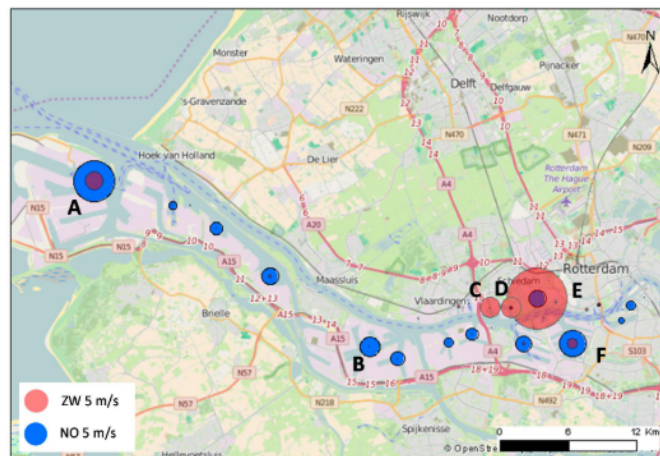
Figure 2.12: Formation of plastic hotspots in the Port of Rotterdam (Clara Chrzanowski, 2016)

Another study by Lammerts (2016) discusses the dynamic movement of marine litter in the Port of Rotterdam using Delft3D PART model and the passive tracer assumption as well. Six different scenarios where modeled, where variations where made on the application of wind, surface litter and submersed litter. Also, the effects of the tide are analyzed. He concluded that the wind was a dominant factor for marine litter at the surface level, but the river flow was dominant for submersed litter. Tidal ranges seemed to have little effect on the marine litter distribution inside the port.

3

EXPLORATORY STUDY ON METHODS

The goal of the exploratory study on methods is to identify validation and verification tools for the numerical model in step III.

Through a literature study and interviews with colleagues a list of potential methods was constructed. Literature studies outside the scope of plastic transport are used, as the variety of methods applied in plastic transport research remains limited. To consider a method for use, it is required to provide a tool for verification/validation of the numerical model output and/or answer one of the research question. Verification/validation methods vary from providing data on distributions of buoyant macro plastics in rivers and provide physical verification according to particle forces and hydrodynamics.

Each of the potential methods were reviewed. A hypothesis was defined for each of the methods to display its goal and use. A feasibility study is performed on the methods; analyzing whether the method is capable to yield results that satisfy the stated hypothesis. Concluding from the feasibility study a final methodology is proposed. Each method is graded on its performance according to multiple requirements. The grading is further explained in Table 3.1. Methods not included in the methodology are discussed as well, to inform the reader on a range of methods and requirements for future use.

Score	Relevance to research questions	Provides validation/verification	Resource costs
++	Delivers on multiple research questions	Good validation/verification	Very low resource costs
+	Delivers on a research question	Moderate validation/verification	Low resource costs
-	Limited delivery on research question	Limited validation/verification	Moderate resource costs
- -	Does not deliver on research questions	No validation/verification available	High resource costs

Table 3.1: Formulation of criteria for constructing methodology

3.1. Results

3.1.1. List of Methods

Using interviews and a broader scope of literature studies a more elaborate list of methods is constructed, see 3.2. A brief description and analysis for each of the methods is provided in Section 3.1.3.

Method	Source
Analytical model	Braudrick et al. (1997), Bosboom and Stive (2015)
Flow study	Graf and Blanckaert (2002),
Web-scraping tool	*Martha Larson, Radboud University*
Drone image analysis	Tauro, Porfiri, and Grimaldi (2016), Garcia et al. (2012)
Satellite image analysis	Goddijn-Murphy, Peters, Van Sebille, James, and Gibb (2018)
Field measurements	van Emmerik et al. (2018)

Table 3.2: List of suggested methods

3.1.2. Methodology

The list of methods is reduced to a methodology. Figure 3.1 shows a schematic of the constructed methodology.
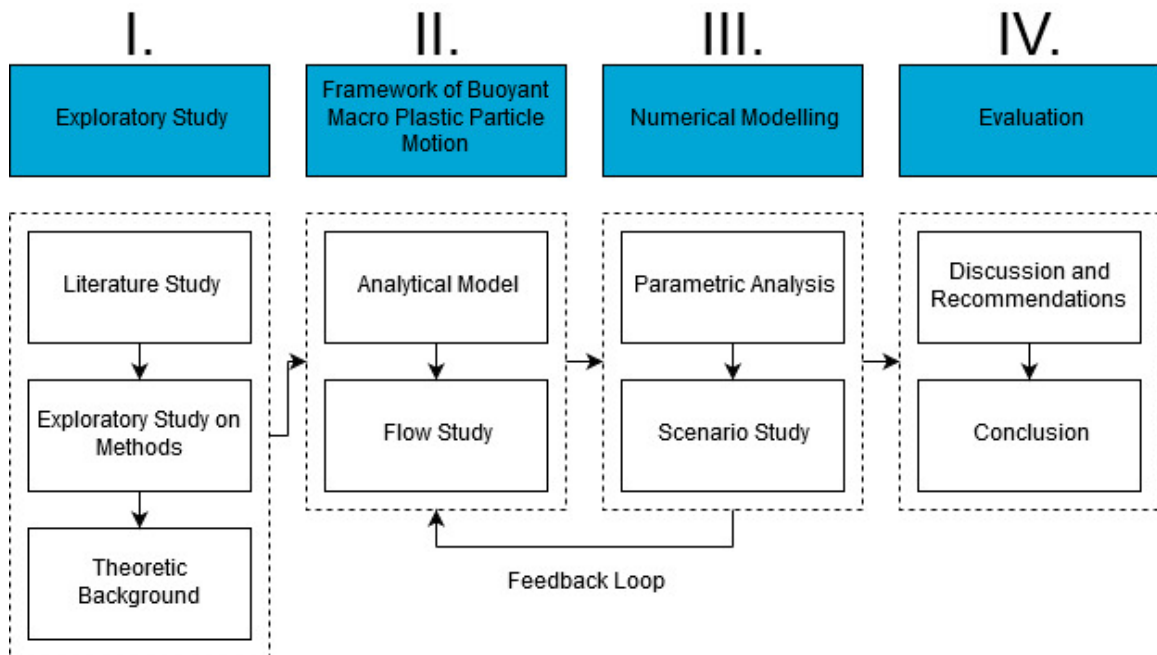
Figure 3.1: Schematic of the methodology

3.1.3. Feasibility Study

ANALYTICAL MODEL

With an analytical model the following is implied; a study on wood and sediment transport to build a transport model of macro plastic transport. The analytical model can be used to identify and study important forces for macro plastic transport in rivers and deliver on research question 1, 3(a) and (c) and can function as a verification tool for the numerical model. This results in the following hypothesis:

> *"Transport models of materials with corresponding properties to macro plastics can be translated to model buoyant riverine macro plastic transport and describe the driving forces for verification of the numerical modelling output"*

The analytical model is useful for describing driving macro plastic forces and verification of existing numerical model functionalities while the resource costs are relatively low, i.e. there is no need of extensive equipment or manpower.

FLOW STUDY

The flow study analyzes flow patterns, induced by a variety of structural or geometrical elements in a river, and their effect on the cross-sectional macro plastic distribution. This delivers on research question 3(b). This can function as a verification for the numerical modelling of river geometry and structures and their effect on the cross-sectional macro plastic distribution. This is summarized in the following hypothesis:

> *"A study on hydrodynamic conditions induced by river geometries and structures can be used to describe the cross-sectional distribution of macro plastics in rivers for verification of the numerical model"*

The flow study provides verification and resource costs are low.

WEB-SCRAPING TOOL

A web-scraping tool can generate a large image dataset of plastic in rivers using a keyword list, machine learning and online image databases, such as Tumblr, Google Images and Instragram. The web-scraping tool auto selects images from the internet, building up an image database. This image dataset of plastic pollution in rivers can help to validate modelling results. A classification tool can be used to classify these images according to certain behaviour. For example, plastic accumulation near structures or riverbanks. As such the following hypothesis is stated for using a web-scraping tool:

> *"By generating and classifying large image datasets from the web consistent behaviour of plastics in rivers can be identified and used for validation of numerical modelling output"*

The effectiveness of a web-scraping tool remains uncertain as it is unclear how accurate the output of the model is. Therefore, a small sample test is performed. As a start the keywords *"plastic river"* were tested in the search engine of the online image databases. Depending on the accuracy of the required data the keywords can be either included into a list of sufficient keywords or discarded. In case of sufficient accuracy of the output the keyword list can be expanded using the supplementary keywords provided from the accurate images. Slowly the list can be expanded while the dataset grows. In Appendix B.1 the first 18 generated images (out of 92) are shown using the keyword *"plastic rivers"*. When looking at these images it is clear that an abundance of plastics is visible, but it remains difficult to classify these images on behaviour.

Development of a web-scraping tool is complicated while the resulting database is often biased, towards either showing or deliberately not showing plastics, and the image quality is very inconsistent. Pictures of plastic pollution are found to be focused on a dramatic portrayal of the plastic pollution, often used for shock effect or creating awareness. On the other side, a lot of pictures are deliberately not including plastic pollution as it also *"pollutes"* the idyllic tourist photos.

DRONE IMAGE ANALYSIS

Drone images provide aerial pictures of rivers. Pictures from plastic polluted rivers can be used to analyze macro plastic transport and the role of river structures and geometry. The spatial and temporal resolution is very high when compared to satellite images. Drone images can be used for validating the numerical modelling output. The image dataset can be used to identify areas that show longer retainment, which suggest interesting behaviour occurs. E.g. river structures can cause plastic flocks to develop. With access to an image database of flock development near multiple rivers structures consistent behaviour can be identified. This is interesting for delivering on research question 3(b) and 5. The following hypothesis is formulated for using a drone image analysis as an indicator for the effect of river elements on macro plastic transport:

> *"Drone images that show longer retainment of marine litter in a river indicate areas with high macro plastic concentrations and impose areas of interest and can function as validation for numerical modelling output"*

Via a research from Radboud University *Frank Collas* a public drone image database was suggested called the Open Aerial Map. When using the Open Aerial Map no decent and consistent public drone images of rivers where available.

SATELLITE IMAGE ANALYSIS

Similar to drone images, satellite images can be used to analyze formation of plastic flocks along river structures or bends. Again, this provides validation for the numerical modelling output. Satellite images of rivers are publicly available and therefore provide a good alternative to drone images. Similar to drone image analysis the hypothesis is stated as follows:

> *"Satellite images that show longer retainment of marine litter in a river indicate areas with high macro plastic concentrations and impose areas of interest and can function as validation for numerical modelling output"*

To properly assess the satellite images as a tool for analyzing macro plastic transport a variety of spectral bands are tested. A proper processing tool is required. Via an interview with *Ellis Penning* from Deltares two tools where identified that provide a large online open-source data-set of satellite images and the necessary processing tools, namely the Google Earth Engine and Sentinel-Hub. The Google Earth Engine is used as it includes a coding application.

A variety of satellite image databases are available. The Sentinel-2 Level-1C is chosen as it has the highest spatial resolution of to 10 metres per pixel and includes a spectral band from B1 - B12. The database covers most of the earth and the records date back to June 25, 2015 with a revisit interval of 5 days. The USGS Landsat satellites provide good alternatives as they provide old records from July 23, 1972 for the Landsat 1. However, the spacial resolution (30 - 60 metres per pixel) and spectral bandwidth (B4 - B7) are limited. The newest Landsat 8 has a maximum spatial resolution of 15 metres per pixel, under-performing to the Sentinel-2 Level-1C.

Goddijn-Murphy et al. (2018) proposed that the visible spectrum (VIS), consisting of spectral bands B4, B3, B2, and the short wave infrared spectrum (SWIR), consisting of spectral bands B12, B8A, B4, are both suitably for hyperspectral remote sensing of macro plastic transport in rivers. Interviews with *Ellis Penning* from Deltares pointed towards a third option, the normalized difference water index (NDWI).

Analyzing images using the VIS, SWIR and NDWI spectra showed a limited ability to allocate transport. Figure 3.2 and B.3 show examples of VIS, SWIR and NDWI spectral images of the Saigon river in Vietnam, a known plastic polluted river (van Emmerik et al., 2018). Appendix B.2 provides a closer look of the satellite images. When using the SWIR spectrum the spacial resolution decreases, as the spectral bands B12 and B8A only have a resolution of 20 metres per pixel as opposed to 10 metres per pixel for the VIS spectrum. The NDWI improved the visuals as dirt streams are more visible. The dirt stream might indicate flow behaviour, but not much can be said on its relation to macro plastic transport. In addition, no retainment/accumulation of marine litter is

visible. Therefore, a higher spatial resolution is advised to distinguish accumulation patterns via a satellite image analysis.

(a) Satellite image of the visual spectrum (VIS)

(b) Satellite image of the short wave infrared spectrum (SWIR)

Figure 3.2: Satellite image processing of the Saigon river, Vietnam with the Google Earth Engine

FIELD MEASUREMENTS
Field measurements provide actual data on macro plastic concentrations in a river. These could provide a tool for validating numerical simulations. Depending on the measurement location and surrounding river elements, the distribution of plastic concentrations can be correlated to hydrodynamic effects of river geometry and structures (research question 3(c)). In case data is available on environmental conditions, i.e. wind and discharge, their impact on the transport and concentration distribution of macro plastics can be analyzed as well. This delivers on research question 3(b). As such the following hypothesis is constructed:

"Actual measurements on macro plastic concentrations could identify effects of river geometry, structures, wind and discharge and will help to validate and calibrate the numerical modelling approach"

Field trips are costly (concerning the required manpower, time and money) and no consensus on a universal measuring method has yet been developed.

3.1.4. GRADING OF METHODS
Table 3.3 shows the grading of each method. Each method is graded on their performance concerning research questions, validation/verification and resource costs. The analytical model, flow study and numerical modelling are included in the methodology.

3.2. DISCUSSION
The web-scraping tool is an interesting method for developing a large database. Due to the complexity of the program and low reliability it is not a desired tool. *Globalalert.org* is a newly developed tool that allows its users to allocate aquatic trash sites in a Global Alert Map and upload photos of these areas (Globalalert, 2016). The web-scraping tool concept could improve significantly in its effectiveness when it has access to the Globalalert database or a similar database. If possible, via machine learning, the database can be used

Method	Relevance to research questions	Provides validation/verification	Resource costs	Final
Analytical model	++	++	++	✓
Flow study	+	++	++	✓
Web-scraping tool	-	-	++	X
Drone image analysis	+	- -	+	X
Satellite image analysis	+	-	++	X
Field measurements	+	++	- -	X

Table 3.3: Final grading of methodology

to classify the plastic content, estimate quantity, identify aquatic environment and correlate this to weather, period and location.

Satellite images could provide an effective tool for analyzing marine debris over large river sections, but spatial and temporal resolutions remain relatively low which make it very difficult to identify any litter behaviour. In addition, studies on spectrum band analysis of plastics are still developing. If access is available to satellite images with higher temporal and spatial resolution using satellite images as a tool for analyzing litter transport in rivers can provide an efficient tool. However, the spatial resolution of satellites is expected to remain a limiting factor as the current maximum resolution is around 0.46 metres per pixel with the GeoEye-1 Satellite (Sat-Imaging, 2017) and is not publicly available. As such, only large objects or collections of litter are observable. Therefore drone imaging, with higher spatial and temporal resolutions, suggest to be a more effective tool.

3.3. Summary and Conclusion

In riverine macro plastic studies the variety of methods applied and the availability of validation/verification tools are very limited. Field measurements are being performed but the data is very protected while measurements cost a lot of resources. This hampers marine plastic pollution studies. A wider variety of methods could improve research and validation/verification for numerical modelling output. Therefore a list of potential methods is constructed and a feasibility study is performed. This results in the construction of a methodology as depicted in Figure 3.1. The grading of each method is displayed in Table 3.3. A variety of methods did not make the cut and require either technical improvements in the future or extensive amount of resources outside of this research capabilities. These "*failed*" methods are discussed as well in this chapter, as macro plastic transport research is relatively new and an improved understanding of what methods are available, why certain methods are chosen and how specific methods should improve for future use is relevant. Such information can hopefully prevent new research projects to follow through the same setbacks as were found in this research.

Several methods did not make the cut and are discussed. Field measurements can provide relevant validation data. A variety of organizations are involved in field measurements of macro plastic transport in rivers but this data is not publicly available. As field measurements cost a lot of resources it is beneficial for future studies to have data on plastic measurements, for example trawling studies of plastics along the rivers cross-section, to be publicly available.

Web-scraping tools can generate large image datasets, using machine learning. These images might poses information on certain behavioural patterns of macro plastic. As limited validation data is available, such databases might be very valuable in the future. In the feasibility study it was found that currently most images are biased, inconsistent and difficult for interpreting behaviour. However, image databases focused on marine plastic pollution are growing, e.g. *Globalalert.org*. These provide a good start for developing an image web-scraping tool for macro plastic transport.

Drone images provide high spatial and temporal resolution and can provide validation data, by constructing images of plastic transport in highly polluted rivers along a variety of river elements. Public drone images of highly polluted rivers are limitedly available and therefore this method is not included in the methodology.

With personal access to a drone, using drone images analysis can be useful for developing validation data and understanding of plastic transport as the user has full control of the image development.

Satellite images are publicly available and can provide useful validation data, but have a significantly lower spatial and temporal resolution compared to drone images. A variety of spectral bands have been tested but no strong cases could be made. Higher spatial (> 10 m per pixel) and temporal resolutions (> image per 5 days) are preferred for future research. Using Sentinel and Landsat public databases were not useful for analyzing the transport of plastic objects and the development of validation data.

4

THEORETICAL BACKGROUND ON PARTICLE DISTRIBUTION

The goal of this chapter is to provide theoretical background on the relation between the Stokes numbers, particle diffusivity and river turbulence and to analyze how this translates to buoyant macro plastic particles. The background study is divided into three sections.

1. Provide background information on turbulence and the effects of Stokes numbers on the particle distribution

2. Determine implications and required assumptions for translating particle diffusion to riverine macro plastic transport

3. Determine how particle diffusivity can be translated into the particle tracking model D-WAQ PART

4.1. RESULTS

In a straight channel with laminar flow macro plastic particles are transported similarly to a passive tracer and motion with the flow. Differences in transport between the range of macro plastic particles is small. When turbulence is included the transport of particles is disrupted. Considering the range of macro plastic properties its behaviour becomes diverse. Ideally, understanding the relative transport of a macro plastic particle between the flow and other macro plastic particles in these turbulent environments will greatly improve the understanding and development of modelling approaches for macro plastic transport. Previous studies on particle transport along eddy structures in rivers are therefore analyzed.

4.1.1. DEFINITIONS

Before providing a theoretical background study the definitions of dispersion and diffusivity used in this study are briefly introduced. Figure 4.1 shows an initial release of particles on the left which are transported downstream towards the right.
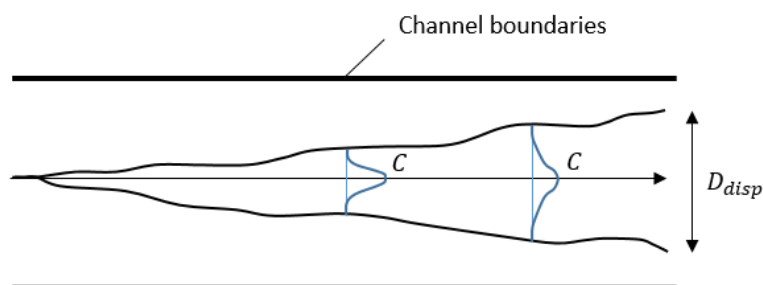

Figure 4.1: Top-down view of channel and the particle diffusion

Concentration: Symbol C represents the particle concentration in kg per m^3. The particle concentration has a Gaussian distribution. The particle concentration peak decreases when travelling downstream.

Particle diffusion: Motion of particles from a high concentration to a lower concentration. In this study only buoyant macro plastics are considered and vertical transport processes are neglected. When considering diffusion of macro plastic particles only diffusion along the free-surface plane in the transverse channel direction is considered. Figure 4.1 shows how the particle concentration decreases downstream. This behaviour is defined as particle diffusion.

Particle dispersion: Particle dispersion is a result of the diffusion process and is a measure for the spreading of the particle cloud in metres. This study focuses on transverse particle dispersion as displayed in figure 4.1 with symbol D_{disp}. When mentioning particle dispersion in this study, transverse dispersion is considered unless mentioned otherwise.

4.1.2. GENERAL FEATURES OF PARTICLE DISPERSION IN TURBULENCE

First work that related diffusivity to statistical properties of homogeneous turbulent flow was performed by Taylor (1922). Taylor described a diffusivity relation according to Equation 4.1.

$$D = u^2 \delta \tag{4.1}$$

u^2 is the mean square velocity in the transverse direction to the flow and δ is the Lagrangian time scale. *Taylor* studied the diffusivity of a fluid particle, but successive studies by Snyder and Lumley (1971) proposed its application for calculating particle dispersion. Soo (1967) reported that the ratio of particle diffusivity to fluid diffusivity is always less than one and that it depends on the ratio of Lagrangian to Eulerian turbulent length scales. This relation is provided by Equation 4.2.

$$K = \frac{\rho_p d_p^2 18 \mu_c}{\delta \sqrt{u^2}} \tag{4.2}$$

ρ_p is the particle density, d_p is the particle diameter, μ is the dynamic viscosity and $\sqrt{(u^2)}$ is the root mean square of the turbulent fluctuations. The numerator is identified with the particle response time (τ_p) and the denominator is defined as the fluid characteristic time or eddy timescale (τ_e). In short, the particle response time is the responsiveness of the particle to a change in fluid velocities. The fluid characteristic time or eddy timescale is the time available for eddy-particle interaction. Hence, the formula represents a general definition of the Stokes number in Equation 4.3.

$$Stk = \tau_r / \tau_e \tag{4.3}$$

Peskin's study suggest that large Stokes numbers imply that the particle does not have enough time to respond to the turbulent fluctuations. Hence, the particles trajectory is dominated by its own inertia. A low Stokes number suggests that the particle responds almost instantly to the turbulent fluctuations and strictly follows the fluid motion. Reeks (1977) assumed a linear drag and body force acted on the particle. *Reeks* showed that particle diffusion increases with particle size and exceeds the dispersion of a fluid particle. This results from the fact that particle dispersion is proportional to the root mean square of particle velocity fluctuations and particle Lagrangian time scale (Equation 4.1).

Brown (1974) identified that free shear flows are characterized by large-scale turbulent structures. Small-scale turbulence may cause local diffusion but the primary source of dispersion follows from these large-scale turbulent structures. Singamsetti (1966) provided a first suggestion of the physical effects of the large-structures on particle motion (in this study a sediment particle) and dispersion. *Singamsetti* explained that the circulatory nature of eddies can cause sediment particles to be thrown out of the eddy due to inertial effects. This resulted in larger and faster lateral spreading of sediment compared to the flow. Successive studies by Householder and Goldschmidt (1968) and Yule (1981) confirmed the statement by Singamsetti when analyzing the dispersion of oil droplets and air sprays. Yule added on *Singamsetti's* physical model and concluded the following:
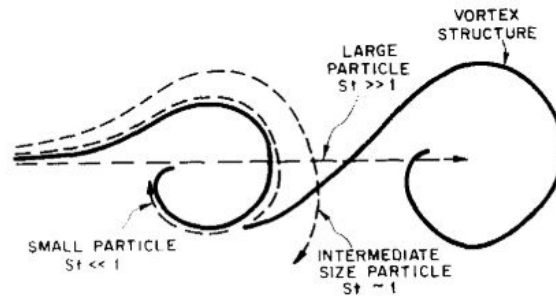
Figure 4.2: Particle trajectory compared with flow for various Stokes numbers (Piccinini, 2011)

> "Coherent large scale eddy structures play an important role in the dispersion, mixing, burning and evaporation of sprays. Small droplets closely follow the gas flow and give good visualization of large eddies. However, large droplets with their smaller drag/inertia ratios, are seen to leave these eddies and penetrate the outer potential flow. Realistic modelling of droplet environments... requires modelling of large eddies and their interaction with the droplets."

It is preferred to quantify conditions for which these large-scale structures dominantly affect particle diffusion. Young et al. (1985) proposed a time scale ratio (Stokes number) that describes the ratio between the particle response time and time scale of large scale structures. The time scale of the large scale structures is defined according to Equation 4.4.

$$\tau_e = \delta / U_m \tag{4.4}$$

Combined with the particle response time this relates to the Stokes number as formulated in Equation 4.5.

$$Stk = \tau_p / \tau_e = \frac{\rho_p d_p^2 U_m}{\delta 18 \mu_c} \tag{4.5}$$

A visual relation of the particle dispersion and Stokes number is provided in Figure 4.2. The figure shows that for small Stokes numbers ($Stk << 1$) the particle response time is much lower than the eddy structure timescale, resulting in the particle diffusing similar to a fluid particle. For high Stokes numbers the ratio of particle and fluid dispersion is well below zero. For intermediate Stokes numbers ($Stk \sim 1$) the particles disperse in relation to the observations of *Singamsetti* and *Yule*. Where particles enter the large structures and get thrown out, due to centrifugal forces, beyond the large-scale vortice.

Crowe, Chung, and Troutt (1988) performed a numerical study on the dispersion concept of the Stokes number. Particle trajectories where modeled through a vortex field and the maximum lateral displacement was recorded. The displacement was dived by size of the vortices representing the inverse Schmidt number. The turbulence Schmidt number is a relevant parameter as it describes the ratio between turbulent transport of momentum and the turbulent transport of mass. The turbulence Schmidt number is a dimensionless number and is generally calculated according to Equation 4.6 (Brethouwer, 2005).

$$S_c = \nu_t / K \tag{4.6}$$

ν_t is the eddy viscosity in m^2/s and K is the eddy diffusivity in m^2/s. In the study by *Crowe* the inverse of the Schmidt number is obtained but instead uses particle and fluid displacement rather than eddy viscosity and diffusivity. This is described by Equation 4.7.

$$1/S_c = D_{eff} / \nu_{eff} \tag{4.7}$$

Here D_{eff} is the lateral particle displacement in metres and ν_{eff} is the vortice size in metres. The results of the numerical study by *Crowe* are presented in Figure 4.3. The numerical results show that for a particle with moderate Stokes number will disperse more than the fluid.
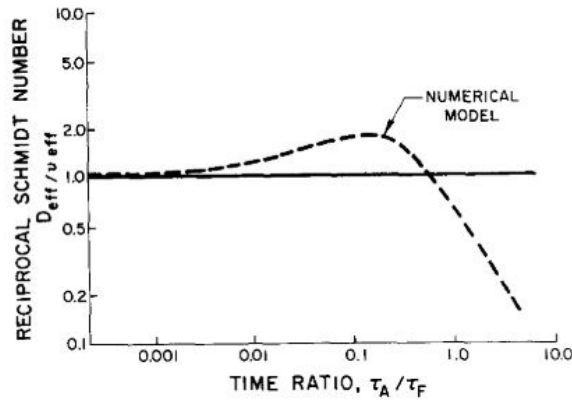
Figure 4.3: Predicted particle/fluid dispersion ratios as function of the Stokes number (Young et al., 1985)

4.1.3. GENERAL FEATURES OF RIVER TURBULENCE

Particles in transport are affected by turbulent flow conditions and affect particle dispersion. To understand particle dispersion in riverine environments it is important to study turbulence characteristics of rivers.

Yokosi (1967) described the character of turbulent structures in rivers on three different scales. Namely, width of the channel B, water depth D and on the Kolmogorov microscale λ_0. In case of a shallow river the regions relate according to $B >> H > \lambda_0$. In this study a shallow river of $B = 250$ metres and $D = 10$ metres are generally assumed. The eddies on the Kolmogorov scale are very small. The eddies on the width scale are limited to the rivers width. This results in very large eddy timescales. The vertical turbulence scale lies in the middle as it is limited to the rivers depth. The vertical turbulence results in turbulence along the free surface level as well. Hickin (2004) described the formation of boils along the water surface in rivers due to vortices shed from irregularities on the bed.

Franca and Brocchini (2015) described the formation of quasi-steady structures due to changes in river geometry or interference of structures; secondary flow in riverbend, eddy formations at riverbend, channel widening, confluence or groyne. These eddies affect the horizontal plane and are of interest for the horizontal particle dispersion. However, these large structures have relative low eddy time scales as the flow speed is low and the structure is large. Particle Stokes numbers are low $Stk << 1$, even for particles with high response times.

4.1.4. TRANSLATING TO BUOYANT MACRO PLASTIC PARTICLES

The previous section described how particle response times relate to the Stokes number and ultimately the particle diffusivity. Considering the different eddy timescales proposed in the previous subsection; turbulence on the free surface level created by vertical turbulence from the bed is of particular interest as it is expected that these structures induce moderate Stokes numbers on macro plastic particles and affect particle diffusivity. To numerically model the relative motion of macro plastic particles towards the flow and one another a motivation is made to translate the response times of macro plastics into particle dispersion coefficients. The particle response time is introduced in Equation 4.5 which translates to Equation 4.8.

$$\tau_p = \rho_p d_p^2 / 18\mu_c \tag{4.8}$$

Observing this equation directly proposes a problem with translating response times to buoyant macro plastics. The response time calculation assumes a fully submerged particle. Buoyant macro plastics, as modeled in chapter 5, are not fully submerged due to their buoyant character. This implies one cannot directly relate the particle response times of buoyant macro plastics to a linear relation with particle densities (ρ_p) and a quadratic relation to particle diameter (d_p^2) as Equation 4.8 proposes.

Therefore a different approach is used. Liu, Vanka, and Thomas (2014) described that the particle response time can be defined as the time needed for a particle to accelerate from a stationary state to 63% of the free stream velocity. This value is derived from calculating the particle velocity by deriving its acceleration and

calculating the particles speed at τ_p. To obtain the particle response times of the different buoyant macro plastic objects the time it takes for each particle to obtain 63% of the free stream velocity is measured. This is performed in chapter 5 for different macro plastic types. According to these measurements a new relation was found between size/density and the particle response time. Figure 4.4 shows the effect of size and density on the response time of a buoyant particle. Interestingly, the response time has a linear relation to size and remains constant for a range of densities. This is a result of the buoyant properties of the particle and the balance between the contact area of the flow induced drag force and change in particle mass. An increase in particle diameter does not result in equal increase of the flow contact area as part of the object is above the water level. An increase in density results in an increase in mass and an increase in flow contact area (as particle draught increases) that balance one another.

(a) Size   (b) Density
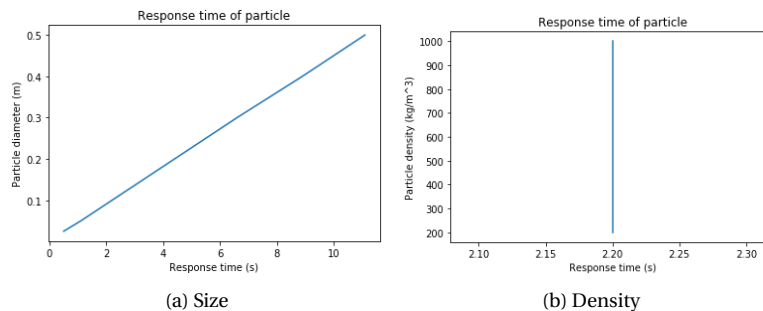
Figure 4.4: Particle response time according to size and density

Before the calculated response times for the different buoyant macro plastic objects can be related to particle diffusion, Stokes numbers need to be calculated. The Stokes number relates to the timescale of the large eddy structures in the flow. This study is interested in riverine transport, therefore an understanding of eddy timescales in rivers is required.

The large vortice structures discussed by *Singamsetti* and *Householder* refer to vortices induced by water and plane jets in experiments. Eddy formations in the riverine environment are different to those induced by water jets. Hence, compatibility of the particle dispersion relations to the Stokes number in riverine environments is questioned. Therefore the derived relation by *Crowe* in Figure 4.3 functions more as a guideline to motivate the translation of buoyant macro plastic response times into dispersion coefficients in the numerical model. Future research (possibly lab experiments) on dispersion of plastic objects in large eddy structures could motivate a better relation between the particle Stokes number of buoyant macro plastic objects and the relative dispersion compared to the flow.

To attribute effects of the particle response time on the relative particle dispersion an eddy timescale needs to be defined. The eddy timescale depends on the riverine environment and the eddies it induces. In Section 4.1.3 horizontal eddy formations induced by the riverbed are introduced. The eddy timescale correlates to $\tau_e = \frac{D}{(U_m)}$. This value is constant for all river cases as modeled in chapter 8 as the dimensions are kept constant in the channel.

4.1.5. TRANSLATE TRANSVERSE PARTICLE DIFFUSION INTO A RANDOM WALK MODEL

D-WAQ PART models particle diffusion using a random walk. The random walk describes a particle path according to a succession of random steps. In this case, when considering transverse particle diffusion, the random steps either go to the left or right. Bigger value for the dispersion coefficient increases the random step size and thus the particle diffusion. A relative increase in particle diffusion can be backtracked to a Stokes number according to Figure 4.3.

The random walk model is limited in describing particle diffusion. In reality, particles with moderate Stokes numbers tend to disperse more as they shoot out of large eddy structures. This cannot be modeled in D-WAQ PART as the particles are modeled as a passive tracer and do not have inertia. The random walk model can only be used to approximate the resulting dispersion. Therefore, in chapter 7 the relative particle diffusion

between the different classes is expressed. A sensitivity study is used to find a dispersion coefficient that fits the particles diffusion.

Fischer, List, Koh, Imberger, and Brooks (2013) described a relation between the diffusivity in a channel and transverse particle mixing. This relation is useful for testing the numerical model (in chapter 8) to determine whether the observed dispersion in the numerical model is physically representative. This relation relies on experiments of transverse mixing in both laboratory and natural channels. For a straight channel the average transverse mixing coefficient is found to be equal to Equation 4.9.

$$\epsilon_t = 0.15 DU f^* \tag{4.9}$$

The transverse mixing coefficient affects particle mixing. The width of the plume, or in other words the transverse particle dispersion, can be calculated according to Equation 4.10.

$$D_{disp} = 4\sqrt{2\epsilon_t x / U_m} \tag{4.10}$$

Equation 4.11 describes the required travelled distance at which a cloud of particles (at point release in the channels centre) are fully mixed. Considering a straight channel design (as proposed in chapter 8) with a mean flow velocity of 1 m/s, channel width of 250 metres and a transverse mixing coefficient of $\epsilon_t = 0.01$ m²/s results in a mixing length of 62.5 kilometres.

$$L_m = 0.1 U_f W^2 / \epsilon_t \tag{4.11}$$

When modelling a passive tracer along a straight channel the particles were fully mixed after only ∼ 12.5 kilometers. This is a significant difference of a factor 5 compared to estimations made by Fischer et al. (2013). Although this is not tested for the other cases, as limited information on the relation to particle diffusion and the transverse mixing coefficient in different cases, an uncertainty in the modelling results of the other cases is expected as well. Within the limits of this thesis this problem is not fully addressed but should be taken into consideration in future studies. As such, the results of chapter 8 provide a limited physical representation. Instead the numerical study in chapter 8 provides first insights in relative behavior of the different macro plastic classes and highlights cases and areas along a channels cross-sectional that are of interest for further investigation.

4.2. DISCUSSION

From literature study it remained clear that a limited understanding is available of turbulence in rivers. Research often focuses on small scale turbulent processes (Kolmogorov scale) where a statistical isotropic approach to turbulence is made. But for macro plastics, the larger quasi-steady structures are much more relevant for describing relative particle dispersion towards the flow. These structures are not as well documented. This results in insecurities in the formulation of the eddy timescale.

Crowe proposed a relation between the relative particle dispersion (towards the flow) and the Stokes number. This relation is based on a numerical study performed by *Crowe*. Insecurities arise for its relevance to buoyant macro plastics. For now, this relation is used as motivation to highlight the difference in particle dispersion between the classes and study its practical use.

The particle response time equation describes the response time for submerged particles. Buoyant macro plastics are emerged particles. Instead, the particle response time is approached by calculating the time it takes for a particle to reach 63% of the carrier fluid velocity. It is not clear whether this assumption is completely true for buoyant macro plastic particles.

Stokes number assumes small particles with low Reynolds numbers. This does not hold for macro plastic particles. However, Stokes number is still used as a relevant parameter to describe particle motion along eddy structures as limited tools are available for describing such behaviour for macro particles.

4.3. SUMMARY AND CONCLUSION

A useful parameter for describing particle diffusion in turbulent vortices is the Stokes number. The Stokes number is expressed as the particle response time divided by the eddy timescale. When the particles response time is significantly lower than the timescale of the eddy, the particle is dominated by the flow and behaves like a passive tracer. In case of a very high response time the particle is dominated by its own inertia. Interesting behaviour occurs along the middle, where particles can shoot out of the eddies and experience increased diffusion relative to the flow. *Crowe* proposed a relation between the relative particle dispersion (compared to the flow) and the Stokes number in figure 4.3. This relation is used for estimating the dispersion of different buoyant macro plastic objects in chapter 7.

To understand the particle diffusion an understanding of turbulence in rivers is important. A range of eddy formations of different scales occur in rivers. The largest eddies are limited by the river width. These structures are very large and result in low Stokes numbers. Such particles move similar to a passive tracer. This is not of interest for the modelling of macro plastic transport. On the small scale, the Kolmogorov scale, eddy timescales are very small. Macro plastic particles will not be affected by these small scale eddies. Vertical structures are limited by the channel depth and can result in turbulence along the water surface in the form of boils. These eddy structures propose of interest for macro plastic transport as the eddy timescale induces moderate Stokes numbers. Calculations on the particle response times and Stokes numbers for different macro plastic particles are performed in chapter 5. Uncertainties arise concerning the modelling results of the numerical model in chapter 8. This, as the expected mixing length (according to Fischer et al. (2013)) is significantly longer than the observed mixing length in the numerical model. This problem is not full addressed and should be taken into account in future studies.

II. Framework of Buoyant Macro Plastic Particle Motion

5

ANALYTICAL MODEL

The goal of the analytical model is to 1) classify macro plastic objects according to behaviour, 2) calculate the relating response times that functions as input for the numerical model and 3) provide an understanding of the macro plastic drivers and effects of size, density, wind and discharge on macro plastic transport for verification of the numerical modelling output.

5.1. METHOD

5.1.1. CLASSIFICATION OF BUOYANT MACRO PLASTIC BEHAVIOUR

A plastic diagram is constructed based on the formulation of response time in Section 2.6.3. Equation 2.7 shows that particle response time has a positive linear relation with the particle density and a positive quadratic relation with the particle diameter. This relation holds for submerged particles. For buoyant macro plastics the relation found in Figure 4.4. A plot is created, with density and size on the x- and y-axis, showing indications of the response time of a variety of macro plastic objects. Objects that depict relative extreme behaviour are selected and classified. For each class a representative object is chosen and characteristics values, such as weight, size and density, are calculated.

5.1.2. FORCE MODEL

In Section 2.5 on a selection of materials in riverine transport and the particle dynamics of motion are provided. The characteristics of these materials are compared with plastics. Wood and sediment are a good fit and provided equations can be translated relatively easily to macro plastics. Using analytics from these equations a force model is constructed. Two regimes are identified, namely a buoyant and non-buoyant regime. Studies on oil and ice are found not to be very compatible with macro plastic transport.

The study on the particle dynamics of motion in Section 2.6 of the literature study provides extra information to improve the force model. The pressure gradient is responsible for the downstream flow. As the drag forces already represent the downstream flow component the pressure gradient is not included as an extra constituent. Added mass is included in the force model. Plastic objects, e.g. plastic bags, have the ability to enclose large volumes of water in the form of added mass.

5.1.3. COMPUTATIONAL MODEL

To analyze the force model and the effect of particle properties on its transport a computational model is constructed in Python 3.7.1, using the Jupyter interface. The model focuses on buoyant material in line with the research objective and questions. Two models are constructed; one with and one without added mass.

WITHOUT ADDED MASS

The basic force model, excluding added mass, is described with Equation 5.1. Equation 5.2 represents a more elaborate description. The model assumes a perfectly buoyant particle; buoyancy and gravity forces are in balance. Assume a spherical body; neglecting orientation and rotation. Neglects (vertical) turbulent effects. Drag coefficients for the wide variety of macro plastic shapes are barely described. Therefore the drag coefficient is assumed to be equal to one, neglecting shape effects.

$$F_{xy,ytotal} = F_{xy,wind} + F_{xy,flow} \qquad (5.1)$$

$$m_p \vec{a}_p = \frac{1}{2}\vec{U_w}^2 C_D p_w \frac{4\pi r^3}{3} + \frac{1}{2}\vec{U_f}^2 C_D p_f \frac{4\pi r^3}{3} \tag{5.2}$$

A step-by-step particles path can be calculated with a differential equation. The force balance is rewritten into the differential Equation 5.3. This is translated into the python model via a discretization. The discretization is forward in time and backward in space, providing Equation 5.4.

$$\frac{\partial U_{p,xy}}{\partial t} = \frac{1}{2m_p} C_D \rho_f A_f (U_{f,xy} - U_{p,xy})^2 + \frac{1}{2m_p} C_D \rho_w A_w (U_{w,xy} - U_{p,xy})^2 \tag{5.3}$$

$$U_{p_i}^{n+1} = \frac{C_D \Delta t}{2m_p}\left(\rho_f A_f (U_{f_i}^n - U_{p_i}^n)^2 + \rho_w A_w (U_{w_i}^n - U_{p_i}^n)^2\right) + U_{p_i}^n \tag{5.4}$$

WITH ADDED MASS

The added mass term is derived from Section 2.6. This results in a new force balance, see Equation 5.5. The added mass effect in air is negligible compared to the flow ($\rho_{air} << \rho_w$) and is neglected. Again, a differential equation is formulated (see Equation 5.6) which is discretized forward in time and backward in space (Equation 5.7). The pressure force is not included as it the pressure gradient in the channel imposes no relative behaviour on a particle.

$$F_{xy,ytotal} = F_{xy,wind} + F_{xy,flow} + F_{addedmass} \tag{5.5}$$

$$\frac{\partial U_{p,xy}}{\partial t} = \frac{C_D \rho_f A_f}{2m_p}(U_f - U_p)^2 + \frac{C_D \rho_w A_w}{2m_p}(U_w - U_p)^2 + \frac{\pi d_p^3 p_f}{12m_p}\left(\frac{\partial U_f}{\partial t} - \frac{\partial U_p}{\partial t}\right) \tag{5.6}$$

$$U_{p_i}^{n+1} = \frac{C_D \Delta t}{2m_p(1 + 12\pi p_f d_{p,wet}^3)}\left(\rho_f A_f (U_{f_i}^n - U_{p_i}^n)^2 + \rho_w A_w (U_{w_i}^n - U_{p_i}^n)^2\right)$$
$$+ \frac{\frac{\pi d_p^3 g p_p}{12}}{(1 + \frac{\pi p_f d_{p,wet}^3}{12})m_p}(U_{f_i}^{n+1} - U_{f_i}^n) + U_{p_i}^n \tag{5.7}$$

INPUT

For each of the modules the standard input values are displayed in Figure 5.1, unless specified otherwise. The timestep and simulation time vary per modeled case.

```python
import numpy as np
from matplotlib import pyplot as plt

#general values
g = 9.81 #gravity constant in m/s^2
p_f = 1000 #density water in kg/m^3
p_w = 1 #density air in kg/,^3
w_river = 25 #width of river
p_p = 800 #particle density in kg/m^3
d_p = 0.1 #particle diameter in meters
uf = 1 #flow speed in m/s
uw = 5 #wind speed in m/s

#timestep
nt = 250 #amount of steps
dt = 0.5 #timestep
```

Figure 5.1: Standard input for computative model

Figure 5.2 shows the channel design, modeled flow profile and wind direction that are used as input for the model. A uniform velocity profile is modeled. Such a velocity profile is typical for a shallow river where the channel width is significantly larger relative to its depth ($B >> d$). Here, a channel width of 25 meter is used. The wind is modeled perpendicular to the downstream flow. In this study perpendicular oriented wind is most dominant in affecting the particles trajectory and faith (due to increased possibility of interference with riverbank) and makes wind effects easier to analyze.
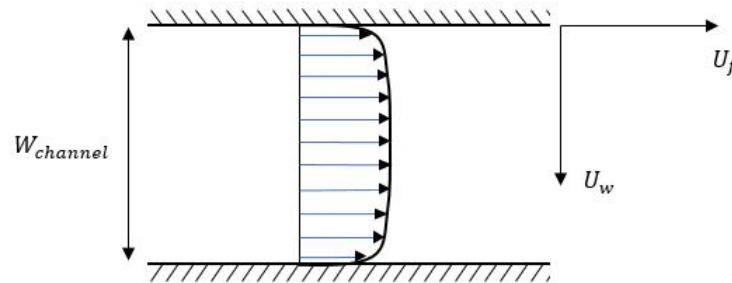

Figure 5.2: Schematic of channel design and modeled flow profile and wind direction

Each classified plastic type is modeled. These objects vary in dimensions and shapes, but are modeled as a sphere. With known variations of the typical object weight, density and/or volume a calculation is made on the required diameter of the object to model it as a sphere. This is done according to Equation 5.8.

$$d_p = 2\sqrt[3]{\frac{3\frac{m_p}{\rho_p}}{4\pi}} \tag{5.8}$$

5.1.4. CALCULATING STOKES NUMBERS
The response time of a particle is an important parameter as it is used for calculating the Stokes number. The Stokes number is an important parameter for describing horizontal buoyant macro plastic dispersion in the numerical model. Calculations are made on the effect of particle characteristics (density and size) and external forcing (wind and discharge) on the response time. The response time for each of the three plastic classes and relating Stokes numbers are calculated according to Section 4.1.4. The numerical model in step III models multiple river cases with $B = 250$ metres, $D = 10$ metres and an average flow speed of $U_m = 1.0 m/s$. Assuming surface level eddy formations from vertical eddy structures (chapter 4) provides an eddy timescale of $\tau_e = 10$ second. In a high discharge case the flow speed increases to $U_m = 2.2 m/s$ and a eddy timescale of $\tau_e = 0.45$ seconds is used.

5.2. RESULTS
5.2.1. CLASSIFICATION OF BUOYANT MACRO PLASTIC BEHAVIOUR
Because of the complex nature of buoyant macro plastics properties and behaviour a classification of buoyant macro plastics is proposed. The classification is based on the cornerstones in extreme behaviour of buoyant macro plastic objects and is used to define a framework of buoyant macro plastic particle motion. Such a classification tool can also improve the predictability of buoyant macro plastic riverine transport. For a specific location X the macro plastic litter input in the river can be classified according to formulated cornerstones. Subsequently, a prediction on the transport and fate of the characteristic macro plastic litter distribution of location X can be made in relation with the riverine environment (provided that descriptions of behaviour are already present according to plastic types and river characteristics). Figure 5.3 shows a diagram with on the x-axis particle density and on the y axis the objects longest dimension in metres. Section 4.1.4 explained that instead of a positive relation between particle response time and particle density, this relation is constant. This is included in Figure 5.3. Hence, the response time increases for increasing particle size.

Within the plot a variety of macro plastic objects are displayed according to their characteristic density and longest dimension. Objects with expected low response times are those with relative small size, such as empty water bottles (PET), foam (EPS) and empty soap bottles (HDPE). Food packaging (PP), full water bottles and plastic bags have similar densities and size. Plastic bags (LDPE) are very flexible and can enclose a significant amount of water up to 100 times its own weight. This phenomena is expected to significantly increase the response time of a plastic bag and is not described by the figure. Massive objects such as plastic chairs (PP) show a long response time.
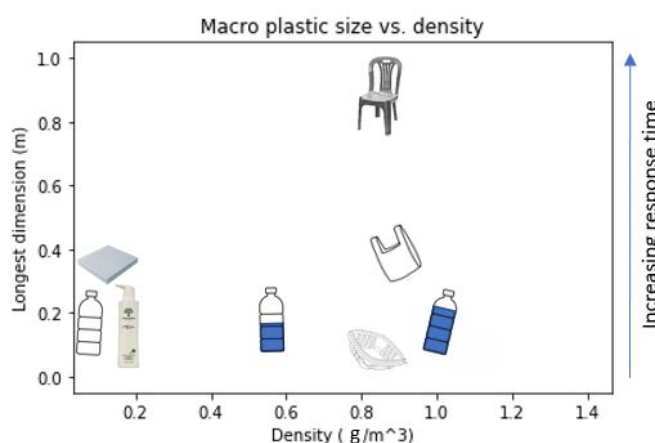
Figure 5.3: Indication on the response of different macro plastic particles

From the plastic diagram three distinctive classes are identified according to isolated transport characteristics and differences in the particle response time. In Table 5.1 the three buoyant macro plastic classifications are described. The added mass class represents particles that transport a large amount of added mass opposed to their own plastic mass. An example are plastic bags. Extremely low density macro plastic material is very buoyant and more exposed to the wind. Their response time is low. A good example are empty water bottles that are filled with air. Finally, massive objects have large dimensions and are generally heavier. Examples are plastic furniture (chairs), plastic suitcases or plastic car parts. Massive particles have high response times.

Classification	Characteristics	Representative type
Added mass	Large added mass opposed to plastic mass	Plastic bag
Dominance of buoyancy	Extremely low density, high wind exposure and low mass	Empty water bottle, foam, empty jug
Massive objects	Large size and mass	Furniture, luggage, car parts

Table 5.1: Classifications for buoyant macro plastics

Table 5.2 shows the characteristics for each of the representative buoyant macro plastic types as formulated in Table 5.1. Plastic bags are a dominant plastic polluter and have unique behaviour due to their flexible structure and capacity of trapping water. To simplify, the entrapment of water is not included in the density value described in Table 5.2. Instead, an added mass factor is used in calculations to compensate for the extra transport of water. Plastic bag sizes vary from 10 to 120 centimetres (Packeverything, 2019) (*Plastic Bag Suppliers*, 2019). Weight varies from 5 grams for small bags, 11 grams for medium sized bags and 18 grams for large bags (Ecomerge, 2011).

A range of low density plastic particles exist, such as foam and empty bottles. Empty water bottles are used as a representative object for this class as water bottles are often single-used and pose a threat as a dominant polluter.Water bottles can vary in size and weight; from 500 ml to 2000 ml bottles with weights of 10 - 54 grams (American-Samoa, 2009).

There are a range of massive plastic objects. Plastic chairs are used as representative objects as information on their weight and dimensions are easily available from online retailers (Alibaba, 2019). Figure 5.4 provides a visualization of each class representative macro plastic type.

Object	Resin	Weight (grams)	Longest dimension (cm)	Density kg/m^3
Plastic bag	LDPE	5 - 18	10 - 120	910 - 930
Empty water bottle	PET	10 - 54	20 - 30	20 - 27
Plastic Chair	PP	1900 - 4000	60 - 90	830 - 850

Table 5.2: Properties for each representative macro plastic type

(a) Plastic bag   (b) Water bottle   (c) Plastic Chair

Figure 5.4: Visualization of macro plastic objects

5.2.2. FORCE MODEL

TRANSLATING WOOD AND SEDIMENT TRANSPORT

Combining the formulated forces of wood and sediment two regimes are formulated; namely the buoyant and non-buoyant regime. For a still standing particle released instantaneously into the environment a force diagram is developed as shown in Figure 5.5. For a perfectly buoyant particle the gravity and buoyant forces are in balance ($F_{gravity} = F_{buoyancy}$). The friction force ($F_{friction}$) is very small and the downstream gravity component ($F_{gravity,downstream}$) is negligible compared to the drag forces. Both are therefore neglected. Only the buoyant regime is studied.
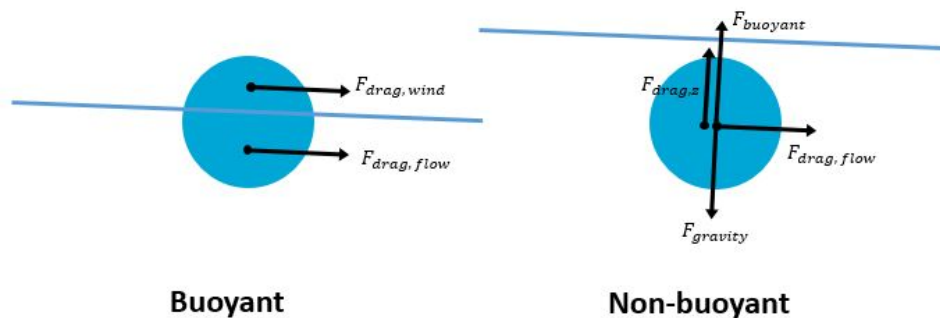
Figure 5.5: Force model of a still standing buoyant and non-buoyant particle

INCLUDING ADDED MASS

In reality a particle in transport has a boundary layer and interferes with the fluid. A particle in motion can accelerate some of the surrounding fluid, when the particle has a net positive acceleration with the fluid, or can enclose volumes of water. This extra volume of water that is accelerated functions as added mass. Depending on the characteristics of the object the amount of added mass displaced differs. Added mass is expected to be a dominant contributor to macro plastic transport and is included into the model.
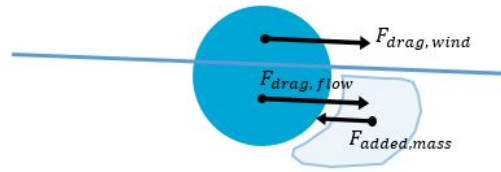
Figure 5.6: Force model including added mass

5.2.3. PARTICLE TRANSPORT

MODELLING SIZE AND DENSITY

In relation to research question 2(a) the effects of size and density on the particle displacement and response are modeled and analyzed. Figure 5.7 shows the particle displacement for varying size and density input. Larger particles are slower in adjusting to the longitudinal flow and cross-sectional wind forces. Lower density results in more exposure to the wind as the particles draught decreases. This results in lower density particles experiencing more cross-sectional displacement. The effect on particle size and density on the response time is plotted in Figure 5.8 and already discussed in chapter 4.

(a) Size   (b) Density
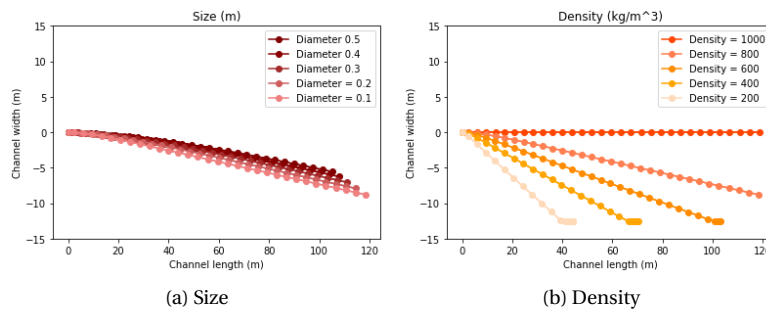
Figure 5.7: Top down view of river and size- and density effects

(a) Size   (b) Density
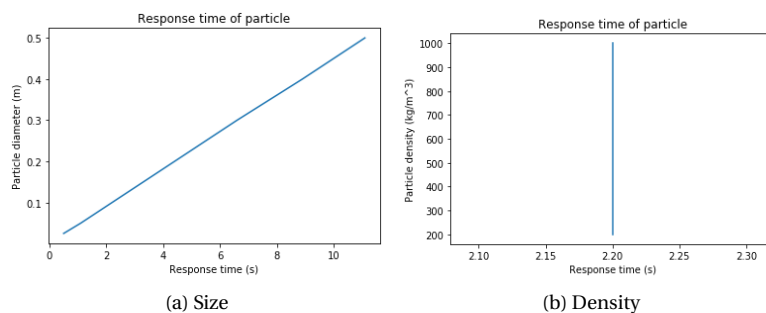
Figure 5.8: Particle response time according to size and density

Appendix C.1 shows particle displacement including added mass and corresponding response times are plotted in Figure 5.9. The response time is the time required for a released particle in rest to achieve 63% of the free stream velocity (Schwarzkopf et al., 2011). Without the inclusion of added mass the response time is constant for varying densities. The decrease in mass and contact surface area with the flow are in balance, resulting in a constant response time of 2.2 m/s. Larger particles have higher response times. The increase in volume (and thus mass) is larger than the increase in contact area. This increases the particles response time. With the inclusion of added mass density effects on the response time change. A decrease in density results in a decrease in the response time. For very low densities this no longer holds and the response times increases. This follows from a strong decrease in contact area with the flow. In reality it is expected that very light particles have low response times. The relation between response time with and without added mass for

size and density is plotted in Appendix C.2. For high densities the added mass effect is more pronounced. This, as particles submerge more as density increases.

(a) Size
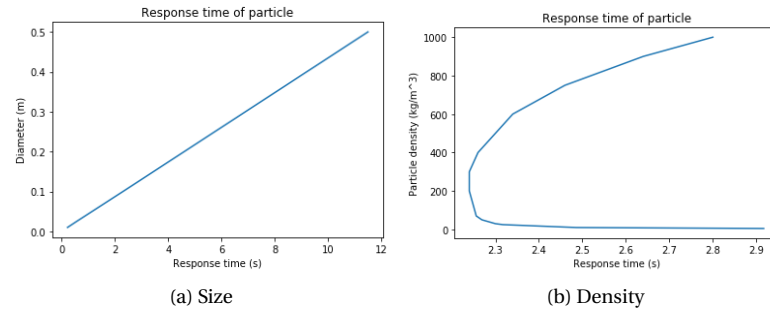
(b) Density

Figure 5.9: Particle response time according to size and density including added mass

MODELLING WIND AND FLOW

In relation to research question 2(c) the effects of wind and flow on the particle displacement and response time are modeled and analyzed. Figure 5.10 shows higher wind speeds increase cross-sectional displacement and an increase in flow increases longitudinal displacement. Corresponding response times are plotted in Figure 5.11. The pattern for wind and flow is very similar, but response times are significantly lower for flow ($\approx$ factor 10). This is expected as the density of water is thousand times greater than the density of air.

(a) Wind speed

(b) Flow speed
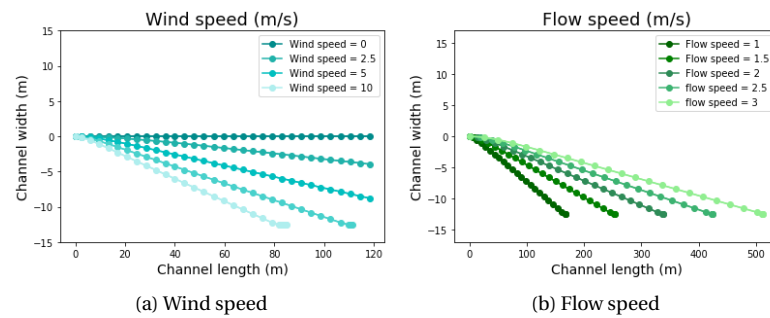
Figure 5.10: Top down view of river and wind- and flow effects

(a) Wind speed

(b) Flow speed
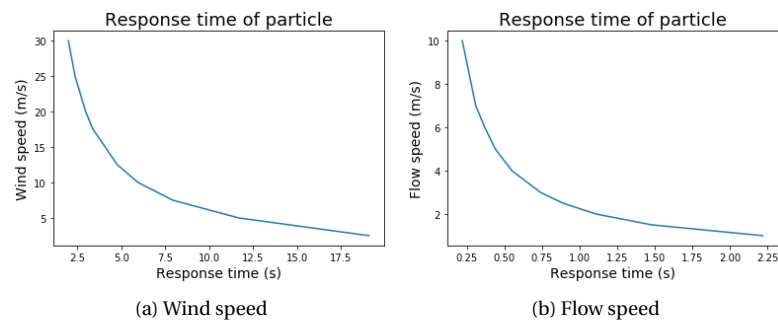
Figure 5.11: Particle response time according to wind and flow

Appendix C.3 shows the particle displacement including added mass. The particle response time, including added mass, is plotted in Appendix C.4. The response time with and without added mass are compared in Appendix C.5. Including added mass increases the response time remains relatively the same for both wind and flow and change around a factor 1.02 for wind and 1.04 for flow.

MODELLING PLASTIC CLASSES

Transport plots of the three plastic classes are displayed in Figure 5.12. For the modelling of the plastic bags an added mass factor of 100 is used to represent the ability of plastic bags to enclose a volume of water equivalent to 100 times its own mass. The cross-sectional displacement develops the slowest for the plastic bag as it is less exposed to wind and has a large amount of added mass. The empty water bottle interacts with the riverbank quickly as its exposure to wind is high and its inertia is low. In Figure 5.13 the response time for each plastic object is plotted, for a normal and high discharge case. Appendix C.6 shows the relative response time of a plastic bag between a case with and without added mass. The difference is significant and constant, with $t_{0\,AM}/t_0 \sim 5.4$, and shows the dominance of the added mass effect for plastic bags.

(a) Graph of plastic bag   (b) Graph of empty water bottle   (c) Graph of plastic chair
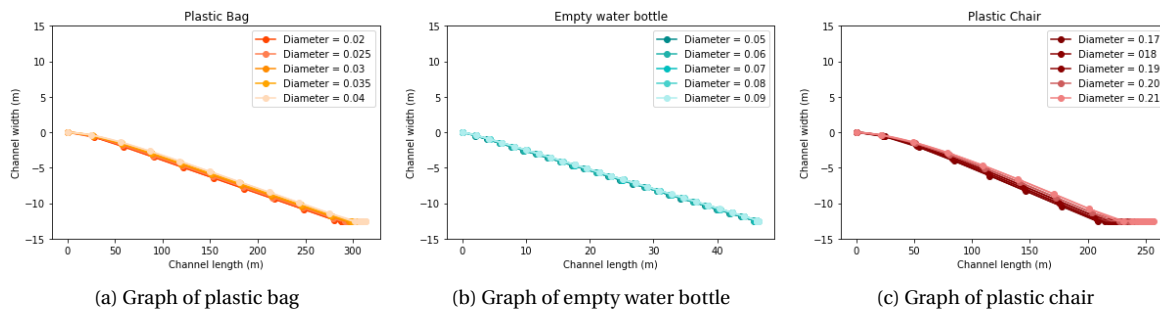
Figure 5.12: Top down view of the transport of the plastic types for different diameters

Figure 5.13 shows plots of the response time development for each of the various plastic types. The response time for a plastic bag varies between 2.4 and 4.72 seconds, for an empty water bottle it varies between 0.45 and 0.72 seconds and for the plastic chair this varies between 3.92 and 4.84 seconds.
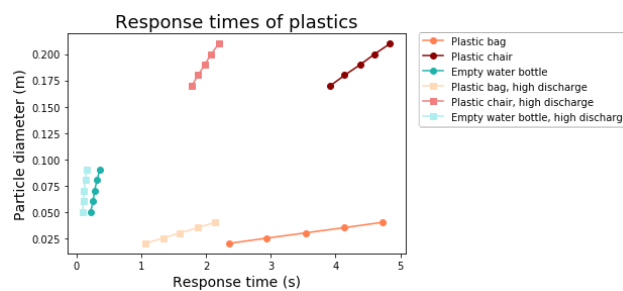
Figure 5.13: Particle diameter plotted against the response time for different plastic objects with normal and high discharge

CALCULATING STOKES NUMBERS

The Stokes numbers are calculated for each plastic object and presented in Table 5.3. This is important for understanding particle dispersion of each macro plastic type subjected to bottom induced surface level turbulence (chapter 4). Both the plastic bag and chair have moderate Stokes $Stk < 1$. The empty water bottle has a stokes number much smaller than one ($Stk << 1$). In addition, also Stokes numbers are provided for a high discharge case. As flow velocities increase the eddy timescale decreases. Interestingly, the response time decrease and eddy time scale decrease are in balance and result in equal Stokes numbers. Figure 5.14 shows a relation between the particle dispersion relative to the dispersion of a fluid particle (y-axis) and Stokes number (x-axis). Particle dispersion is greatest for the plastic bag. The empty water bottle disperse the least compared to a fluid particle. Increasing the discharge does not results in a change of the Stokes number as the decrease in eddy timescale and response time are of equal magnitude.

5.3. DISCUSSION

In the analytical model the effect of wind on the flow is neglected. In reality the top part of the water column is affected by the wind and partially adjusts to the wind direction. As a result, wind is expected to be more

Object	Response time (s)	High discharge response time (s)	Stokes number (-)	High discharge Stokes number (-)
Plastic bag	2.4 - 4.72	1.06 - 2.14	0.24 - 0.47	0.24 - 0.47
Empty water bottle	0.22 - 0.36	0.1 - 0.16	0.02 - 0.04	0.02 - 0.04
Plastic chair	3.92 - 4.84	1.78 - 2.2	0.39 - 0.48	0.39 - 0.48

Table 5.3: Stokes number for each macro plastic type
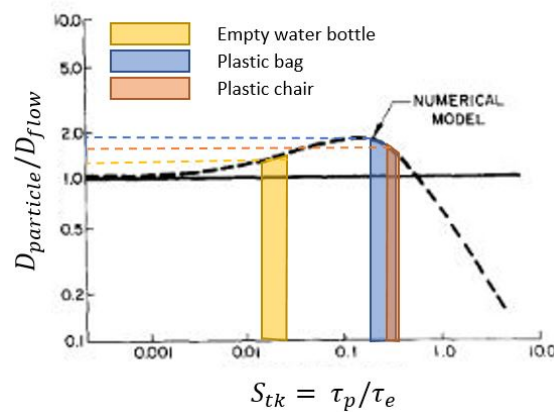
Figure 5.14: Relation between Stokes number and relative particle dispersion (compared to a fluid particle) for each plastic object

dominant than perceived from the analytical model results.

Buoyant macro plastics consist of a wide variety of shapes and are affected by both wind and flow. This complicates modelling with drag coefficients. Therefore, in the analytical model a constant value of 1 is used for the drag coefficients. Both wind and flow drag coefficients are set at 1. In reality, wind has a different kinematic viscosity compared to water and this relates to different drag coefficients resulting in different particle motion.

The particles in the analytical model are modeled as perfectly spherical objects. As a result rotation and orientation can be neglected. In reality macro plastic objects are not perfectly spherical and therefore rotation and orientation are important. Once an object rotates its orientation towards the flow regime changes resulting in a different drag, potentially affecting its rotation and so on. This process is chaotic and is especially complicated when considering a wide variety of macro plastic shapes.

In this study a velocity profile is chosen that corresponds to a shallow channel. This results in a uniform velocity profile along the channel width. However, a parabolic velocity profile can occur for narrow channels. This is expected to result in a different particle motion.

The analytical model does not take into account the shape of an object and therefore limitedly addresses the wind exposure. For example, a plastic bag will barely have any wind exposure even when floating. While a floating (empty) water bottle has more exposure and is more subjective to wind forcing.

The flow in the model is laminar. In reality turbulence streams constantly develop along a river. As turbulent conditions are very complex they are not included in the analytical model. Instead, the numerical model in step III does model large vortice structures.

Figure 5.9 (b) suggests that low density objects have high response times. According to the model calculations the particles draught and thus contact area with the flow decreases significantly for lower densities. This results in a very low flow induced drag force for low density particles. This effect is not expected to be so pronounced in reality.

Each of the three plastic types are modeled as spheres. To do so, particle weight, density and/or volume are used to calculate the diameter. As plastic bags and empty water bottles are very light their diameter distribution is also relatively low. In reality, large differences in plastic bag sizes and bottles are observed (see Table 5.2). This affects the flow and wind induced transport of the particle.

The plastic bag is modeled as a sphere. This results in an error in the calculation of the added mass effect as the sphere does not represent the enclosing properties of a plastic bag. Therefore, an added mass factor of 100 is used. Because of this significant factor it is expected that small changes in size have significant effect on the amount of added mass and therefore relative behaviour. However, Figure 5.12 (a) does not show a large difference in behaviour between different sized particles. In reality this effect is expected to be much more pronounced as the dimensions of a plastic bag are not condensed to a sphere but have a much wider range (see Table 5.2).

5.4. SUMMARY AND CONCLUSION

The analytical model uses transport equations of wood and sediment to construct a force model to analyze the effects of plastic characteristics (size and density) and external forcing (wind and discharge). In addition, plastic response times are calculated that function as input for the numerical model. To do so, a classification of macro plastic objects is proposed according to cornerstones in behaviour. Three distinct classes and representative types are identified and presented in Table 5.1.

The model suggests that an increase in particle size results in a linear increase of the response time. An increase in particle density results in lower particle response times. For very low particle densities, the particle contact area with the flow is very small. Hence, an increase in particle response time is observed (Figure 5.9). Including the added mass effect results in an increase of the particle response time. This effect is dominant for high density particles (Figure C.2). Wind and flow speeds have significant effect on the particle displacement and particle response time (Figure C.3 and C.4).

The response time of each representative plastic, namely plastic bag, empty water bottle and plastic chair, are calculated for normal and high discharge conditions. Plastic chairs have the highest response time quickly followed by plastic bags. The response time of an empty water bottle is significantly lower (see Figure 5.13). Plastic bags are not sensitive to wind forcing as their exposure is minimal and inertia is high. Due to their significant added mass effect their response time is increased by a factor 5.4 (Figure C.6). Empty water bottles have low response times and significant exposure and adjust quickly to wind forcing. For all plastics, an increase in flow speed results in significant decrease of the response time.

For each plastic object Stokes numbers are calculated. The Stokes number provides a relation to the particle dispersion, which is relevant for translating each plastic object into the numerical model in step III. The Stokes numbers for normal and high discharge conditions are calculated in Table 5.3. An increase in flow speed does not affect the particle Stokes number as the decrease in particle response time is of the same magnitude as the decrease in eddy timescale.

Concluding on the analytical model a framework of macro plastic particle motion is proposed in Table 5.4. This description of behaviour is used as a guideline for building hypotheses on expected behaviour of macro plastic transport in different riverine environments (chapter 7).

Representing object	Behaviour
Plastic bag	Particle experiences increased dispersion relative to the flow. Particle has barely any wind exposure and is therefore not very subjective to wind. High response time results in slow adjustment to flow changes.
Empty water bottle	Particle dispersion is similar to dispersion of fluid particle. Particle is easily affected by wind due to large wind exposure. Low response time, thus adjusts quickly to flow changes.
Plastic chair	Particle experiences increased dispersion relative to the flow. Particle has some wind exposure but also high response time, therefore moderately effected by wind. High response time results in slow adjustment to flow changes.

Table 5.4: Framework for macro plastic particle motion based on the three cornerstone classes and riverbed induced turbulence on the surface level

6

FLOW STUDY

The goal of the flow study is to construct hypotheses on the transport of buoyant macro plastic types (as introduced in chapter 5) in a range of riverine environments. These hypotheses are used for verification of the hydrodynamic and particle tracking output in the numerical model (chapter 8).

6.1. METHOD

The flow study uses information from the literature study of the geometrical and structural river elements, as described in Section 2.3. The framework of buoyant macro plastic particle motion, provided by the analytical model in Table 5.4, is used to analyze the effect of different flow features on the macro plastic transport. For each river element a hypothesis is constructed of its expected effect on the cross-sectional macro plastic concentration distribution and how it affects the three macro plastic objects.

6.2. RESULTS

6.2.1. RIVER BEND

In a river bend, the secondary flow in the top layer of the water column is directed towards the outer bend. Near the bottom an inward secondary flow pattern develops. In addition, an outer-bank cell develops near the outer bend. The outer-bank cell only develops in strongly curved and smooth bends and are rarely observed in reality. Therefore the effect of the outer-bank cell on buoyant macro plastic transport is neglected.

A schematic of the flow patterns is shown in Figure 6.1. Highly buoyant materials such as empty water bottles have a much lower response time. It is expected they subject quicker to the secondary flow and are likely to reach the outer-bank. During high discharge conditions it is expected that secondary flow velocities increase. Higher concentrations towards the outer bend are expected. Downward motion of the secondary flow suggests vertical mixing of macro plastics is possible. Buoyant dominant particles have high rising velocities and are not very subjective to vertical mixing. Particles with near water densities, such as plastic bags, are possibly sensitive to vertical mixing by secondary flow. The vertical transport of macro plastics due to secondary flow imposes an interesting research topic but will not be assessed further in this study. Since vertical transport processes are not analyzed in the analytical model no verification of vertical processes is made.
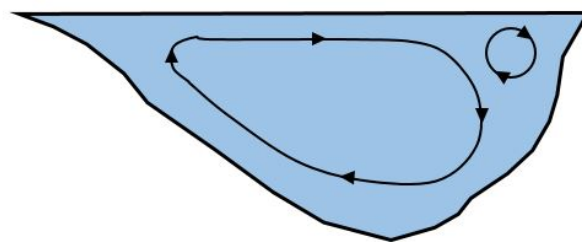

Figure 6.1: Schematic of the cross-sectional flow features in a river bend

Figure 6.2 shows a top down view of a river and flow conditions. Number 1 and 3 show the development of a point bar along the inner bank, where advective transport decreases strongly and gyres can occur. Along strong river bends bank embayments can develop where gyres occur. These are not taken into account in the numerical modelling study. In both cases macro plastic material in transport can accumulate in these areas. Table 6.1 provides a conclusion on the expected behaviour of the three buoyant macro plastic classes.
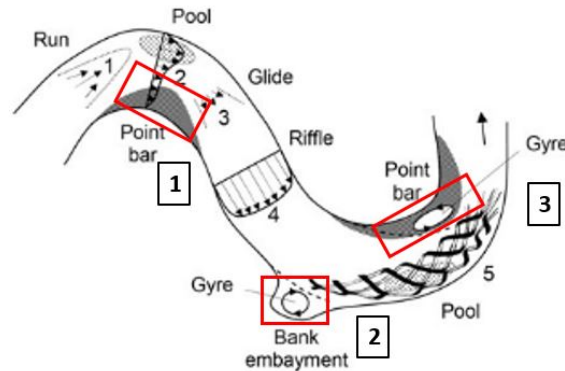
Figure 6.2: Top down schematic of flow features in a river bend

Combining this information results in the following hypothesis for river bends and their effect on the cross-sectional macro plastic distribution in rivers:

"Flow conditions imposed by river bends increase the concentration of buoyant macro plastics along the outer bend, when neglecting wind. An increase in discharge results in an increase of secondary flow conditions and particle concentrations near the outer bend."

Object	Suggested behaviour
Plastic bag	Less influenced by secondary flow. More concentrated towards the channels centre.
Empty water bottle	Low response time and therefore more affected by the secondary flow which results in higher concentrations near outer bend. Responsive to wind, which can potentially counteract secondary flow effects
Plastic chair	Less influenced by secondary flow. More concentrated towards the channels centre

Table 6.1: Expected behaviour for macro plastic types in a river bend (neglecting wind)

6.2.2. CHANNEL WIDENING

In Figure 6.3 two areas of interest are identified. Number 1 shows the formation of eddies due to the sudden channel expansions. Material can get trapped in these eddies due to wind and/or horizontal dispersion. This results in an increase of particle concentrations along the channels boundaries. Number 2 illustrates a redistribution of the transport material along the river width as the eddies decrease in size. This results in spreading of macro plastic concentration along the channels width and a relative decrease of material in the channels centre. The particle dispersion of plastic bags and chairs is relatively high. These particles distribute more towards the channels sides compared to the empty water bottle, and are more likely to interfere with the large eddy structures increasing their concentration along the channel boundaries. The following hypothesis is constructed:

"Channel widening results in a relative decrease of macro plastic concentrations in the channels centre and an increase along the channels boundaries."

Table 6.2 summarizes the expected behaviour in a channel widening for the different plastic types.

Object	Suggested behaviour
Plastic bag	Particles tend to disperse more towards channel boundaries and interact with the large eddy structures; increasing concentration along the channels boundaries
Empty water bottle	Particles disperse less towards channel boundaries
Plastic chair	Particles tend to disperse more towards channel boundaries and interact with the large eddy structures; increasing concentration along the channels boundaries

Table 6.2: Expected behaviour for macro plastic types in a channel widening
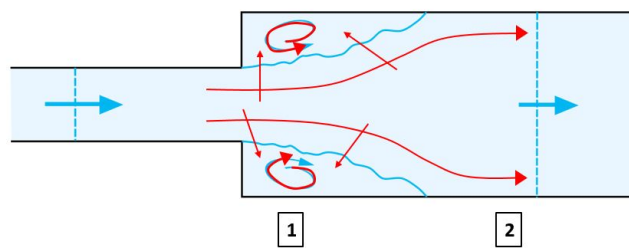
Figure 6.3: Schematic of flow features along a channel widening

6.2.3. RIVER CONFLUENCE

In figure 6.4 three factors are illustrated that affect the plastic distribution due to a river confluence. Number 1 demonstrates the input of extra material and therefore increasing the macro plastic concentration in the main channel. Number 2 shows a separation zone, where circular flow develops. Buoyant macro plastics can migrate into these zones which increase particle retainment. This increases the concentration of particles along the tributary side of the channel. Number three shows the redistribution of plastic concentrations along the channels width. Particles with increased dispersion are more likely to transport into the separation zone and retain longer, increasing their concentrations.
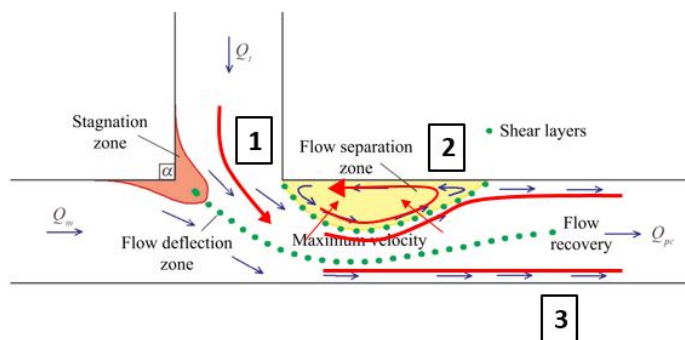
Figure 6.4: Schematic of flow features near a river confluence

This results in the following hypothesis for a river confluence and the macro plastic transport distribution:

> *"Confluence hydrodynamics impose a relative increase in plastic concentrations along the tributary side of the river"*

Table 6.3 shows the expected behaviour of the different plastic types in a river confluence.

Object	Suggested behaviour
Plastic bag	Relatively high dispersion results in more interference with separation zone. This results in an increase in particle concentrations near the tributary side of the channel
Empty water bottle	Concentrated more towards the channels centre and is less likely to be affected by separation zone
Plastic bag	Relatively high dispersion results in more interference with separation zone. This results in an increase in particle concentrations near the tributary side of the channel

Table 6.3: Expected behaviour for macro plastic types in a river confluence

6.2.4. Groyne

Groynes cause a sudden disruption in flow. Material in transport is likely to accumulate directly upstream of the groyne as the groyne is obstructing the passage of material (number 1 in Figure 6.5). This results in a decrease of plastic concentrations along the groyne side of the river. Downstream of the groyne the disruptance results in a recirculating zone. In case of wind and/or horizontal dispersion macro plastic material in transport can enter the recirculating zone and accumulate over time (number 2). This increases particle concentrations along the groyne side. As the groyne motivates particles to transport along the groyne free side of the channel, strong wind and/or horizontal dispersion is required to have particles enter and retain in the recirculating zone. Therefore, it is expected that the concentration increase due to the large eddy structure behind the groyne is of limited effect. Further downstream the recirculating zone decreases in size and the macro plastic concentration re-distributes itself along the river width (number 3).
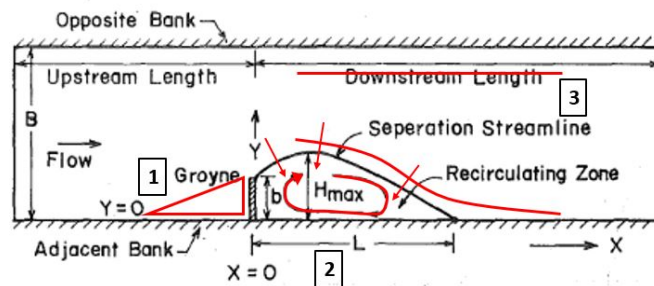

Figure 6.5: Schematic of flow features along a groyne

This following hypothesis is formulated:

> *"The occurrence of groynes in rivers results in a reduction of plastic transport concentrations along the groyne side of the river"*

Table 6.4 shows the expected behaviour of the macro plastic objects along a groyne.

Object	Suggested behaviour
Plastic bag	Increased dispersion results in increased interaction with eddy structure behind groyne and a slight increase in particle transport along the groyne side of the channel compared to the empty water bottle. Overall, the particle concentration increases along the groyne free side of the channel.
Empty water bottle	Concentrated more towards channels centre and therefore results in a increase in particle concentration along the groyne free side of the channel.
Plastic chair	Increased dispersion results in increased interaction with eddy structure behind groyne and a slight increase in particle transport along the groyne side of the channel compared to the empty water bottle. Overall, the particle concentration increases along the groyne free side of the channel.

Table 6.4: Expected behaviour for macro plastic types near a groyne

6.3. DISCUSSION

In reality smooth and steep bends do not occur often and therefore the strength and development of secondary flow and especially the outer-bank cell is limited. Considering the dominance of wind and advective flow, the real effects of secondary flow on the cross-sectional macro plastic distribution remain uncertain. Furthermore, the meandering nature of rivers where multiple river bends occur in succession while secondary flow effects are constant shifting, suggest that the effects on the horizontal plastic distribution might counteract one another. Research on in-situ data is required to provide information on the relevance of secondary flow on the cross-sectional distribution of buoyant macro plastics.

Along a river confluence it is expected that the flow separation zone is responsible for reducing the macro plastic concentration along the tributary side of the river. It is unclear how the (macro) plastic input from the tributary distributes along the river width and how this affects the macro plastic distribution. This also varies with the incoming discharge of the tributary channel, which affects the size of the separation zone and thus macro plastic transport.

Groynes have an abrupt effect on the flow and are expected to be relevant for their effects on the macro plastic transport distribution. As opposed to river bends, the occurrence of groynes is less frequent and therefore possible its relevance.

Plastic bags and chairs are very similar in behaviour and have similar descriptions for each case. This is a result of the similar Stokes numbers attributed to both particles. In reality, different behaviour is expected as a plastic chair and bag greatly differ in shape and size. Due to the limitations of the analytical model this is not represented in the calculation of the Stokes number.

6.4. SUMMARY AND CONCLUSION

The flow study performs a study on flow features induced by a range of river elements. Using the framework of buoyant macro plastic particle motion, hypotheses are proposed on the effects of these flow features on the buoyant macro plastic distribution of each macro plastic class.

In a river bend a secondary flow develops. Along the top of the water column the secondary flow motions towards the outerbend. When neglecting wind, buoyant macro plastic material transports towards the outer bend, increasing concentrations near the outer bend. It is expected to find greater concentrations of empty water bottles near the outer bend, as their response time is low.

An abrupt widening of the channel geometry results in the development of eddies at the widening location. These eddies increase the retainment of macro plastic material. Hence, the concentrations increase near the channels boundaries. This effect is more pronounced for more dispersive particles such as plastic bags and

chairs as they are more likely to interact with the eddy formations, resulting in retain longer and increased concentrations.

In a river confluence two rivers merge. The tributary channel introduces new material to the main channel, increasing the plastic concentration. In addition a separation zone develops. The separation zone can retain material. This increases the concentration along the tributary side of the channel, where the separation zone develops. More dispersive material (plastic bag and chair) are more likely to be affected by the separation zone and have increased concentrations along the tributary side of the channel.

Groynes obstruct the flow and passage of transport material. Due to blockage an increase in macro plastic concentrations is expected along the groyne free side of the channel.

III. Numerical Modelling

7

ANALYSIS ON NUMERICAL PARAMETERS

The goal of the parametric analysis is to define relevant parameters in Delft3D FLOW and D-WAQ PART for describing buoyant macro plastic transport. For each macro plastic class input values are motivated, which are used in chapter 8.

7.1. METHOD

7.1.1. CONSTRUCTING A LIST OF PARAMETERS

Delft3D FLOW and D-WAQ PART are the software packages of choice for performing numerical modelling. As this study is performed in cooperation with Deltares access and guidance to these software packages is granted. Delft3D FLOW is used to model the hydrodynamics and D-WAQ PART is used for particle tracking. To represent each buoyant macro plastic class an analysis on the numerical parameter of Delft3D FLOW and D-WAQ PART is performed to determine which parameters can be used to describe differences in behaviour of the buoyant macro plastic classes in relation to the results from chapter 5.

The manual of Delft3D FLOW, D-WAQ PART and the program interface are analyzed to propose a list of parameters that can describe transport relevant for buoyant macro plastic objects. D-WAQ PART offers two different modules for modelling particles. One is a tracer module and the other is an oil module. When neglecting all oil processes in the module (see Table 7.1), the oil module functions as a tracer module. In addition, the oil module is also compatible with wind settings in D-WAQ PART. This is not the case for the tracer module. Therefore the oil module is chosen as the desired particle tracker.

Parameter	Value
Evaporation fraction per day	0
Oil dispersion	0
Stickyness probability	0
Volatile fraction	0
Emulsification parameter	0
Maximum water content	1
Fraction at which emulsification starts	1

Table 7.1: Oil module settings for modelling macroplastics

7.1.2. DEFINING PARAMETER VALUES

The particle response time of each macro plastic class, calculated in chapter 5, is translated into input values for the numerical model. Chapter 5 briefly describes a relation between the Stokes number (see Table 5.3 for calculated values per class) and particle dispersion.

No absolute calculation on the amount of dispersion is made. Instead a moderate amount of dispersion is attributed to the empty water bottle. The moderate amount of dispersion is defined according to a sensitivity

study on the horizontal dispersion coefficients and their effect on particle dispersion. The ratio of relative particle dispersion (compared to the flow) for the other plastic objects is translated into an amount of particle dispersion by relating the objects relative to the empty water bottle. According to the sensitivity study on the horizontal particle dispersion coefficient on particle dispersion, values for the horizontal particle dispersion coefficient are attributed to each macro plastic object.

In the sensitivity study a straight channel is modeled with a maximum depth of 10 metres. A depiction of the cross-sectional and longitudinal velocities are provided in Figure 7.1 (a) and (b). The vertical bounce is excluded from the model as well, as this simulates reflection of particles at the bottom and water level boundary. This behaviour is not desired for modelling plastics and is switched off in the input file.

(a) Cross-sectional view   (b) Top down view
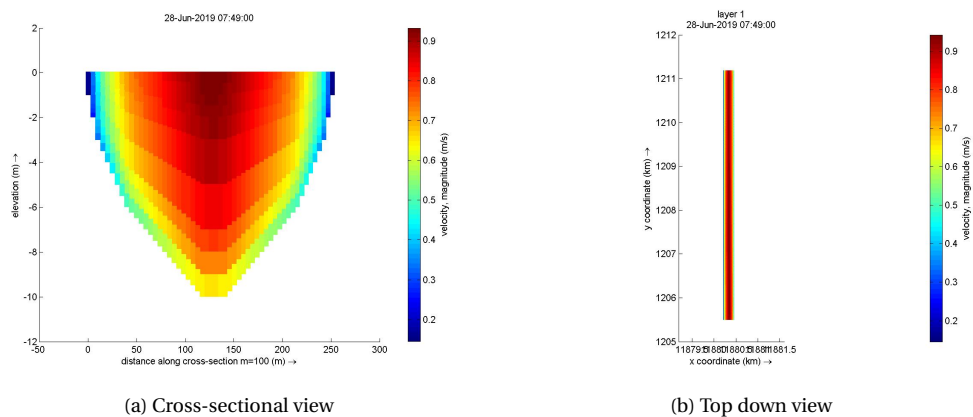
Figure 7.1: View of flow velocities in reference model

7.2. RESULTS

7.2.1. LIST OF PARAMETERS

DELFT3D FLOW

To understand relative particle motion towards the flow, it is important to have an understanding of the flow features modeled by Delft3D FLOW. Correct modelling of eddy formations is important and effect eddy timescales. Eddy timescales effect the Stokes number (see Equation 2.8) and thus particle dispersion. For 1D modelling scenarios the depth and width velocity profile is averaged to a single point. This includes averaging of eddy formations. Eddy viscosity coefficients are used to account for eddy formations in a 1D model. Formulating a representative value of the viscosity coefficients is very complicated, especially for a range of river geometries. These complications can be bypassed by modelling a 3D channel, where there is no need for flow averaging. Horizontal and vertical eddy viscosity values have limited effect on the hydrodynamic output in a 3D modelling environment. Hence, there is no need to formulate horizontal and vertical eddy viscosity input.

Wind can be modeled in Delft3D FLOW. However, D-WAQ PART also provides tools for modelling wind which cost less computing power. Wind is therefore modeled in D-WAQ PART. Discharge boundaries are applied in Delft3D FLOW and affect the flow velocity in the channel. The flow velocity is an important parameter in describing the eddy timescale and thus particle dispersion.

Table 7.2 shows the available parameters in D-WAQ PART that could be used to model macro plastic transport. In Section 5 calculations are made on the response time of the different buoyant macro plastic classes along the horizontal plane. Vertical effects (vertical dispersion and rising velocity) are therefore not further included in this research as they cannot be verified with the results from the analytical model. The horizontal dispersion coefficient b is neglected as no value for each of the macro plastic classes could be motivated. The horizontal dispersion coefficient a is further analyzed in the next section.

Parameter	Effect	Translating to buoyant macro plastic transport
Vertical dispersion coefficient	Increase step size of vertical random walk and subsequently the vertical dispersion	Accounts for vertical mixing of particles. Particles with near water densities are more subjective to vertical mixing.
Rising velocity	Describes the upward velocity of a submerged particle	Account for the different densities and thus rising velocities of plastic particles.
Horizontal dispersion coefficient a	Increase step size of horizontal random walk and subsequently the horizontal dispersion.	A relation between the amount Stokes number and particle dispersion is described in chapter 4. The dispersion coefficient can be used to model according to the experience particle dispersion and represent the particle Stokes number.
Wind drag percentage	Percentage of wind forcing that effects particle.	Can be used to account for the amount of wind exposure for particles, where exposed objects have a higher drag percentage.

Table 7.2: Available parameters in D-WAQ PART that are relevant for the modelling of macro plastic transport

7.2.2. PARAMETER VALUES
The horizontal dispersion is modeled as a random walk, where the dispersion coefficient relates to the step size and ultimately the amount of dispersion. In Section 2.6.4 a relation is described between the particle and fluid dispersion ratio and the Stokes number. This relation is used as a starting point for defining a dispersion coefficient for the different macro plastic classes.

The models sensitivity to the dispersion coefficient is described in Table 7.3. A moderate amount of dispersion is valued at 100 metres. This value is used as a baseline for modelling the relative dispersion between the three macro plastic classes. Figure 7.2 shows the relative particle diffusion for each class, according to the relation found by Crowe et al. (1988). Accordingly, the horizontal dispersion of each class is calculated and a horizontal dispersion coefficient is attributed (based on the sensitivity study). These are described in Table 7.4.

Description	I	II	III	IV	V
Horizontal dispersion coefficient a	0	0.001	0.01	0.1	1
Horizontal dispersion (m)	20	80	100	250	290

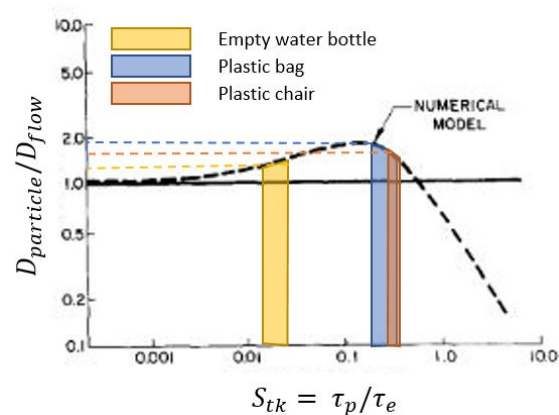Table 7.3: Sensitivity study on the horizontal dispersion coefficient a

Figure 7.2: Relation between Stokes number and dispersion for each plastic object

Object	Relative ratio particle and fluid dispersion (-)	Horizontal dispersion (m)	Horizontal dispersion coefficient D_H (m^2/s)
Plastic bag	1.9	135	0.03
Empty water bottle	1.4	100	0.01
Plastic chair	1.7	120	0.02

Table 7.4: Horizontal dispersion coefficient values for each macro plastic object

In Table 7.5 the input values for the wind drag percentage per class are shown. No sensitivity study is performed on the wind drag percentage, due to time constraints. Conclusions from the analytical model (chapter 5) suggest that the empty water bottle is very subjective to wind forcing. The plastic bag was found to be least influenced by wind. forcing

Description	Plastic bag	Empty water bottle	Plastic chair
Wind drag percentage (%)	1	12	2

Table 7.5: Wind drag percentage per class

7.3. Discussion

The values provided in Table 7.5 represent a relative difference in wind induced behaviour between each class. The values are poorly motivated and are not representative for real behaviour but do provide insight on the relative effect of wind. In addition, the wind modeled in D-WAQ PART does not affect the hydrodynamics, only the particle. In reality, the flow is affected by wind and amplifies wind effects. In the analytical model the same assumption is applied.

Table 7.4 provides horizontal dispersion coefficients motivated according to their relative difference in dispersion according to studies by Crowe et al. (1988). Definitive values of the dispersion coefficient for the different macro plastic are not defined, and are likely to provide different results. Measurements on the amount of dispersion for different macro plastics types, e.g. in a lab environment, can reduce insecurities on this matter.

Vertical dispersion is not included in the sensitivity study as no verification can be provided with the analytical model. It is expected that vertical dispersion is important for the distribution of macro plastic particles, due to the logarithmic velocity profile along the vertical. In combination with the large difference in rising velocities between the classes this could result in a significant difference in behaviour.

7.4. SUMMARY AND CONCLUSIONS

The parametric analysis performs an analysis on Delft3D FLOW and D-WAQ PART, the numerical models of choice for modelling cases in chapter 8, to define a list of parameters that are relevant for the modelling of buoyant macro plastic transport. A range of input values are motivated, using results from chapter 5, and are applied in chapter 8.

In Delft3D FLOW the hydraulic boundary conditions are defined. Here, the discharge and thus flow velocity of the channel is simulated. Flow velocity plays an important role in describing eddy timescales and thus particle dispersion. It is therefore a very relevant parameter for describing macro plastic transport.

Multiple parameters are available in D-WAQ PART that provide tools to describe relative behaviour between macro plastic particles. Two parameters are important for describing vertical behaviour. The vertical dispersion coefficient accounts for vertical mixing. Near density objects, such as plastic bags, are more subjective to vertical mixing than buoyant dominant objects. Rising velocities vary strongly between different particles and are expected to influence the vertical mixing resistance of a particle. These vertical parameters are not used in chapter 8 as no verification with the analytical model can be made (vertical process are not studied in chapter 5).

D-WAQ PART provides horizontal particle dispersion coefficients which describe horizontal particle dispersion via a random walk. The horizontal dispersion is related to the Stokes number, and thus response time, of a particle and are calculated by the analytical model for each class. The amount of dispersion increases for moderate Stokes numbers compared to low Stokes numbers. This results in a significant difference in dispersion between objects with higher Stokes numbers, namely plastic bags and chairs, and empty water bottles which have low Stokes numbers. This relation between the Stokes number and amount of dispersion provides an entry point for motivating dispersion coefficients for the different macro plastic classes. D-WAQ PART uses a random walk approach for describing the particles dispersion. The amount of horizontal dispersion can be adjusted according to the input value of the horizontal dispersion coefficient in the model. With the Stokes numbers calculated in the analytical model and the given relation between Stokes number and amount of dispersion from the literature, a value for the dispersion coefficient of each class is proposed in Table 7.4. The effect of these input values are tested in the case study.

Wind conditions can be modeled in D-WAQ PART. The particle exposure to wind can be represented in the model using the wind drag percentage, which describes the amount of wind forcing to affect the particle. The analytical model concludes that each of the macro plastic classes reacts differently to the wind, due to difference in wind exposure. The empty water bottle is most sensitive to wind, plastic bags are the least sensitive (Table 7.5).

8

CASE STUDIES

In this chapter the macro plastic classes are modeled according to input values defined in chapter 6. Particle tracking is performed in a number of riverine environments as proposed by chapter 5. The goal of this chapter is to analyze the performance of the particle tracking results and compare these with the framework of buoyant macro plastic motion.

8.1. METHOD

8.1.1. GRID

For each case a grid is designed, as introduced in Section 6, using the RGFGRID tool. The grids are designed according to a set of rules to ensure grid quality:

- Grid must be orthogonal, where grid lines must intersect perpendicularly.

- Grid spacing must vary smoothly

Figure 8.1 displays the constructed grids and used reference points. The riverbend grid also contains a wind direction. This is the only case were wind conditions are modeled. A southern wind direction is chosen as it has a dominant counter-effect on the secondary flow. A high discharge case is modeled in the riverbend as well. This, to analyze the effects of discharge on secondary flow and cross-sectional particle distribution. The river bend case is analyzed more in depth as it is occurrence is frequent. The straight grid is used for modelling the reference case and the groyne case, using the thin dam tool in Delft3D FLOW. Each grid has a width of 250 metres.
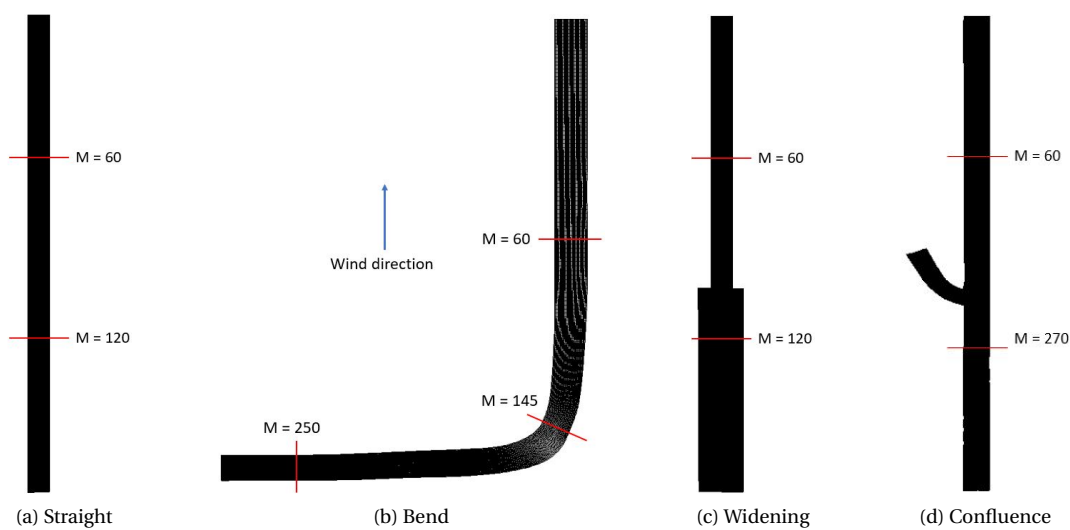

Figure 8.1: Constructed grids in RGFGRID for Delft3D FLOW

8.1.2. Bathymetry

The bathymetry file is created in the QUICKIN tool. A maximum depth of 10 metres is used for all grids. This coheres with the modelling of a shallow river where $B >> d$. The bathymetry of the reference, riverbend and groyne case are modeled in line with studies from Rosgen (1994). The hydrodynamic output of all cases are verified with the defined hydrodynamics from the literature study in Section 2.3.

8.1.3. Settings Delft3D FLOW

Apart from the grid and bathymetry, the settings in Delft3D FLOW are the same for each case. Ten depth layers are modeled to calculate the vertical velocity profile accordingly. The layer thickness is smaller near the top and bottom of the water column as these are the areas where the particles are located and bottom interaction with the flow occurs. A time frame of 12 hours is used, this is sufficient for modelling the particles complete trajectory from release to exit out of system and to prevent interference with spin up time. The time step is set at 1 minute.

The upstream boundary is governed by the discharge and consists of a constant value of $Q = 1250$ m^3/s. The downstream boundary is governed by the water level and remains constant with a value of 0 metres. The bottom roughness is included according to the Chezy formula with U = 65 and V = 65. The wall roughness has a length of 0.02 metres, simulating grass land (Hong, Zhao, & Zhu, 2018).

The physical representation of different values for the eddy diffusivity is not completely clear and for simplification purposes the value is remained constant along each case. Fischer et al. (2013) showed from multiple laboratory studies in a rectangular open channel that the horizontal eddy diffusivity can be between orders of 0.0001 and 1.0 m^2/s. For this study the value 0.0001 m^2/s is used. Uncertainties arise whether this value is applicable for the different cases (different values might be applicable due to hydrodynamic changes per case), but due to modelling instabilities with high values for the horizontal eddy diffusivity higher values are less functional. Vertical mixing is not included in the study thus a value for the vertical eddy diffusivity is not provided.

8.1.4. Settings D-WAQ PART

The oil model is used for particle tracking, while neglecting all oil processes (Table 7.1). A number of 10000 particles are released, as a large sample is desired for statistical representative results. Particles are released instantaneously at M = 25, with a radius of 10 metre. The horizontal dispersion settings align with the results from the parametric analysis in Table 7.4.

The modelling of wind requires three input values, namely speed, direction and wind drag percentage. A constant speed of 5 m/s is used, equal to wind speed used in chapter 4.

8.1.5. Calculating Particle Distribution

Particle distributions along the cross-section are calculated and compared between upstream and downstream locations. The cross-section is divided in 100 cells, which equals 2.5 metres per cell. For each cell the amount of particles passing through during the simulation time is calculated at an upstream and downstream location. The upstream measurement location is set at cell M = 60. This is located well below the initial release (but above the river element), at cell M = 25, where the particles are well mixed and better represent the litter distribution of a river. The downstream location varies according to the case and is located downstream of the river element. For the straight channel, widening and groyne case the downstream measurement location is set at M = 120. For the riverbend the downstream measurement location is located at M = 250. The downstream measurement location of the river confluence is located at M = 270.

The QUICKPLOT tool, which is integrated in the D-WAQ PART interface, does not provide tools to plot the particle counts along the channel cross-sections. Therefore, a code is written in Python 3.7.1 that reads the export MAT file of the D-WAQ output. At each location, upstream and downstream, the amount of particles passing through at each cell is calculated. Then, the upstream particle count is subtracted from the downstream particle count to calculate the relative particle count between the downstream and upstream locations. This is done for each of the 100 cells, representing the relative particle count across the cross section, and plotted against the channel width.

8.2. RESULTS

For each of the cases the hydrodynamics are modeled and the resulting particle tracking. A calculation is made on the effect of the hydrodynamic conditions on the cross-sectional particle distribution for each case.

REFERENCE CASE

In Appendix D.1 the flow velocities at M = 60 and M = 120 for the reference case are displayed. Location M = 60 is located more upstream than location M = 120. The traveling distance between these two points is around 1700 metres. As the bathymetry and grid are very constant no changes in flow velocities are observed between these two locations. The flow velocity reduces near the wall and bottom due to bottom and wall roughness.

Figure 8.2 shows the cross sectional distribution of each macro plastic class compared between the locations. For all three modeled plastic objects little variation in the cross-sectional concentration distribution is observed. This is expected as the hydrodynamics are very constant. A slight reduction in the centre and an increase near the river edges is observed, a result of the dispersion from the initial release in the centre of the channel.
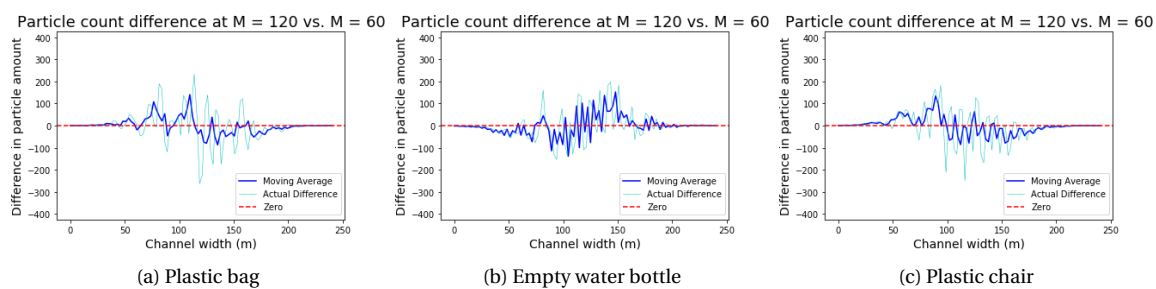

| (a) Plastic bag | (b) Empty water bottle | (c) Plastic chair |

Figure 8.2: Cross-sectional distribution of particle tracking for the reference case between M = 60 and M = 120

RIVERBEND

The flow velocity at location M = 60, M = 145 and M = 250 are plotted in figure 8.3. M = 60 represents the location before the riverbend, M = 145 represents the location in the middle of the bend and M = 250 is after the riverbend. After the bend a small change in the velocity profile is observed with a slight increase in velocity towards the right.

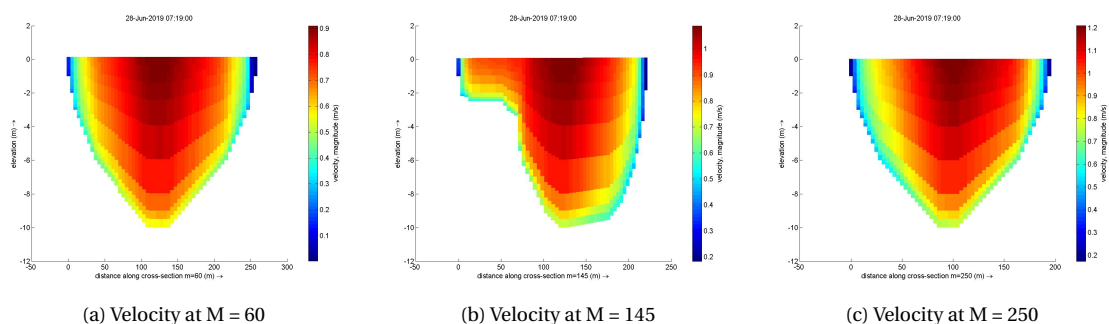| (a) Velocity at M = 60 | (b) Velocity at M = 145 | (c) Velocity at M = 250 |

Figure 8.3: Flow velocity along different cross-sections for riverbend case

Figure 8.4 displays the vertical velocity in the middle of the riverbend at M = 145. Maximum vertical velocities of $0.006 - 0.008$ m/s occur. These velocities are relatively low. Wind directed against the secondary flow, can possibly neglect the secondary flow effects. This is studied in Section 8.2.2.

In Figure 8.5 the cross-sectional concentration distribution is plotted. The plastic bag shows a significant shift in the concentration distribution towards the outerbend with a peak particle difference of 200 per cell. The
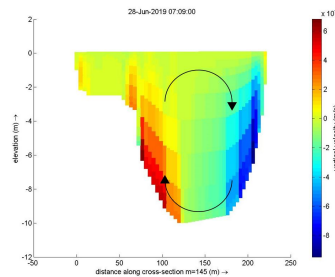
Figure 8.4: Vertical velocities at M = 145

plastic chair distribution is similar to the plastic bag but with lower extreme values and a maximum particle count increase of around 100 particles per cell. Significant changes in the particle concentration distribution of the empty water bottle occur, but does not develop a clear pattern. This contradicts the hypothesis in chapter 6, which stated that empty water bottles are affected the most by the secondary flow (due to their low response time).

(a) Plastic bag   (b) Empty water bottle   (c) Plastic chair
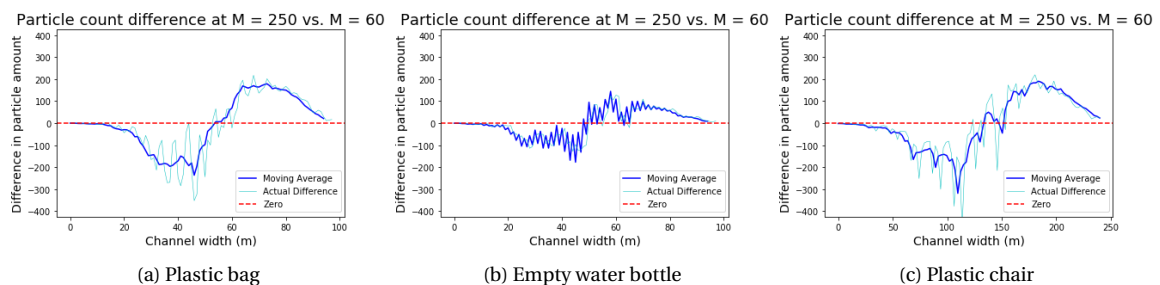
Figure 8.5: Cross-sectional distribution of particle tracking along a riverbend between M = 60 and M = 250

CHANNEL WIDENING

Appendix D.2 displays the velocity profile up- and downstream of the widening. A disturbance in the flow field occurs after the widening. Figure 8.6 shows the formations of eddies downstream of the channel widening. This is in line with hydrodynamics in a channel widening from the literature study. In Figure 8.7 the distribution of particles before (at M = 60) and after (at M = 120) the channel widening are compared. For all classes a strong reduction of plastic concentration occurs in the channel centre. A concentration increase on the channels left and (more significantly) right occurs.
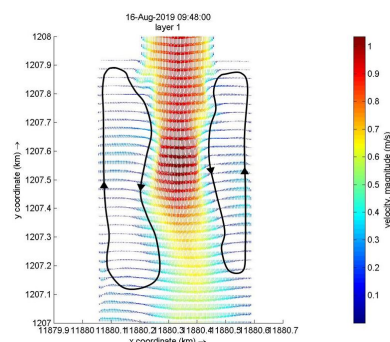

Figure 8.6: Eddy formations near channel widening

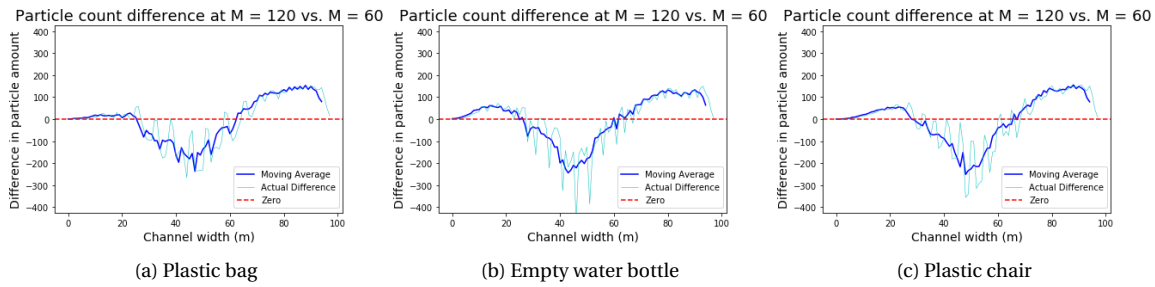(a) Plastic bag   (b) Empty water bottle   (c) Plastic chair

Figure 8.7: Cross-sectional distribution of particle tracking along a channel widening between M = 60 and M = 120
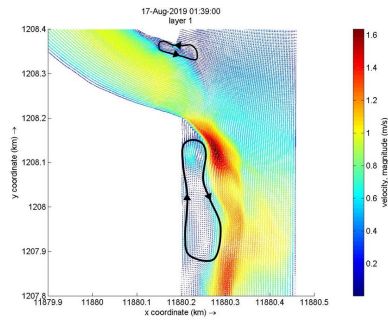

Figure 8.8: Eddy formations near confluence

RIVER CONFLUENCE

Appendix D.3 shows the velocity profiles of a river confluence. Upstream of the confluence, at M = 60, the flow velocity is significantly lower. This, as the upstream discharge boundaries are split along the tributary channel and main channel. Downstream of the confluence the total discharge is similar to the other cases, hence velocity profile looks more similar. Figure 8.8 shows the formations of eddies. This align with the literature study from Section 2.3 as a stagnant zone and separation zone are observed. Figure 8.9 displays the cross-sectional distributions of the macro plastic classes. For all types an increase in particle counts along the tributary side of the channel is observed of similar value.

(a) Plastic bag   (b) Empty water bottle   (c) Plastic chair
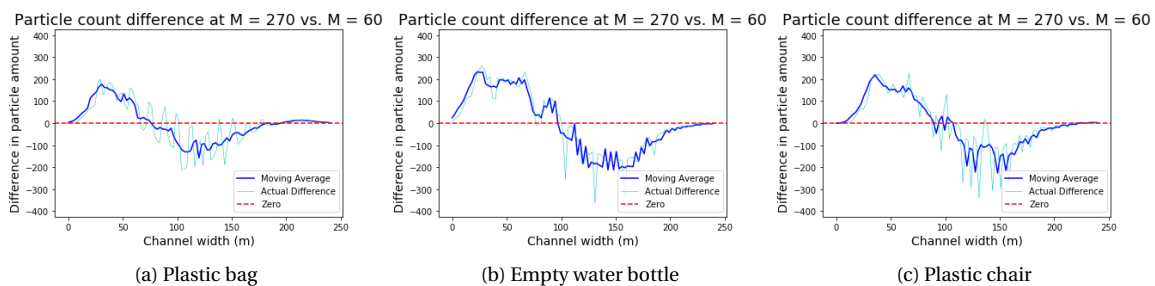
Figure 8.9: Cross-sectional distribution of particle tracking along a channel confluence between M = 60 and M = 270

GROYNE

The modeled groyne is 80 metres long, is located at M = 90 and induces a strong disturbance in the flow. Figure 8.10 shows the hydrodynamics near the groyne. As formulated in Section 6, a recirculating zone develops behind the groyne.

Figure 8.11 displays the relative cross-sectional macro plastic concentration distribution between two locations; M = 60 located upstream of the groyne and M = 120 located downstream of the groyne. A shift in the concentration distribution of plastic bags to the right is observed, with a maximum increase of over 300 particles per cell. Plastic chair concentrations shifts to the right as well with an increase of maximum of 250

(a) Velocity

(b) Velocity at cross-section M = 90

Figure 8.10: flow velocity near groyne structure

particles per cell. The empty bottle concentration decreases behind the groyne and increases on the right side of the river with a maximum of around 200 particles per cell.
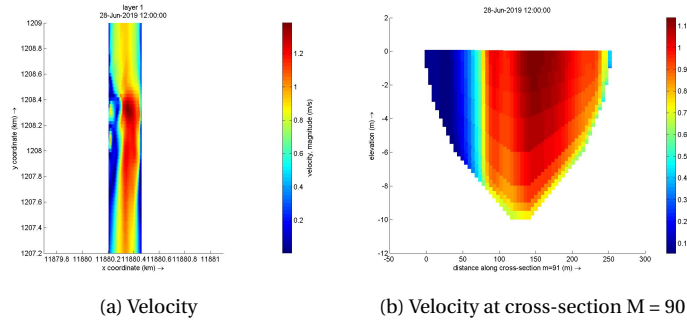

(a) Plastic bag

(b) Empty water bottle

(c) Plastic chair
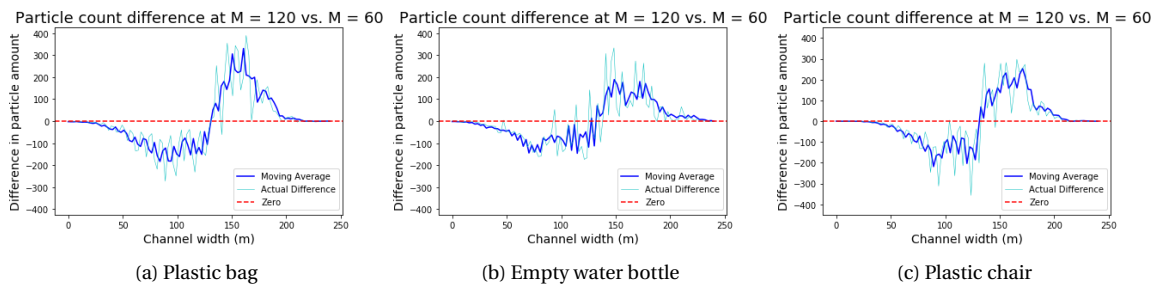
Figure 8.11: Cross-sectional distribution of particle tracking along a groyne between M = 60 and M = 120

8.2.1. DISCHARGE

The effects of increased discharge on the secondary flow and particle distribution are analyzed. The river bend case is now subjected with a doubling of the discharge, from 1250 kg/m^3 to 2500 kg/m^3. In Appendix D.4 the velocity profiles are displayed at M = 60, M = 145 and M = 250. Maximum channel velocities vary from 1.6 m/s upstream of the bend to 2.2 m/s downstream of the bend.

Figure 8.12 shows a significant increase in vertical flow velocities, compared to normal discharge case in Figure 8.4 to 0.01 m/s. In Figure 8.13 the difference in the cross-sectional distribution between M = 60 and M = 250 are plotted. In a high discharge case, the distribution of each plastic object changes. Both the plastic bag and chair disperse very little and concentrate towards the channels centre. The water bottle increases in dispersion and is concentrated more towards the outerbend.

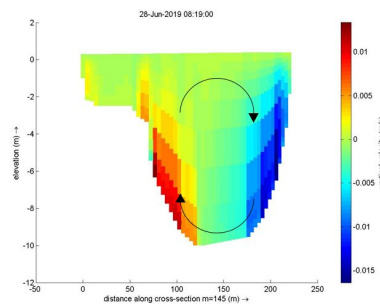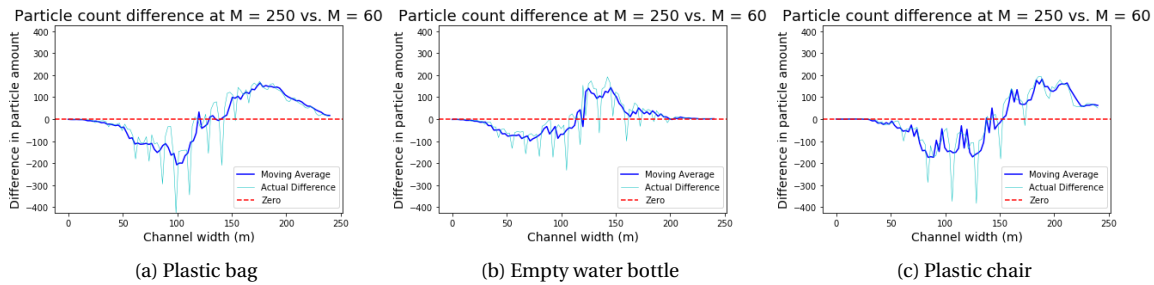Figure 8.12: Vertical velocities at M = 145 with high discharge

Figure 8.13: Cross-sectional distribution of particle tracking along a riverbend with high discharge between M = 250 and M = 60

8.2.2. WIND

In this case wind is included along a riverbend. The wind drag percentages defined in Table 7.5 are used. In Figure 8.14 the cross-sectional particle distribution is displayed, comparing between M = 60 and M = 250. Both the plastic bag and chair have relatively low wind drag percentages, and wind effects are not observed. The empty bottle does show significant transport towards the left side of the river (inner bend) compliant with the given wind direction.
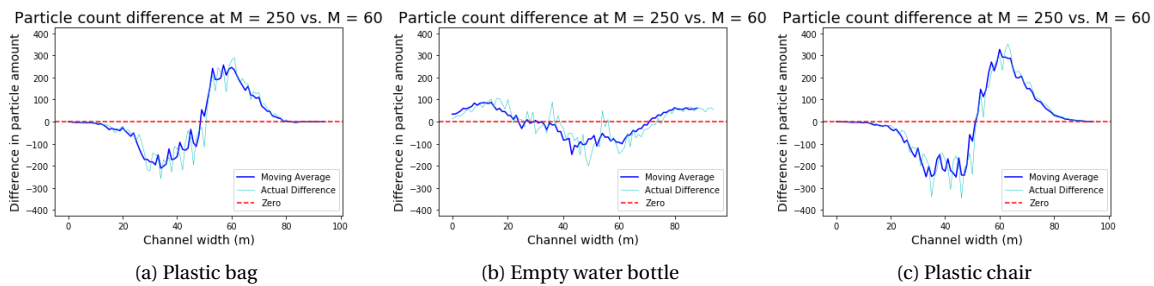
Figure 8.14: Cross-sectional distribution of particle tracking along a riverbend with wind forcing between M = 250 and M = 60

8.3. DISCUSSION

The constructed bathymetries for each case provide moderate representations of reality. For better representation and modelling results, it is advised to perform a case study.

A study on the effect of changes in wind and discharge on the cross-sectional particle distribution along a riverbend are performed. It is expected that riverbend characteristics also effect the particle distribution, i.e. riverbend angle. This accounts also for the other cases, e.g. groyne length, widening ratio etc.

The value for a horizontal eddy diffusivity is motivated according to laboratory results as described by Fischer et al. (2013). In addition, these values are held constant for the different scenarios to simplify the modelling process. This simplification provides an uncertainty to the results.

The effect of the wind is modeled in D-WAQ PART. Similar to the analytical model, only the particle is affected by the wind. The top of water column is not. In reality, the top of the water column adjusts (partially) to wind conditions and enhances wind effects. Wind effects are therefore expected to be more pronounced in reality, even for plastic bags which have barely any wind exposure, and are expected to reduce secondary flow effects. A possibility to account for theis is the modelling of wind in the hydrodynamics (Delft3D FLOW), but this does require more computing power.

The numerical models did not display any retention of particles. For example, in the flow study it was hypothesized that groynes can retain large amounts of material. Whether the model performs poorly on simulating accumulation or these are expected results regarding chosen input values is not clear. Further testing of the model and, if possible, validation data is required.

The expected particle diffusion according to Fischer et al. (2013) is a factor 5 larger than what is observed from the numerical model. This identifies uncertainties within the model results. Regarding future studies, this problem should be addressed. Therefore the current results of the numerical model provide a limited physical representation. Instead these should be interpreted as first insights in relative behavior of the different macro plastic classes which highlights specific cases and areas along a channels cross-sectional that are of interest for further investigation.

When modelling a passive tracer along a straight channel the particles where fully mixed after only ∼ 63 kilometers. This is a significant difference of a factor 100 compared to estimations made by Fischer et al. (2013). Within the limits of this thesis this problem is not addressed but should be taken into consideration in future studies. As such, the results of chapter 8 provide a limited physical representation. Instead the numerical study in chapter 8 provides first insights in relative behavior of the different macro plastic classes and highlights cases and areas along a channels cross-sectional that are of interest for further investigation.
Vertical mixing is neglected. In reality such behaviour has a significant effect on longitudinal particle diffusion due to the logarithmic velocity profile along the vertical.

8.4. Summary and Conclusion

The case study uses the numerical models Delft3D FLOW and D-WAQ PART to model the hydrodynamics and particle tracking for the proposed river elements from Section 6. The macro plastic particles in the numerical models are described using the dispersion and Stokes number relation formulated in chapter 7.

First a straight channel is modeled. Little change in the particle distribution is observed as expected. When each of the macro plastic classes are subjected to a river bend case an increase in the particle concentration near the outerbend is observed, especially for the plastic bag and chair. The general hypotheses in chapter 6 for the river bend is confirmed, but for the different plastic objects a difference is observed. The empty water bottle seems to be barely effected by the secondary flow. This is not expected as chapter 6 concluded that the empty water bottle is more responsive to secondary flow and concentrate more along the outer bend. The numerical model is not able to model the particle response time, but only the effect of the particle response time on the particle dispersion. This is not the same and particle response time and Stokes number related dispersion seem to behave counter intuitively when looked at separately.

The channel widening imposes a similar cross-sectional distribution for all three classes. In the centre a relative decrease in concentration is observed. An increase near the channel boundaries occur. This is in line with the formulated hypothesis in chapter 6. The empty water bottle does not show very different particle distribution, although a relative increase along the channel centre (compared to the plastic bag and chair) is expected (Table 6.2).

The river confluence also shows similar cross-sectional distributions for all three classes. An increase in particle concentrations at the tributary side of the channel is observed. This is in line with the predictions in chapter 6. However, the empty water bottle seems to transport more towards the tributary side in comparison with the plastic bag and chair. This contradicts the predictions made in Table 6.3.

The groyne shows again a similar distribution for all three classes. A increase in particle concentrations along the groyne free side of the river are observed. This is in line with hypotheses formulated in chapter 6. Plastic bags show the larges increase in particle count along the groyne free side of the channel, with a maximum of 300 particles per cell. This is less than 200 for the empty water bottle. Table 6.4 predicted that empty water bottles would show relative increase in particle concentrations near the groyne free side of the channel compared to the plastic bag and chair.

An increase in discharge showed a significant increase in secondary flow conditions. A slight increase in particle concentrations near the outerbend for the empty water bottle and plastic chair is observed. A slight decrease is observed for the plastic bag and chair. The increase in outer bend concentrations for the empty water along the outer bend is expected, but strangely no increase in concentrations for the plastic bag and chair are observed.

The modelling of wind does not have impact on the cross-sectional distributions of the plastic bag or chair. The empty water bottle does show a significant impact. This is expected due to the high wind drag percentage of wind.

For all most all cases the general hypothesis is confirmed. Individual expectations for each macro plastic type cohere less with the results. Often expected differences between the empty water bottle and plastic bag and chair are not very pronounced. Only the riverbend, with normal discharge conditions, and wind case behave as expected. For the other cases, the difference in relative dispersion is of limited effect to the cross-sectional particle distribution or partially confirms expected behaviour of each plastic object. This proposes that either 1) using the horizontal dispersion coefficient is not a very effective tool in describing relative horizontal particle dispersion, 2) the amount of 10000 modeled particles is not enough to give a statistical representation of particle transport or 3) the dispersion relation as described by *Crowe* is not sufficient for describing buoyant macro plastics dispersion and 4) the constructed hypotheses for each class are not correct.

IV. Evaluation

9

DISCUSSION

9.1. DISCUSSION

This study has identified the significance, diversity and complexity of macro plastic particles in riverine environments. It highlights the need for classification and simplification to facilitate modelling and still be able to obtain relevant results. Describing macro plastics according to cornerstones in behaviour, proposed by Table 5.1, provides a tool for simplifying modelling to a select group of plastics. Coupling of different macro plastic classes to a range of riverine environments and understanding the differences in behaviour (in this study the cross-sectional distribution is used as a benchmark to analyze their behaviour) provides much practical use.

As an example a hypothetical situation is constructed where a framework of macro plastic particle motion and macro plastic classification are fully developed. Rio lives near a river and wants to reduce the plastic pollution in his river as the water quality is deteriorating. Rio knows that his river is mainly polluted by single type plastics such as plastic bags and empty water bottles. Rio can analyze the characteristic river elements and wind conditions that occur along his river. According to the framework of macro plastic particle motion and the dominant polluting plastic classes, Rio can now start to predict where the different plastic classes are concentrated and monitor at these locations. This is effective and time-saving for Rio as a limited amount of samples are required to identify areas of interest for possible extraction of macro plastics. Rio has good insight how and what kind of plastics concentrate along the river. This scenario greatly simplifies the macro plastic pollution problem of Rio's river.

Tools such as satellite and drone imaging will help to validate modelling results. Together with the classification of macro plastics and the developed understanding of the different types, targeted areas can be mapped and plastic pollution hotspots can be identified. In case vertical macro plastic transport processes are included in future models and more data is available on how bottom and surface level plastic concentrations relate, modelling approaches together with satellite or drone imaging can provide 3D mapping of the plastic pollution in rivers on a global scale.

With a developed understanding of the cross-sectional distribution for different macro plastic classes ultimately effective monitoring locations along the channel cross-section can be identified. Currently research in field studies perform measurements along the top layer of the water column (van Emmerik et al., 2018), mainly due to limitations on proper vertical measuring tools, and have a limited understanding of how their measurements represent the true plastic composition of the river. With an improved understanding of the cross-sectional distribution of macro plastics in rivers along different riverine environments (i.e. river bend or groyne) and the vertical distribution of plastics, representative monitor locations can be identified. Together with improved modelling techniques, transport can be extrapolated along the river which limits the amount of sampling required.

10

CONCLUSION AND RECOMMENDATIONS

10.1. CONCLUSION

The objective of this thesis is stated as follows:

"Improve the modelling and understanding of buoyant macro plastic forces and their effect on the cross-sectional distribution of buoyant macro plastics in rivers"

To improve the modelling and understanding of buoyant macro plastic transport simplifications are required. Using a classification tool according to cornerstones in behaviour provides an interesting tool to reduce modelling complexity. Three distinct classes are identified; Added mass (represented by plastic bag), dominance of buoyancy (represented by an empty water bottle) and massive objects (represented by a plastic chair). The particle response times for each class are used to describe their relative behaviour, where empty water bottles show low response times and plastic bags and chairs have high particle response times. Particle response times are generally used for submerged particles. As buoyant macro plastics are not fully submerged a new relation between particle response times and particle density and size is found. Where particle density does not affect the response time, due to a balance in change between drag area and weight, and particle diameter results in a linear increase in the particle response time.

According to the relation between particle response times and particle diffusivity particle transport for each of the classes is translated into a numerical model. Here, the cross-sectional particle distribution in a variety of cases is analyzed to compare behaviour between each class. For all scenarios the general hypothesis on the buoyant macro plastic distribution is confirmed. This provides that river bends increase the macro plastic concentration along the outer bend. Channel widening increases the concentration along the boundaries. A river confluence increases the concentration along the tributary side of the channel. A groyne increases the macro plastic concentration along the groyne free side of the channel. Differences in the cross-sectional particle distribution between the different classes are only observed for the river bend case. Along the river bend case natural separation between the empty water bottle and plastic bag and chair is observed which proposes areas of interest for validation.

1) What are expected forces that drive buoyant macro plastic transport in rivers?

Buoyant macro plastic particles are exposed to wind, water current and gravitational forces. Plastic bags have minimal exposure and experience less wind drag. Empty water bottles have a significant wind exposure and interact with the riverbank ten times faster than plastic bags and chairs with lateral wind conditions. As the river width is small compared to its length lateral wind conditions are likely to cause particle interaction with the riverbank. This can result in a temporary sink.

Added mass is found to be an important factor that contributes to the response time. Especially for plastic bags which can enclose a volume of water 100 times its own mass. This results in a significant increase of the response time of a plastic bag.

2) How can existing numerical modelling functionalities be used for the modelling of horizontal buoyant macro plastic particle dispersion in rivers?

Particle response times and their relation to Stokes number and particle dispersion proposes an interesting tool for the modelling of relative particle motion towards the flow and the different macro plastic objects. The modelling results are mixed. Along a river bend significant difference in behaviour is modeled between empty water bottles and plastic bags and chairs. For the other scenarios the model does not always satisfy the hypotheses (those formulated specifically for each plastic type) and the difference in cross-sectional distributions is often very small. Validation data is required to give a definitive answer on the model performance.

3a) What is the effect of macro plastic characteristics (size and density) on particle dispersion?

Generally the particle response time is described for submerged particles. Buoyant macro plastics, as modeled in the analytical model, are not fully submerged. Hence, a different relation between particle size and density and the particle response time develops. A linear relation between size and response time is observed and a constant relation between density and particle response time (when neglecting added mass). This is a result of the buoyant properties of the particle and the balance between the contact area of the flow induced drag force and change in particle mass. An increase in particle diameter does not result in equal increase of the flow contact area as part of the object is above the water level. An increase in density results in an increase in mass and an increase in flow contact area (as particle draught increases) which balances one another.

Massive particles experience a high response time. This results in a moderate Stokes number $Stk \sim 1$. Due to centrifugal forces of large eddy structures massive particles disperse more, given the rive bed induced surface level turbulence.

Low density particles experience low response times. An example are the empty water bottles. Interestingly, the analytical model provides that an increase in response time occurred for extremely low densities. This is caused by the extremely low draught of extremely low density particles. In reality this effect is expected to be less pronounced.

3b) What is the effect of river geometry and structures on the cross-sectional distribution of buoyant macro plastics in rivers?

The river bend hydrodynamics have a significant effect on the cross-sectional distribution. Especially for the plastic bag and plastic chair, which show a significant shift of the distribution towards the outer bend. The effects on the empty water bottle are less pronounced. This contradicts the hypotheses in the flow study, which assumes that due to the low response time of empty water bottles they are more subjected to the secondary flow. Using the dispersion coefficient as a parameter for describing macro plastic transport in the numerical model is not sufficient to explain this behaviour.

For all scenarios the general hypothesis on the buoyant macro plastic distribution is confirmed. This provides that river bends increase the macro plastic concentration along the outer bend. Channel widening increases the concentration along the boundaries. A river confluence increases the concentration along the tributary side of the channel. A groyne increases the macro plastic concentration along the groyne free side of the channel.

The individual hypothesis per macro plastic object follows less agreement with the modelling results. This proposes that either 1) using the horizontal dispersion coefficient is not a very effective tool in describing relative horizontal particle dispersion, 2) the amount of 10000 modeled particles is not enough to give a statistical representation of particle transport or 3) the dispersion relation as described by *Crowe* is not sufficient for describing buoyant macro plastics dispersion and 4) the constructed hypotheses for each class are not correct.

3c) What is the effect of external forcing (wind and discharge) on particle dispersion?

Lateral wind conditions against the secondary flow are modeled. Particles sensitive to wind (empty water bottle) show that the secondary flow effect can be counteracted by wind, reducing the particle dispersion. Furthermore, wind can also increase dispersion and cause interaction with the riverbank. An increase in discharge is expected to increase secondary flow effects and therefore dispersion towards the outer bend. However, this was limitedly observed from the modelling.

4) How can buoyant macro plastic behaviour in rivers be classified?

Macro plastics have a wide range of properties, which is complicating the modelling of riverine transport. Classifying macro plastics according to cornerstones in behaviour proposes an efficient tool to mitigate the complexity. These cornerstones are the boundaries where within macro plastics behave and provide a framework of (buoyant) macro plastic particle motion. An introduction to classifying macro plastics is made in this study. This study focuses on three distinct classes, namely added mass, dominance of buoyancy and massive particles. The particle transport of each class varies. This suggests that classifying macro plastics is a relevant tool for describing behaviour and improves modelling approaches. In addition, classification of plastics provides practical use. In relation to model findings for the different classes, local classification of plastic litter input can be used for predicting transport and motivates locations for monitoring or plastic extraction.

5) What areas along a river are of interest for macro plastic monitoring and the application of riverine plastic extraction?

River bend modelling indicate natural separation occurs between dispersive and less dispersive particles, in this case plastic bags and chairs and empty water bottles, between the outerbend and channel centre. This proposes an interesting area for extraction of plastic bags and chairs along the outer bend and along the channel centre for water bottles. Depending on the dominant litter input of the river, for either of these areas a motivation for the type of plastic extraction can be made.

In the other scenarios the difference in particle distributions between different classes is limited, hence the use of natural separation does not apply. For these locations interesting extraction locations are at the areas where concentration is along the cross-section are the highest. Suggested areas are; along the channel boundaries downstream of a channel widening, along the confluence side of a channel downstream of the confluence and downstream of the groyne along the groyne free side of the channel.

Monitoring locations that are of interest are those that impose validation for this study and ultimately the use of Stokes number and horizontal particle dispersion coefficients for the modelling of relative particle motion between flow and different particles. Of particular interest is the modeled difference in cross-sectional distribution of plastic bags and chairs between the empty water bottle. Field samples could identify whether such natural separation is observed in real rivers.

10.2. Recommendations

The results from this study promote the simplified modelling of macro plastic transport according to plastic classification and particle response times. Simplified modelling is desired, but research is still in its early stage. Due to many assumptions and complex nature of macro plastic transport the results from this research should be used carefully. As such, these results are preferably used to motivate further classification of macro plastics and the use of response times to simplify modelling and motivate areas along the river cross-section for field measurements to validate results.

Interestingly, the relation between particle response time and particle density and size, as described by Equation 4.8, does not hold for buoyant macro plastic particles. Particle density does not effect the particle response time of a buoyant macro plastic particle and particle diameter shows a linear relation with the particle response time. This result suggests that particle density does not play a role in defining particle response times for buoyant material. Whether this relation holds in reality can be researched in future studies using laboratory tests.

The numerical model results involve uncertainties regarding the physical representation of the modeled particle diffusion. Differences are observed between the expected mixing length of released particle based on laboratory and field studies compared to results from the numerical model. Regarding future studies, this problem should be addressed.

This study proposes first steps in classifying macro plastics and their transport. Three classes are identified, namely added mass, dominance of buoyancy and massive particles. For future studies it is recommended to further investigate and expand on the proposed classifications.

Vertical mixing of macro plastics is expected to be relevant for the fate of macro plastic particles. Due to the range of properties, some particles are subjected to vertical mixing and others are not, e.g. plastic bags vs. empty water bottles. In combination with logarithmic vertical velocity profiles vertical mixing induces longitudinal dispersion of material. In addition, wind effects become practically non-existent for particles that are easily mixed vertically. In future studies it is recommended to investigate the possibilities of modelling vertical mixing within existing numerical functionalities. In Chapter 6 a proposal is made of parameters in D-WAQ PART which relate to vertical transport of macro plastic particles.

The effect of wind and discharge on the macro plastic distribution is briefly modeled in Chapter 7. Within the limits of this thesis the effects of wind and discharge are only modeled for a river bend scenario. A more elaborate study on the effect of wind and discharge on macro plastic transport for each class is beneficial as environmental conditions constantly change and vary in strength.

In Chapter 7 suggestions are made on the behaviour of macro plastics along specific scenarios. Modelling results show natural separation can occur along a river bend. This provides an interesting area for plastic extraction solutions. Measuring macro plastic concentrations along the outer bend and channel centre can be used for validation. Ideally a case is modeled, where bathymetry, wind, discharge data and plastic measurements are available. This not only provides a representative topography and grid for improved numerical modelling, but also strengthens validation.

This study proposes the use of particle response times and the relation to Stokes numbers and particle dispersion as a tool for modelling relative behaviour of macro plastic particles. The model output showed some promise, the effects of river geometries and structures often aligned with the formulated hypothesis from chapter 6. Relative motion between the different classes was in some cases less than expected. A more elaborate study on the effect of characteristics of the river elements, e.g. river bend angle or groyne length, larger range of wind and discharge conditions in the numerical model could provide more insight in the models performance, especially in combination with validation data.

In this study the particle dispersion compared to the flow is modeled using the horizontal particle dispersion coefficient in D-WAQ PART. The dispersion in D-WAQ PART is derived from a random walk model, applied on top of a tracer particle. Chapter 4 described the increased dispersion of different macro plastic particles in eddies is a result of particles shooting out of vortice structures, beyond the vortice reach, due to the particles inertia. The numerical model is a simplified representation of this dispersive behaviour. Other models with different horizontal dispersion modelling techniques can be used to understand what model best approaches real dispersion.

This research considers the use of river bed induced surface plane turbulence for calculating the Stokes number and eventually particle dispersion. Multiple forms of turbulence occur in rivers and on a range of scales. Expansion on the effects of other types of turbulence in rivers is advised to characterize dominant turbulence types in rivers for buoyant macro plastics.

Only limited field data of macro plastic transport in rivers is publicly available. Availability of data should increase and diversify more in the future. Here, diversify refers to; more measurements along different river scenarios and areas along the rivers cross-section. As limited data of field measurements are publicly available, validation of studies is hampered. Field measurements are time consuming and expensive and limits the growth of executed measurements. This study suggests the buoyant macro plastic cross-sectional distributions are characterized by the riverine environment. These areas impose of direct interest for field studies.

REFERENCES

Alibaba. (2019). *Plastic chair weight.* https://www.alibaba.com/products/F0/plastic_chair_weight.

American-Samoa. (2009). Weight of aluminum cans and pet beverage bottles without caps. *American Samoa Power Authority Materials Management Office.*

Andrady, A. L., & Neal, M. A. (2009). Applications and societal benefits of plastics. *Philosophical Transactions of the Royal Society B: Biological Sciences, 364*(1526), 1977–1984.

Armanini, A. (2018). Introduction to sediment transport. In *Principles of river hydraulics* (pp. 33–47). Springer.

Atkin, E. (2018). The global crisis of plastic pollution. *The New Republic.*

Bahrami, M. (2009). *Fluid mechanics.* Simon Fraser University.

Battjes, J. A., & Labeur, R. J. (2017). *Unsteady flow in open channels.* Cambridge University Press.

Best, J. L., & Reid, I. (1984). Separation zone at open-channel junctions. *Journal of Hydraulic Engineering, 110*(11), 1588–1594.

Blettler, M. C., Abrial, E., Khan, F. R., Sivri, N., & Espinola, L. A. (2018). Freshwater plastic pollution: Recognizing research biases and identifying knowledge gaps. *Water research.*

Borda-carnot equation. (2018). https://en.wikipedia.org/wiki/Borda\T1\textendashCarnot_equation.

Bosboom, J., & Stive, M. J. (2015). *Coastal dynamics 1.* Delft Academic Press.

Braudrick, C. A., & Grant, G. E. (2000). When do logs move in rivers? *Water resources research, 36*(2), 571–583.

Braudrick, C. A., Grant, G. E., Ishikawa, Y., & Ikeda, H. (1997). Dynamics of wood transport in streams: a flume experiment. *Earth Surface Processes and Landforms: The Journal of the British Geomorphological Group, 22*(7), 669–683.

Brethouwer, G. (2005). The effect of rotation on rapidly sheared homogeneous turbulence and passive scalar transport. linear theory and direct numerical simulation. *Journal of Fluid Mechanics, 542,* 305–342.

Brown, J. K. (1974). *Handbook for inventorying downed woody material.* USDA Forest Service.

Cartwright, J. H., Feudel, U., Károlyi, G., De Moura, A., Piro, O., & Tél, T. (2010). Dynamics of finite-size particles in chaotic fluid flows. In *Nonlinear dynamics and chaos: Advances and perspectives* (pp. 51–87). Springer.

Chias, J. (2018). For animals, plastic is turning the ocean into a minefield. *National Geographic.*

Clara Chrzanowski, M. T. W. K., Dana Stuparu. (2016). *Transport van plastics in de haven van rotterdam.* Deltares.

Crowe, C., Chung, J., & Troutt, T. (1988). Particle mixing in free shear flows. *Progress in energy and combustion science, 14*(3), 171–194.

Ecomerge. (2011). *The weight of paper and plastic.* http://ecomerge.blogspot.com/2011/02/weight-of-paper-and-plastic.html.

Einstein, A. (1926). The cause of the formation of meanders in the courses of rivers and of the so-called baer's law. *Die Naturwissenschaften, 14*(11), 223–224.

Engineering toolbox. (2019). https://www.engineeringtoolbox.com/liquids-densities-d_743.html.

The facts 2017. (2017). PlasticsEurope.

Finlay, W. H. (2019). Chapter 3 - motion of a single aerosol particle in a fluid. In W. H. Finlay (Ed.), *The mechanics of inhaled pharmaceutical aerosols (second edition)* (Second Edition ed., p. 21 - 52). London: Academic Press. Retrieved from http://www.sciencedirect.com/science/article/pii/B9780081027493000038 doi: https://doi.org/10.1016/B978-0-08-102749-3.00003-8

Fischer, H. B., List, J. E., Koh, C. R., Imberger, J., & Brooks, N. H. (2013). *Mixing in inland and coastal waters.* Elsevier.

Franca, M. J., & Brocchini, M. (2015). Turbulence in rivers. In *Rivers–physical, fluvial and environmental processes* (pp. 51–78). Springer.

Garcia, X.-F., Schnauder, I., & Pusch, M. (2012). Complex hydromorphology of meanders can support benthic invertebrate diversity in rivers. *Hydrobiologia, 685*(1), 49–68.

Gasperi, J., Dris, R., Bonin, T., Rocher, V., & Tassin, B. (2014). Assessment of floating plastic debris in surface water along the seine river. *Environmental pollution, 195,* 163–166.

Globalalert. (2016). *Globalalert.org.* http://globalalert.org/.

Goddijn-Murphy, L., Peters, S., Van Sebille, E., James, N. A., & Gibb, S. (2018). Concept for a hyperspectral remote sensing algorithm for floating marine macro plastics. *Marine pollution bulletin, 126*, 255–262.

González, D., Hanke, G., Tweehuysen, G., Bellert, B., Holzhauer, M., Palatinus, A., . . . Oosterbaan, L. (2016). Riverine litter monitoring—options and recommendations. *MSFD GES TG Marine Litter*.

Gourmelon, G. (2015). Global plastic production rises, recycling lags. *New Worldwatch Institute analysis explores trends in global plastic consumption and recycling. Recuperado de http://www. worldwatch. org*.

Graf, W., & Blanckaert, K. (2002). Flow around bends in rivers. , 24–28.

Gregory, M. R. (2009). Environmental implications of plastic debris in marine settings—entanglement, ingestion, smothering, hangers-on, hitch-hiking and alien invasions. *Philosophical Transactions of the Royal Society B: Biological Sciences, 364*(1526), 2013–2025.

Guerrero, L. A., Maas, G., & Hogland, W. (2013). Solid waste management challenges for cities in developing countries. *Waste management, 33*(1), 220–232.

Hickin, E. J. (2004). *River hydraulics and channel form.* Wiley, Chichester.

Hong, S.-W., Zhao, L., & Zhu, H. (2018). Saas, a computer program for estimating pesticide spray efficiency and drift of air-assisted pesticide applications. *Computers and Electronics in Agriculture, 155*, 58–68.

Hoult, D. P. (1972). Oil spreading on the sea. *Annual review of Fluid mechanics, 4*(1), 341–368.

Householder, M., & Goldschmidt, V. (1968). Turbulent diffusion and turbulent schmidt number of small particles. In *Part i, am. soc. civil engr., national meeting on environmental engineering, chattanooga, tenn.*

Huang, S.-l., Jia, Y.-f., Hsun-Chuan, C., & Sam, S. (2009). Three-dimensional numerical modeling of secondary flows in a wide curved channel. *Journal of Hydrodynamics, Ser. B, 21*(6), 758–766.

Jambeck, J. R., Geyer, R., Wilcox, C., Siegler, T. R., Perryman, M., Andrady, A., . . . Law, K. L. (2015). Plastic waste inputs from land into the ocean. *Science, 347*(6223), 768–771.

Ji, Z.-G. (2008). *Hydrodynamics and water quality: modeling rivers, lakes, and estuaries.* John Wiley & Sons.

Kooi, M., Besseling, E., Kroeze, C., Van Wezel, A. P., & Koelmans, A. A. (2018). *Modeling the fate and transport of plastic debris in freshwaters: review and guidance.* Springer, Cham.

Lammerts, M. (2016). *Marine litter in port ares - developing a propagation model.* TU Delft.

Lebreton, L., Slat, B., Ferrari, F., Sainte-Rose, B., Aitken, J., Marthouse, R., . . . others (2018). Evidence that the great pacific garbage patch is rapidly accumulating plastic. *Scientific reports, 8*(1), 4666.

Lebreton, L. C., Van der Zwet, J., Damsteeg, J.-W., Slat, B., Andrady, A., & Reisser, J. (2017). River plastic emissions to the world's oceans. *Nature communications, 8*, 15611.

Li, A., & Ahmadi, G. (1992). Dispersion and deposition of spherical particles from point sources in a turbulent channel flow. *Aerosol science and technology, 16*(4), 209–226.

Littler, J., & Thomas, R. (1984). Waste disposal and utilization. In *Design with energy: The conservation and use of energy in buildings* (p. 293–303). Cambridge University Press. doi: 10.1017/CBO9780511627248.011

Liu, R., Vanka, S. P., & Thomas, B. G. (2014). Particle transport and deposition in a turbulent square duct flow with an imposed magnetic field. *Journal of Fluids Engineering, 136*(12), 121201.

Marshall, J. (2005). *Environmental health: Megacity, mega mess...* Nature Publishing Group.

Materialen, G. (n.d.). *Soortelijk gewicht.*

Morritt, D., Stefanoudis, P. V., Pearce, D., Crimmen, O. A., & Clark, P. F. (2014). Plastic in the thames: a river runs through it. *Marine Pollution Bulletin, 78*(1-2), 196–200.

Ottevanger, W., Blanckaert, K., & Uijttewaal, W. (2012). Processes governing the flow redistribution in sharp river bends. *Geomorphology, 163*, 45–55.

Packeverything. (2019). *Plastic bag.* https://www.packeverything.com.sg/index.php?route=product/category&path=51.

Penna, N., De Marchis, M., Canelas, O., Napoli, E., Cardoso, A., & Gaudio, R. (2018). Effect of the junction angle on turbulent flow at a hydraulic confluence. *Water, 10*(4), 469.

Peters, G., Butsch, C., Krachten, F., Kraas, F., Namperumal, S., & Marfai, M. A. (2015). Analyzing risk and disaster in megaurban systems â€"experiences from mumbai and jakarta. *Planet@ Risk, 3*(1).

Piccinini, R. B. (2011). *Eulerian-lagrangian simulation of a turbulent evaporating spray* (Unpublished doctoral dissertation). Master's thesis, ITA.

Plastic bag suppliers. (2019). https://www.plasticbagsuppliers.co.uk/clear-plastic-bags/.

Rebolledo, E. L. B., Van Franeker, J. A., Jansen, O. E., & Brasseur, S. M. (2013). Plastic ingestion by harbour seals (phoca vitulina) in the netherlands. *Marine pollution bulletin, 67*(1-2), 200–202.

Reeks, M. (1977). On the dispersion of small particles suspended in an isotropic turbulent fluid. *Journal of fluid mechanics, 83*(3), 529–546.

Rochman, C. M., Tahir, A., Williams, S. L., Baxa, D. V., Lam, R., Miller, J. T., . . . Teh, S. J. (2015). Anthropogenic debris in seafood: Plastic debris and fibers from textiles in fish and bivalves sold for human consumption. *Scientific reports*, *5*, 14340.

Rosgen, D. L. (1994). A classification of natural rivers. *Catena*, *22*(3), 169–199.

Sascha Klein, J. E. T. P. K., Ian K. Dimzon. (2018). *Analysis, occurence, and degradation.* SpringerOpen.

Sat-Imaging. (2017). *Geoeye-1.* https://www.satimagingcorp.com/satellite-sensors/geoeye-1/.

Schmidt, C., Krauth, T., & Wagner, S. (2017). Export of plastic debris by rivers into the sea. *Environmental science & technology*, *51*(21), 12246–12253.

Schulz, E. F., Wilde, R. H., & Albertson, M. L. (1954). Influence of shape on the fall velocity of sedimentary particles. *MRD Sediment Series; no. 5.*

Schwarzkopf, J. D., Sommerfeld, M., Crowe, C. T., & Tsuji, Y. (2011). *Multiphase flows with droplets and particles.* CRC press.

Shen, H. T., & Yapa, P. D. (1988). Oil slick transport in rivers. *Journal of Hydraulic Engineering*, *114*(5), 529–543.

Shukman, D. (2018). Giant plastic berg blocks indonesian river. *BBC News.*

Shumate, E. D. (1998). Experimental description of flow at an open-channel junction.

Singamsetti, S. R. (1966). Diffusion of sediment in a submerged jet. *Journal of the Hydraulics Division*, *92*(2), 153–168.

Snyder, W. H., & Lumley, J. (1971). Some measurements of particle velocity autocorrelation functions in a turbulent flow. *Journal of Fluid Mechanics*, *48*(1), 41–71.

Soo, S.-l. (1967). Fluid dynamics of multiphase systems. *WALTHAM, MASS, BLAISDELL PUBLISHING CO, 1967. 524 P, 206 FIG, 8 TAB, 886 REF.*.

Tauro, F., Porfiri, M., & Grimaldi, S. (2016). Surface flow measurements from drones. *Journal of Hydrology*, *540*, 240–245.

Taylor, G. I. (1922). Diffusion by continuous movements. *Proceedings of the london mathematical society*, *2*(1), 196–212.

Thompson, R. C., Moore, C. J., Vom Saal, F. S., & Swan, S. H. (2009). Plastics, the environment and human health: current consensus and future trends. *Philosophical Transactions of the Royal Society B: Biological Sciences*, *364*(1526), 2153–2166.

Tingsanchali, T., & Maheswaran, S. (1990). 2-d depth-averaged flow computation near groyne. *Journal of Hydraulic Engineering*, *116*(1), 71–86.

T. M. van Welsenes, E., van Utenhove, B., van Wijland, J., Memelink, R., & de Klerk. (2018). Pantai project. *TU Delft*.

Uijttewaal, W. S. (2005). Effects of groyne layout on the flow in groyne fields: Laboratory experiments. *Journal of Hydraulic Engineering*, *131*(9), 782–791.

van Emmerik, T., Kieu-Le, T.-C., Loozen, M., van Oeveren, K., Strady, E., Bui, X.-T., . . . others (2018). A methodology to characterize riverine macroplastic emission into the ocean. *Frontiers in Marine Science*, *5*, 372.

Van Franeker, J. (1985). Plastic ingestion in the north atlantic fulmar. *Marine Pollution Bulletin*, *16*(9), 367–369.

von Planta, C., Vogler, D., Chen, X., Nestola, M. G., Saar, M. O., & Krause, R. (2018). Simulation of hydro-mechanically coupled processes in rough rock fractures using an immersed boundary method and variational transfer operators. *arXiv preprint arXiv:1812.08572*.

Wagner, M., Scherer, C., Alvarez-Muñoz, D., Brennholt, N., Bourrain, X., Buchinger, S., . . . others (2014). Microplastics in freshwater ecosystems: what we know and what we need to know. *Environmental Sciences Europe*, *26*(1), 12.

Wentworth, C. K. (1922). A scale of grade and class terms for clastic sediments. *The journal of geology*, *30*(5), 377–392.

Windsor, F. M., Durance, I., Horton, A. A., Thompson, R. C., Tyler, C. R., & Ormerod, S. J. (2019). A catchment-scale perspective of plastic pollution. *Global change biology*.

Yang, R.-J., Hou, H.-H., Wang, Y.-N., Lin, C.-H., & Fu, L.-M. (2012). A hydrodynamic focusing microchannel based on micro-weir shear lift force. *Biomicrofluidics*, *6*(3), 034110.

Yokosi, S. (1967). The structure of river turbulence. *Disaster Prevention Research Institute, Kyoto University*.

Young, A., Stokes, M., & Crowe, M. (1985). The size and strength of the quadriceps muscles of old and young men. *Clinical physiology (Oxford, England)*, *5*(2), 145–154.

Yule, A. (1981). Investigations of eddy coherence in jet flows by. In *The role of coherent structures in modelling turbulence and mixing* (pp. 188–207). Springer.

Zhu, L.-S., Chao; Fan. (1998). *"chapter 18 – multiphase flow: Gas/solid".* Springer.

A

LITERATURE STUDY

A.1. MATERIAL TRANSPORT IN RIVERS

A.1.1. WOOD

textitC.A. Baudrick et al., 1997 described the transport of large woody material (LWD) in river channels Braudrick et al. (1997). LWD is longer than 1 meter and has a minimal diameter of 0.1 meters. LWD can be transported by either debris flow or stream flow. Debris flow catches LWD in its path, resulting in transport. Bigger streams are able to transport LWD further downstream where smaller pieces move further than larger pieces. This demonstrates the importance of piece length to channel width in wood log transport. The threshold for sediment transport is generally defined by the critical shear stress, whereas LWD is defined by the threshold for flotation. Depending on the density of the wood (ρ_{wood}) the flotation threshold varies (See Equation A.1, A.2 and A.3). Floating occurs when the water depth reaches the critical depth (d_c). A description of the formulas is given below:

For $\rho_{wood} < 500 \frac{kg}{m^3}$

$$\frac{\pi \rho_{wood}}{\rho_{water}} = \cos^{-}1\left(\frac{r - d_c}{r}\right) - \frac{r - d_c}{r^2}\sqrt{2d_c r - d_c^2} \tag{A.1}$$

For $\rho_{wood} = 500 \frac{kg}{m^3}$

$$r = d_c \tag{A.2}$$

For $\rho_{wood} > 500 \frac{kg}{m^3}$

$$\pi\left(\frac{\rho_{wood}}{\rho_{water}} - \frac{1}{2}\right) = \sin^{-}1\left(\frac{d_c - r}{r}\right) + \frac{d_c - r}{r^2}\sqrt{2d_c r - d_c^2} \tag{A.3}$$

C.A. Braudrick et al., 2000 described the movement of right-circular cylindrical logs in uniform flow, lying on a smooth immobile planar stream bed in rivers, using a force balance. When this balance is in equilibrium the log starts moving. Figure A.1 shows the force diagram of a cylindrical log lying parallel (Figure A.1 (a)) and normal to the flow (Figure A.1 (b)).

A.1.2. SEDIMENT

TRANSPORT OF SEDIMENT IN RIVERS

J. Bosboom & M. J. F. Stive, 2015 pointed out that in still and clear water sediment particles accelerate up to a certain fall velocity and transport downwards until they settle at the riverbed Bosboom and Stive (2015). The fall velocity follows from a force balance between the downward directed gravitational force (minus the buoyancy effect) and the upward directed drag force. *E.F. Schulz et al., 1954* stated that the fall velocity of an isolated particle in water is influenced mainly by its size, shape and density Schulz et al. (1954). For particles
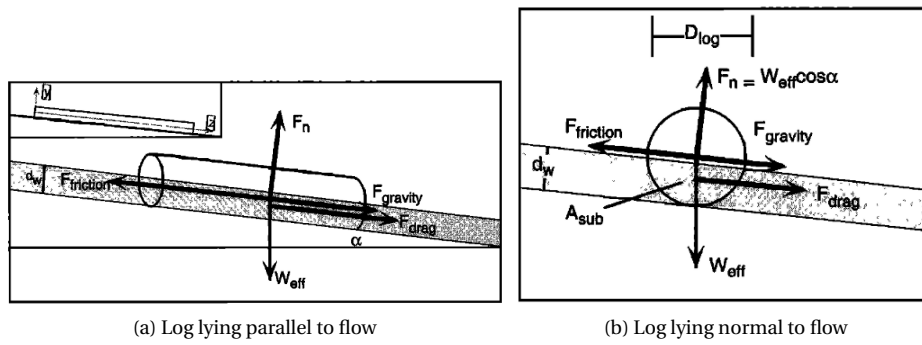
(a) Log lying parallel to flow
(b) Log lying normal to flow

Figure A.1: Log transport in a river Braudrick and Grant (2000)

with a density lower then water the buoyancy forces will dominate the gravity force and result in a rising velocity; as a consequences the drag force and gravity forces rotate 180°.

A. Armanini, 2018 and *J. Bosboom & M. J. F. Stive, 2015* described that the flow regime surrounding a particle influences the experienced drag. The Reynolds number describes the flow regime around the particle and depends on the particle size, fluid viscosity and particle fall velocity. Low Reynolds numbers indicates a laminar flow regime and high Reynolds numbers indicate a turbulent flow regime. Bigger particles are more likely to induce a high Reynolds number, which results in a lower drag coefficient.

A. Armanini, 2018 formulated the effects of the shape factor of sediment particles on its fall velocity Armanini (2018). An example of a shape factor is described by Equation A.4, where d_1, d_2 and d_3 are the longest, intermediate and shortest dimensions of the particle. When using a constant value for the Reynolds number Figure A.2 shows that the shape factor has a large impact on the drag coefficient.

$$SF = \frac{d_3}{\sqrt{d_1 d_2}} \tag{A.4}$$
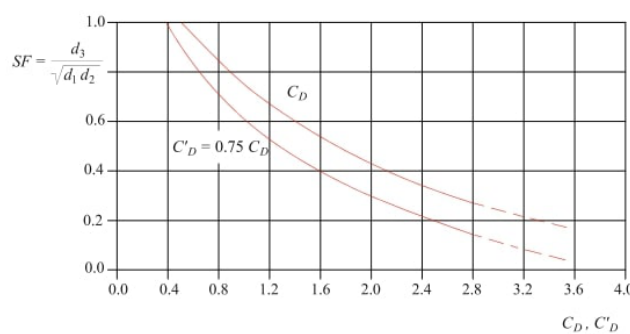
Figure A.2: Graph of the drag coefficient as function of the shape factor with a constant Reynolds number ($Re = 45$) Armanini (2018)

Furthermore, in Figure A.3 multiple fixed values for the shape factor are used to show the dependency of the drag coefficient and Reynolds number. This figure suggests that the drag coefficient reduces for higher Reynolds numbers and the relative effect of the shape factor becomes more dominant for larger particles, which in general have larger Reynolds numbers.
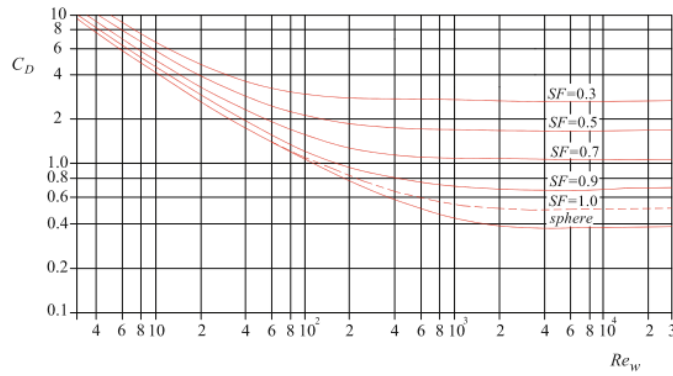
Figure A.3: Graph of the drag coefficient as function of the the Reynolds number Armanini (2018)

A. Armanini, 2018 suggests that a shape factor, as is defined by Equation A.4, does not describe the real conditions properly as natural particles are highly variable in their shape and size. Therefore, a variety of empirical relations exist but many implications still apply.

According to *J. Bosboom & M. J. F. Stive, 2015* sediments that are settled on the riverbed are only transported when the exerted shear stress (τ_b) by the water movement is large enough. When a certain threshold is reached, the critical shear stress (τ_b, cr), the particle initiates motion. The various forces involved in this process are schematized in Figure A.4.

The drag force results from the skin friction on the particle and the pressure difference up and downstream of the particle. The drag force is proportional to the horizontal flow velocity (U^2), the particle surface area (A) and water density (ρ).

Higher flow velocities result in a lower local pressure. Figure A.4 illustrates this contraction of the flow over the sediment particle. Due to this vertical pressure difference an upward lift force occurs, which is proportional to the flow velocity (U^2) and the particle surface area (A). The drag and lift forces are driving forces. The resisting drag force is proportional to the particle density (ρ_p), water density (ρ), gravity constant (g) and particle volume (V). When the resisting forces and driving forces are an equilibrium the particle initiates motion. The Shields parameter describes the initiation of motion of particles by deriving a constant value for C via experiments.
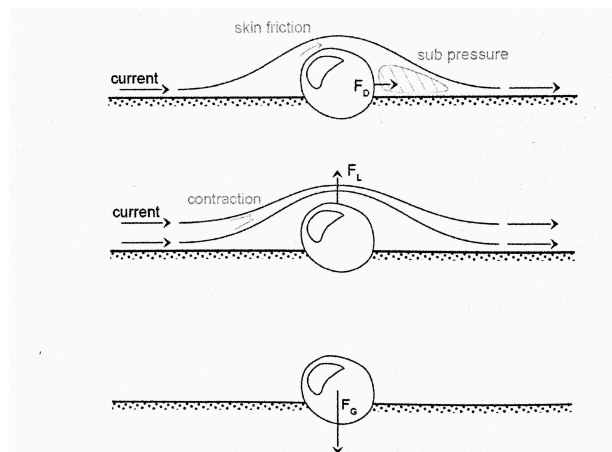

Figure A.4: Schematization of forces on a stationary sediment particle Bosboom and Stive (2015)

A.1.3. OIL
Oil is a buoyant material and is affected by wind transport, similar to macroplastics, and therefore provides a candidate for further study.

OIL CHARACTERISTICS

In Table A.1 the density is given for various types of crude oil*Engineering Toolbox* (2019). The range of properties is described in Table A.2. As shape and size are not applicable to a fluid such as oil only a density value is provided.

Classification	Density $\frac{kg}{m^3}$
Crude oil 48° API	790
Crude oil 40° API	825
Crude oil 35.6° API	847
Crude oil 32.6° API	862
Crude oil, California	915
Crude oil, Mexican	973
Crude oil, Texas	873

Table A.1: Density of various types of crude oil *Engineering Toolbox* (2019)

Density	Size	Shape
790 kg/m^3 - 973 kg/m^3	-	-

Table A.2: Property range of oil

TRANSPORT OF OIL IN RIVERS

H.T. Shen et al., 1988 used a computer model to model oil slick transformations in rivers Shen and Yapa (1988). Figure A.5 shows the variety of processes that oil slick is subjected to in rivers. *H.T. Shen et al., 1988* calculated the advection of oil in open water using Equation A.5 from *D.P. Hoult, 1972* Hoult (1972). Where V_w is the wind velocity at 10 meters above the water level, α_w is the respective drift factor which accounts for the relation of wind and oil transport, V_c is the depth-averaged current velocity and α_c is the drift factor which accounts for the effective of current on oil transport. The wind-induced drift factor varies between 0.01-0.06 and the current-induced drift factor varies between 1.1-1.2. It is suggested that advective transport due to flow is dominant in rivers over wind, especially in the longitudinal direction. Horizontal diffusion of oil in rivers is mainly dependant on the shear velocity, depth of flow and wind condition. The mechanical spreading of oil in open water is dominated by gravitational, viscous and surface-tension forces.
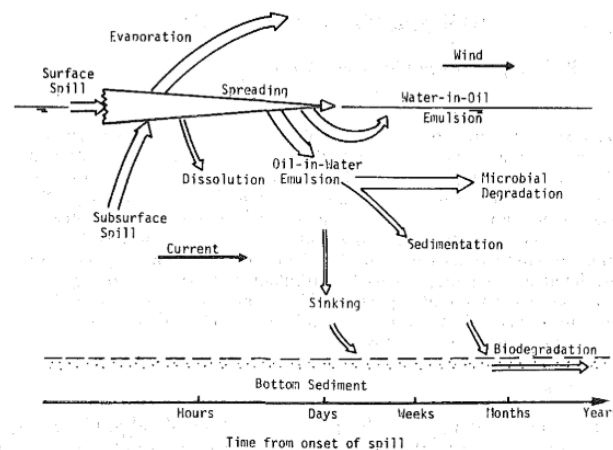

Figure A.5: Schematization of transport processes of oil slick Shen and Yapa (1988)

$$V = \alpha_w V_w + \alpha_c V_c \tag{A.5}$$

B
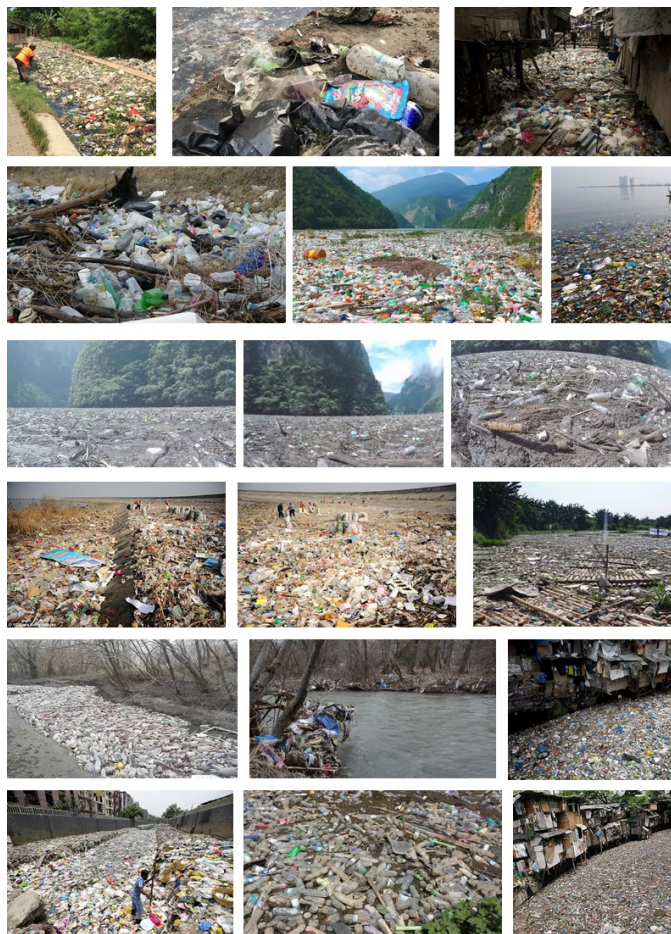
APPENDIX C

B.1. FIGURES

Figure B.1: Output of web scraping tool using the keyword *"plastic river"*

(a) Satellite image of the visual spectrum (VIS)

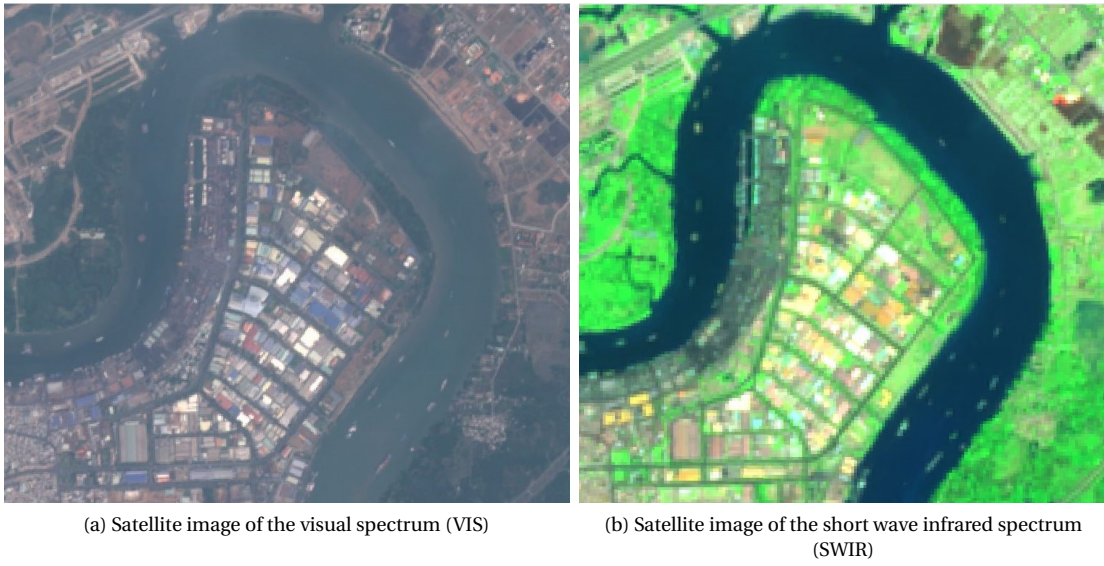(b) Satellite image of the short wave infrared spectrum (SWIR)

Figure B.2: Satellite image processing of the Saigon river, Vietnam with the Google Earth Engine

Figure B.3: Satellite image of the Saigon river, Vietnam of the normalized difference water index (NDWI)
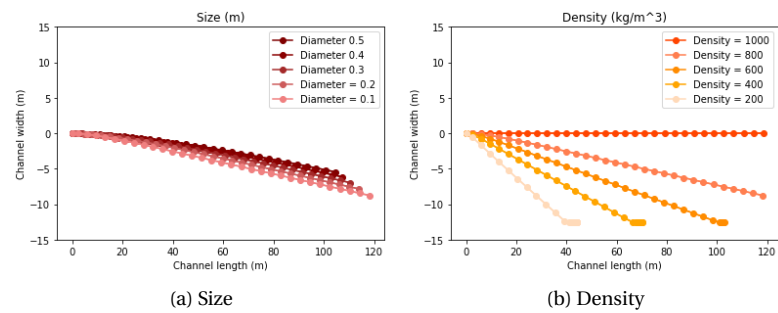
C

ANALYTICAL MODEL

(a) Size

(b) Density

Figure C.1: Top down view of river and size- and density effects including added mass)

(a) Size

(b) Density
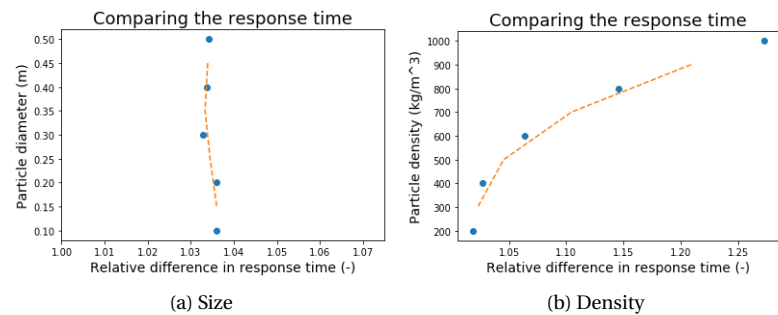
Figure C.2: Comparing particle response time between case with and without added mass

(a) Wind speed

(b) Flow speed
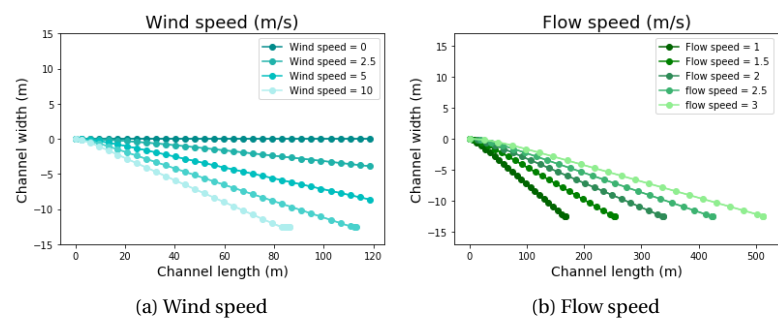
Figure C.3: Top down view of river and wind- and flow effects including added mass

(a) Wind speed

(b) Flow speed
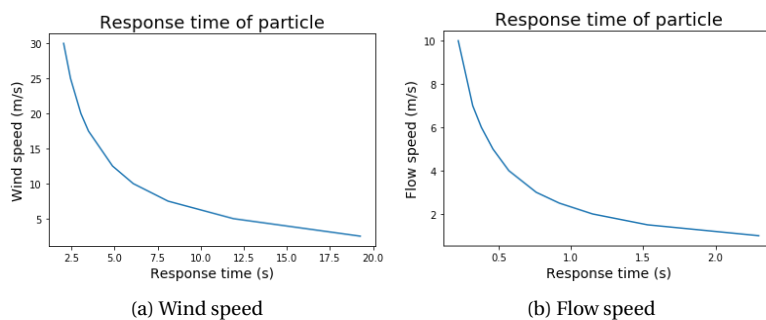
Figure C.4: Particle response time according to wind and flow including added mass

(a) Wind speed

(b) Flow speed
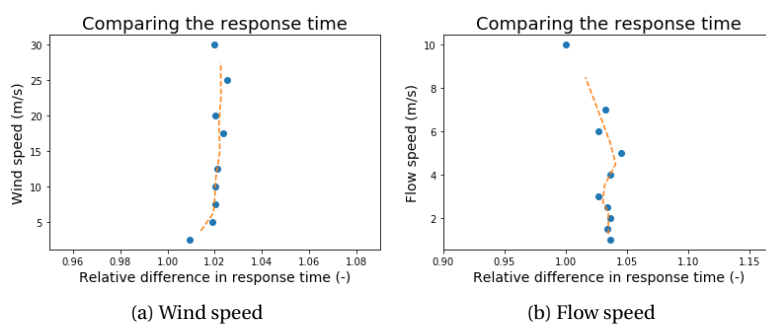
Figure C.5: Comparing particle response time between case with and without added mass
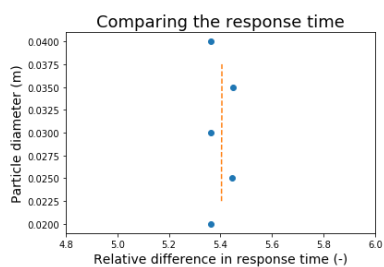
Figure C.6: Relative response time with and without added mass for plastic bag
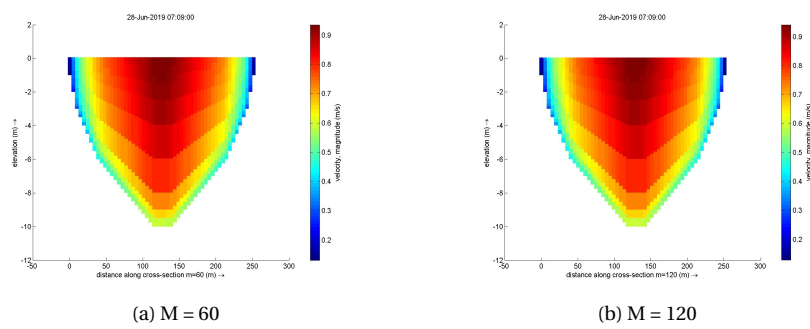
D

SCENARIO STUDY

(a) M = 60   (b) M = 120

Figure D.1: Flow velocity along different cross-sections for reference case

(a) Velocity   (b) Velocity at M = 60   (c) Velocity at M = 120
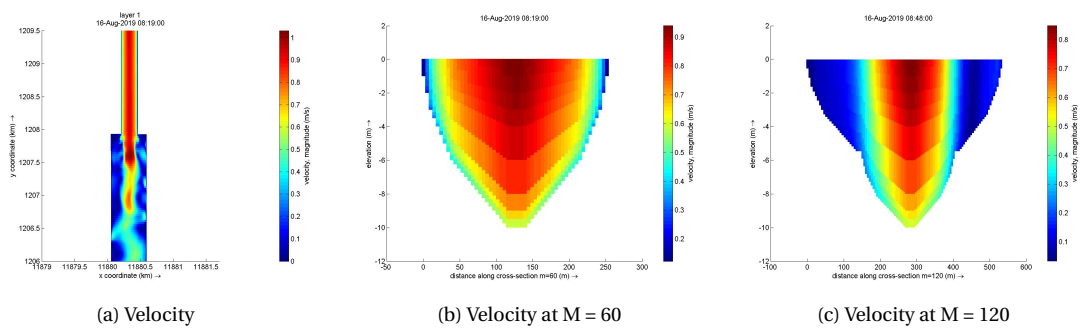
Figure D.2: Flow velocity along different cross-sections for the channel widening case

(a) Top down view of velocity near confluence

(b) Velocity at M = 60

(c) Velocity at M = 270
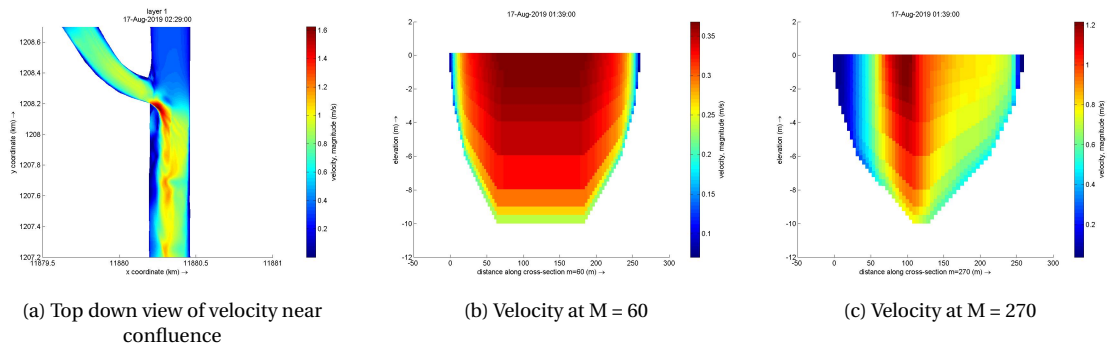
Figure D.3: Flow velocity along river confluence

(a) Velocity at M = 60

(b) Velocity at M = 145

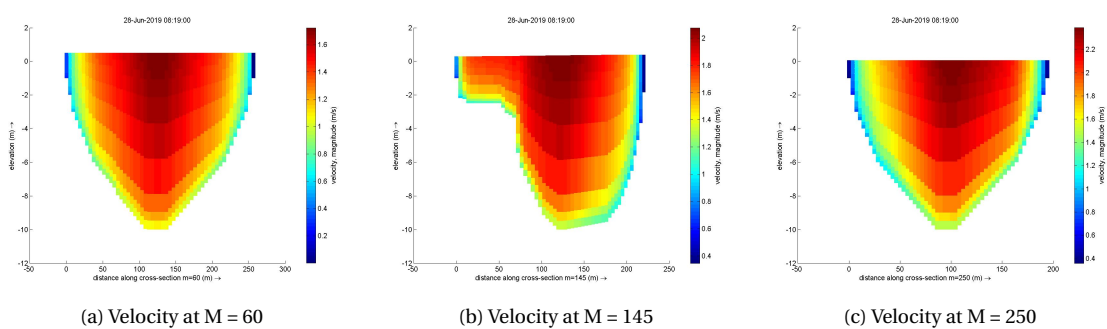(c) Velocity at M = 250

Figure D.4: Flow velocity along different cross-sections for riverbend case with high discharge

This master thesis is conducted in partial fulfillment of the requirements for the degree of Hydraulic Engineering

August 2019